Development of 2-(alkoxycarbonyl)-allyl esters as anticancer agents

A THESIS

PRESENTED TO THE FACULTY OF THE DEPARTMENT OF CHEMISTRY AND BIOCHEMISTRY

UNIVERSITY OF MINNESOTA, DULUTH

BY

CONOR T. RONAYNE

IN PARTIAL FULFILLMENT OF THE REQUIREMENTS FOR THE DEGREE OF MASTER OF SCIENCE

Dr. Venkatram Mereddy
January, 2018

Acknowledgements

First and foremost, I would like to thank my advisor Dr. Venkatram R. Mereddy for all of his guidance, support, motivation, creativity, and endless mentorship throughout my master's degree at UMD. I would also like to thank Dr. Jon Holy for his expertise in training many biological techniques presented in this thesis, and Dr. Joseph Johnson for further guidance throughout my undergraduate and graduate careers at UMD.

Further, I would like to extend my most sincere gratitude to my many colleagues that have helped me grow and learn in the fields of medicinal chemistry and biomedical sciences Sravan K. Jonnalagadda, Shirisha Gurrapu, Grady Nelson, Lucas Solano, Erica Lueth, Tanner Schumacher, and Zachary Gardner. Your help and support has been sincerely appreciated.

Finally, I would like to thank my family for their support in all of my endeavors.

Abstract

Cancer is the second leading cause of human mortality in the United States, with the standard treatment options being surgery, cytotoxic chemotherapy, and radiation therapy. Recently, there has been strong emphasis in developing targeted small molecule therapies which has led to the development of numerous anticancer drugs. However, many of the current cancer chemotherapeutic options are burdened with toxicity and treatment resistance and hence novel therapies with reduced side effects are urgently needed. In the current work, a structurally diverse library of Baylis-Hillman reaction derived 2-(alkoxycarbonyl)-allyl esters have been synthesized, evaluated for their *in vitro* cell proliferation inhibition properties, *in vitro* cellular and molecular mechanisms of action, *in vivo* systemic toxicity study in CD-1 mice, and *in vivo* anticancer efficacy study in a triple negative breast cancer MDA-MB-231 xenograft model in NOD SCID mice. Several of the synthesized compounds exhibit promising in vitro anticancer properties. Further, the lead candidate compound is well tolerated in healthy mice as indicated by normal body weight changes, and exhibits similar if not slightly better tumor growth inhibition properties than clinically available cancer drug doxorubicin.

Table of Contents

List of Schemes

List of Figures

Abbreviations

DNA: Deoxyribonucleic acid
MTIC: Methyl triazino imidazole carboxamide
BH: Baylis Hillman
DABCO: 1,4-diazobicyclo[2.2.2]octane
EWG: Electron withdrawing group
EDG: Electron donating group
RT: Room temperature
S_N2: Bimolecular nucleophilic substitution
LiHMDS: Lithium bis(trimethylsilyl)amide
THF: Tetrahydrofuran
HMPA: Hexamethyl phosphoramide
DMPU: 1,3-dimethyl-3,4,5,6-tetrahydro-2(1H)-pyrimidinone
DME: Dimethoxy ethane
DMF: Dimethyl formamide
DCC: N, N'-dicyclohexylcarbodiimide
DCM: Dichloromethane
DMAP: 4-dimethylaminopyridine
BTF: Benzotrifluoride
NCS: N-dichlorosuccinamide
TFAA: Trifluoroacetic anhydride
MTT: 3-(4,5-thiazol-2-yl)-2,5-diphenyltetrazolium bromide
DMSO: Dimethyl sulfoxide
NMR: Nuclear magnetic resonance
IC_{50}: Inhibitory concentration at 50% cell proliferation
NMO: 4-methylmorpholine-N-oxide
SAR: Structure activity relationship
BrdU: Bromodeoxyuridine
H2AX: Histone variant-2AX
MC: Mitomycin C
PARP: Poly-(ADP-ribose)-polymerase
CD-1: Caesarean derived-1
NOD-SCID: Severely combined immunodeficient mouse
IACUC: Institution of animal care and use committee

Introduction

Cancer is the second leading cause of human mortality behind heart disease in the United States.[1] In fact, it is estimated that in coming years, cancer will become the number one cause of death overtaking heart diseases. According to the 2017 American Cancer Society statistics, ~1.7 million new cases of cancer have been reported with around 600,000 of these cases resulting in mortality this year. Across both genders lung cancer is the highest in terms of incidence followed by prostate and breast cancer respectively and colorectal cancer being the third highest among both.[1] The standard treatment options for cancer involve surgery, cytotoxic chemotherapy and radiation therapy. Recently, there has been a strong emphasis on developing targeted therapies including small molecules, monoclonal antibodies, and immuno-therapeutics to deal with aggressive solid tumors and improve the overall therapeutic outcome.[2-23] Classic chemotherapy involves treating the patients with cytotoxic agents that target cellular DNA, tubulin/microtubules, and antimetabolites. DNA is a critical cellular component with well-defined primary, secondary, and tertiary structures. The genetic information encoded in DNA is critical for cell survival and proliferation. Since cancer cells are highly proliferative, they need heightened levels of DNA replication, transcription, and translation. Hence, targeting DNA is an attractive choice for anticancer therapy.[24-31] The presence of nucleophilic nitrogen atoms in DNA (i.e., N7-guanidine) also makes it an ideal target for designing electrophilic alkylators. Drug molecules that target DNA can be subdivided into DNA alkylators (crosslinkers), DNA topoisomerase inhibitors, DNA-double and single strand breakers and DNA code reading agents (**Figure 1.1**). [32]

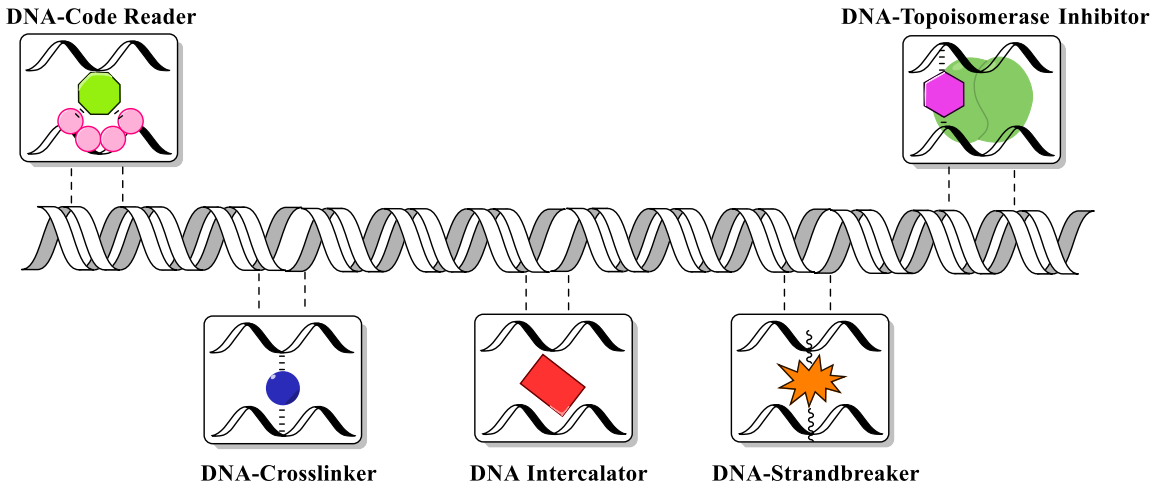

Figure 1.1: Different reactive modes of DNA-interaction with DNA-targeting drugs.

1A.Classical Alkylating Agents

Classical alkylating agents introduce alkyl groups onto the nucleophilic DNA. Some of the clinically used examples are listed in (**Figure 1.2**).

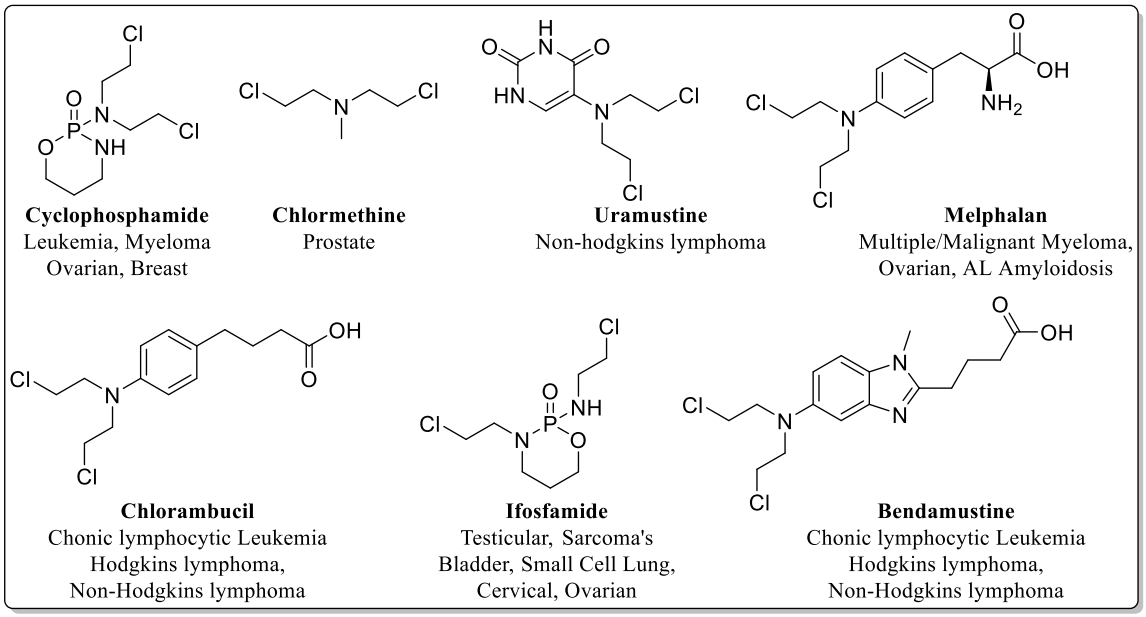

Figure 1.2: Examples of nitrogen mustard based DNA alkylating agents.

The mechanism of action of nitrogen mustards involves conversion of chloroethylamine group in to a reactive cyclic aziridinium intermediate which acts as an electrophile for interaction with nucleophilic DNA in covalent fashion. The presence of a second chloroethyl group leads to covalent interlinkage of two strands of DNA (**Figure 1.3**). The nucleophilic N7 nitrogen atom of guanine (G) reacts with the aziridinium to form G-G linkages resulting in DNA damage leading to cellular apoptosis.[33-36]

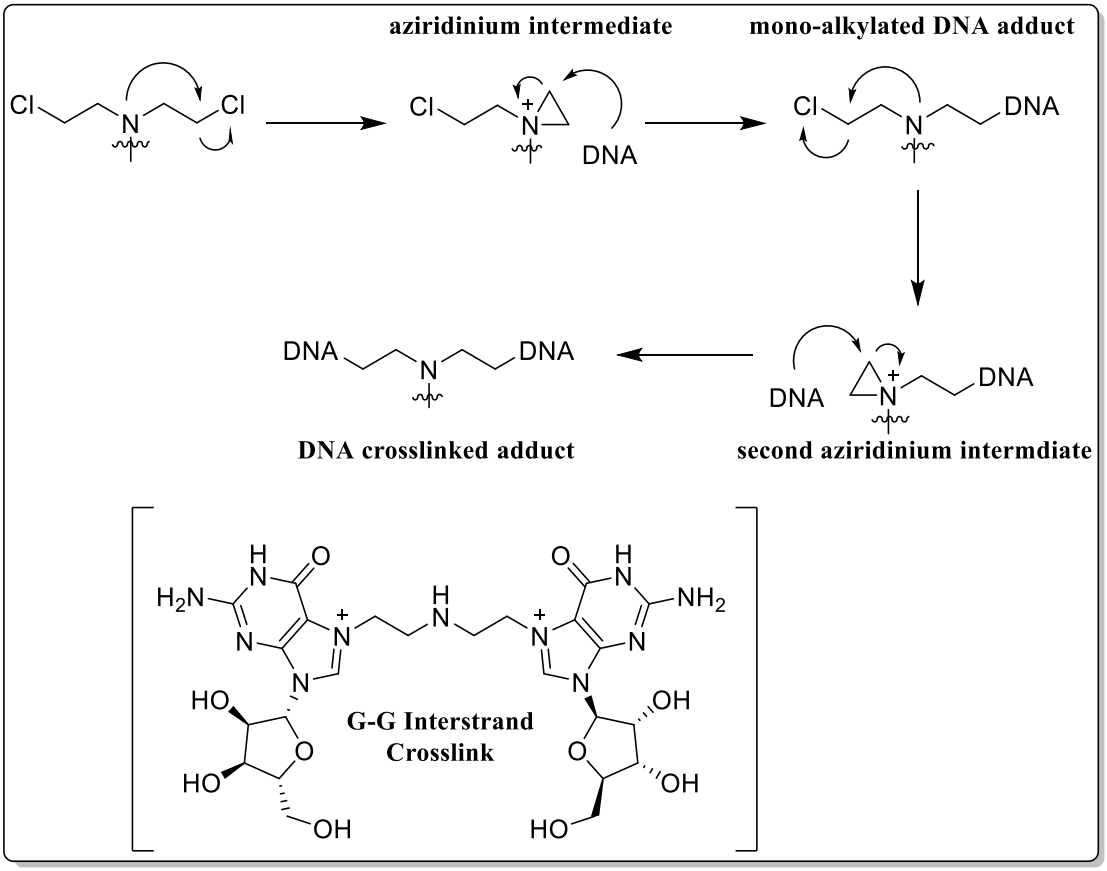

Figure 1.3: General mechanism of action of nitrogen mustard based DNA alkylating agents.

A second class of classical alkylating agents includes N-nitrosoureas, which similarly add an alkyl group to nucleophilic N7 of guanine, but differ in mechanism (**Figure 1.4**). For example, N-nitrosourea in carmustine undergoes extensive metabolic degradation to generate the reactive chloroethyl cation intermediate and chloroethylisocyanate. Chloroethyl cation causes crosslinks in DNA and the isocyanate intermediate carbamoylates protein components both resulting in cell death pathways (**Figure 1.5**).[37-39]

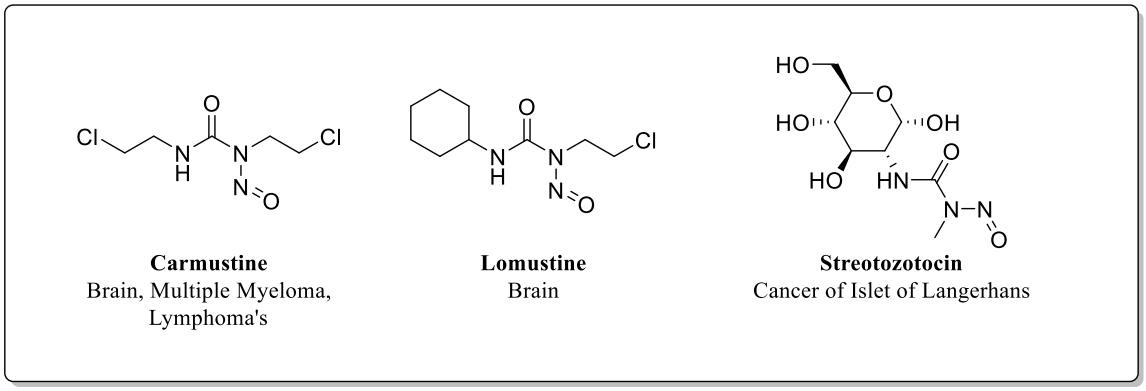

Figure 1.4: Examples of nitrosourea containing DNA alkylating agents.

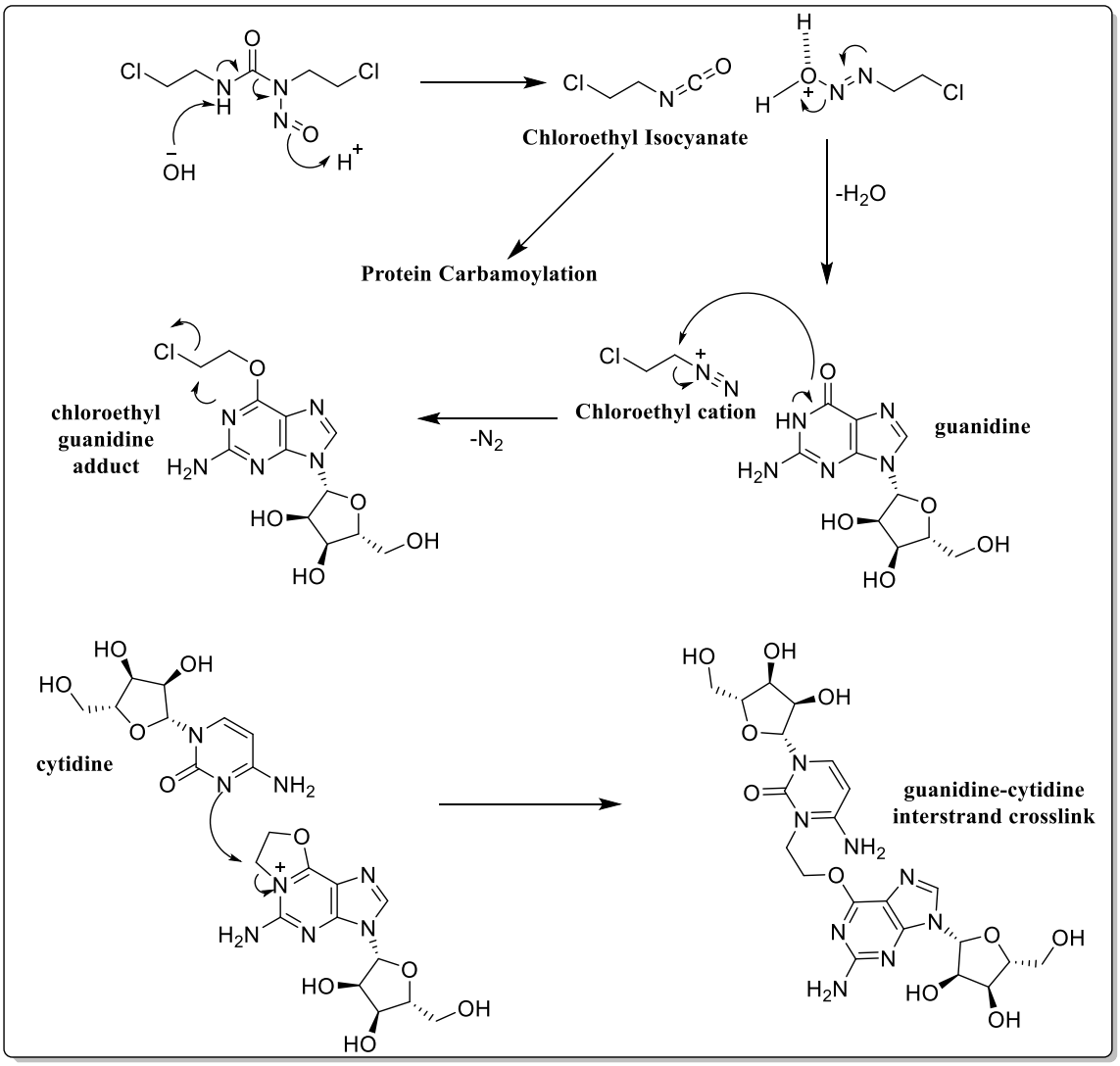

Figure 1.5: General mechanism of action of N-nitrosourea based DNA alkylators.

Another example of a classical DNA alkylating agent used for cancer therapy is busulfan which is a dimesylate derivative of 1,4-butanediol (**Figure 1.6**).

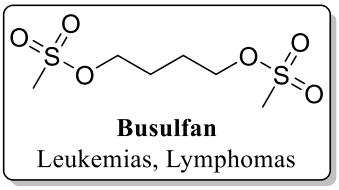

Figure 1.6: Structure of busulfan.

In the presence of a strong nucleophilic atom such as the N7 nitrogen atom of guanine, the mesylate leaving group can be nucle.ophilicly displaced in S_N2 fashion to form a covalent linkage. The presence of two mesylate leaving groups causes crosslinking of the two DNA strands resulting in damage to DNA and cell death pathways (**Figure 1.7**).[40-43]

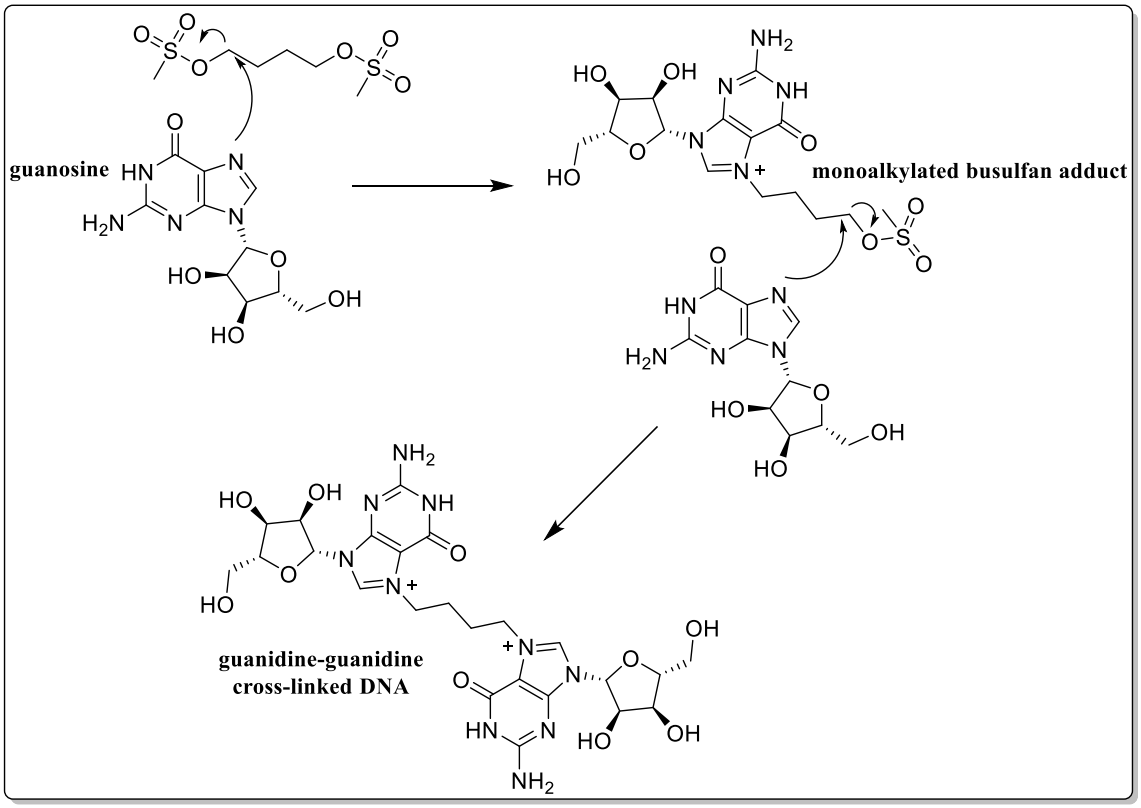

Figure 1.7: General mechanism of action of busulfan.

1B. Platinum based alkylating-like DNA interacting agents

Alkylating-like agents, including platinum based drugs interact with DNA to make covalent bonds, however these drugs do not have any alkyl groups to alkylate DNA in a classical way. Some of the examples of platinum based clinical and pre-clinical anticancer agents are listed in (**Figure 1.8**).

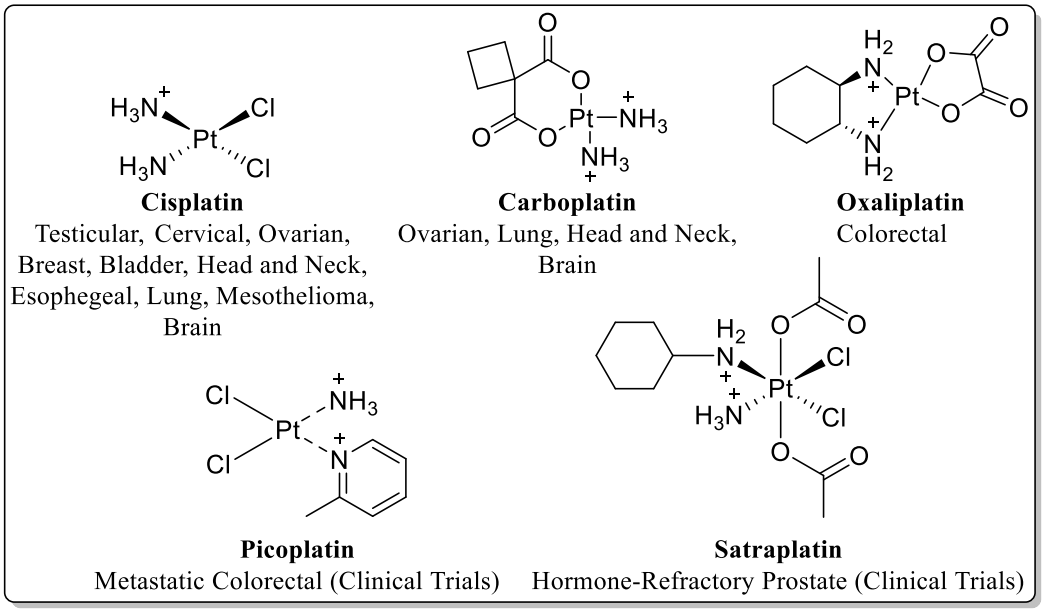

Figure 1.8: Examples of platinum based DNA interacting agents.

Cisplatin has two leaving groups in the form of chlorines. One of the chlorides is replaced by H_2O *in vivo* to provide the aqua-complex $[PtCl(NH_3)_2H_2O]^+$ (**Figure 1.9**). This species undergoes further nucleophilic displacement by two guanine nucleobases on the same strand of DNA to form $[PtCl(guanine\text{-}DNA)_2(NH_3)_2]^+$ (**Figure 1.9**).[44] Although many types of cisplatin-DNA adducts are reported, the predominant one involves 1,2-intrastrand crosslinks with guanine bases d(GpG). The mechanisms of action of other

platinum drugs are similar to that of cisplatin. In these cases, the reactive chloride ions are replaced with more stable Pt-O bonds (**Figure 1.9**).[44]

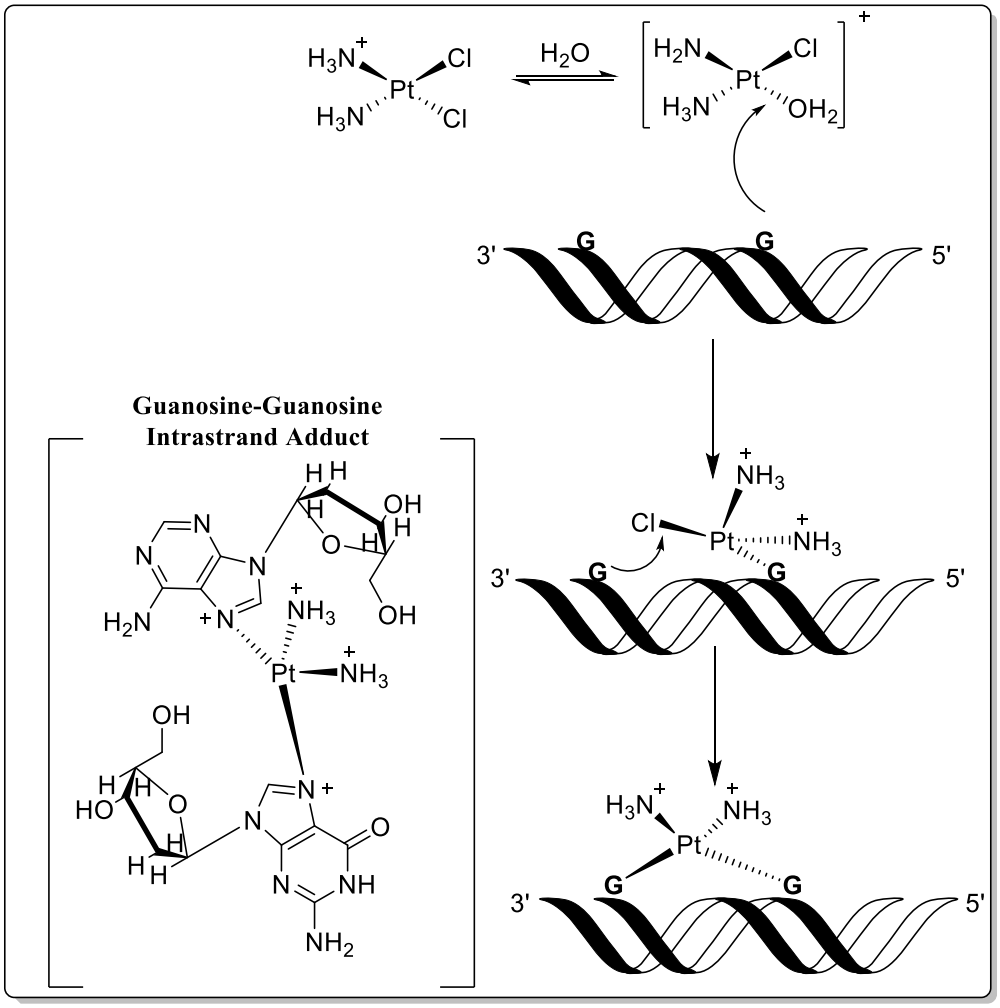

Figure 1.9: General mechanism of action of platinum based DNA interacting agents.

1C. Non-classical DNA interacting agents

Non-classical alkylating agents include hydrazine based procarbazene and triazene based dacarbazine and temozolomide (**Figure 1.10**). Again, these drugs act as electrophiles for the alkylation with nucleophilic DNA. However, the mechanism of

action and metabolic activation are different from that of classical alkylating nitrogen mustards and platinum agents. Hence, they are listed as non-classical alkylating agents.

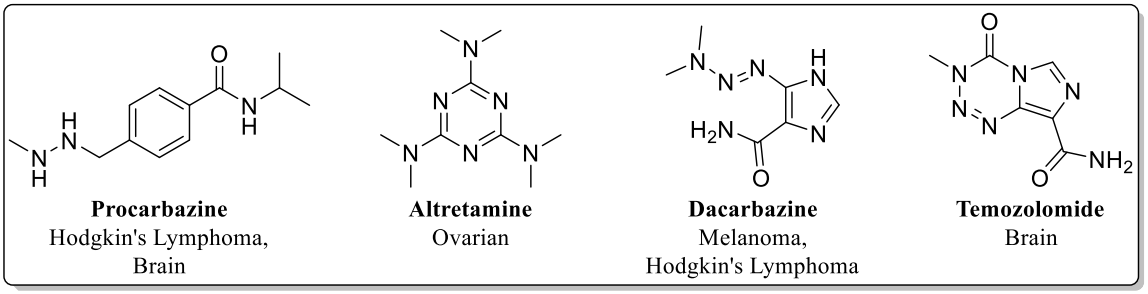

Figure 1.10: Examples of non-classical DNA alkylating agents.

Temozolomide is a lipophilic prodrug of dacarbazine. It is highly orally bioavailable and due to its small size and high lipophilicity it crosses the blood-brain-barrier with high efficiency (30% brain versus blood plasma). It undergoes metabolic activation to reactive methyl triazino imidazole carboxamide (**MTIC**) (**Figure 1.11**). This species further generates reactive electrophilic units which alkylate at N7 and O6 positions of guanine residues, and N3 of adenine (**Figure 1.12**).[45-46] This results in cellular apoptosis due to the failure of cellular repair mechanisms due to alkylated DNA.

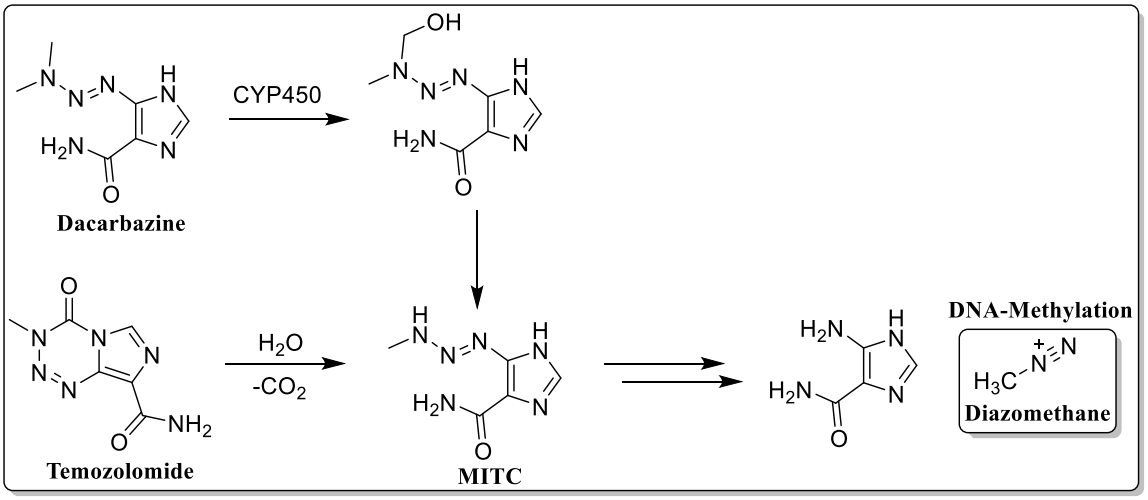

Figure 1.11: General mechanism of action of temozolomide.

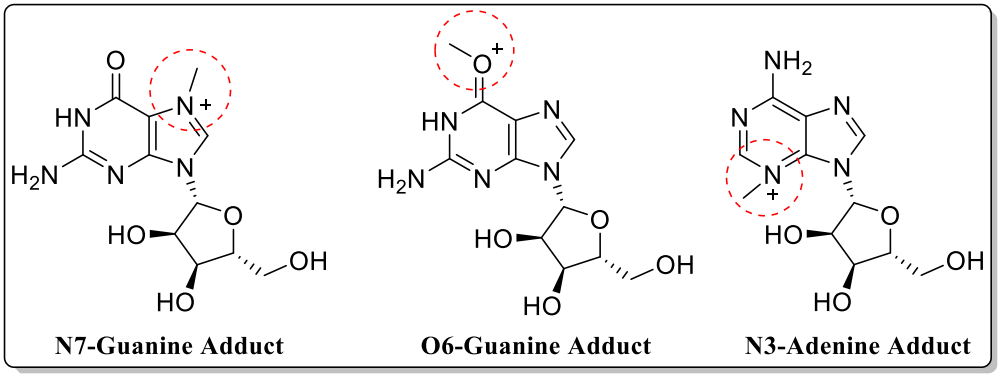

Figure 1.12: Sites of alkylation of temozolomide.

1D. DNA topoisomerase inhibitors

Other classes of antineoplastic agents that do not directly alkylate or bind to nitrogenous bases, but interact with and disrupt DNA functions include topoisomerase 1 and 2 inhibitors (**Figure 1.13** and **1.14**). In these cases, the flat topology of the molecule helps intercalate with the DNA strands, and the polar functional groups form a tight hydrogen bonding with phosphodiester backbone of DNA.

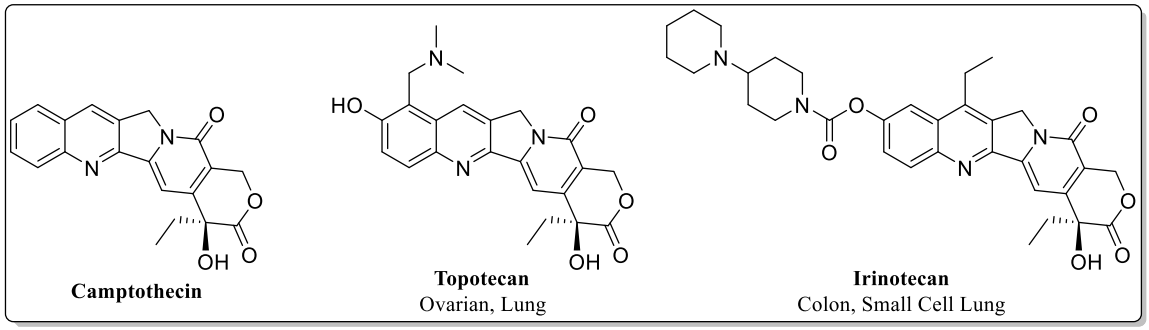

Figure 1.13: Examples of topoisomerase 1 inhibitors.

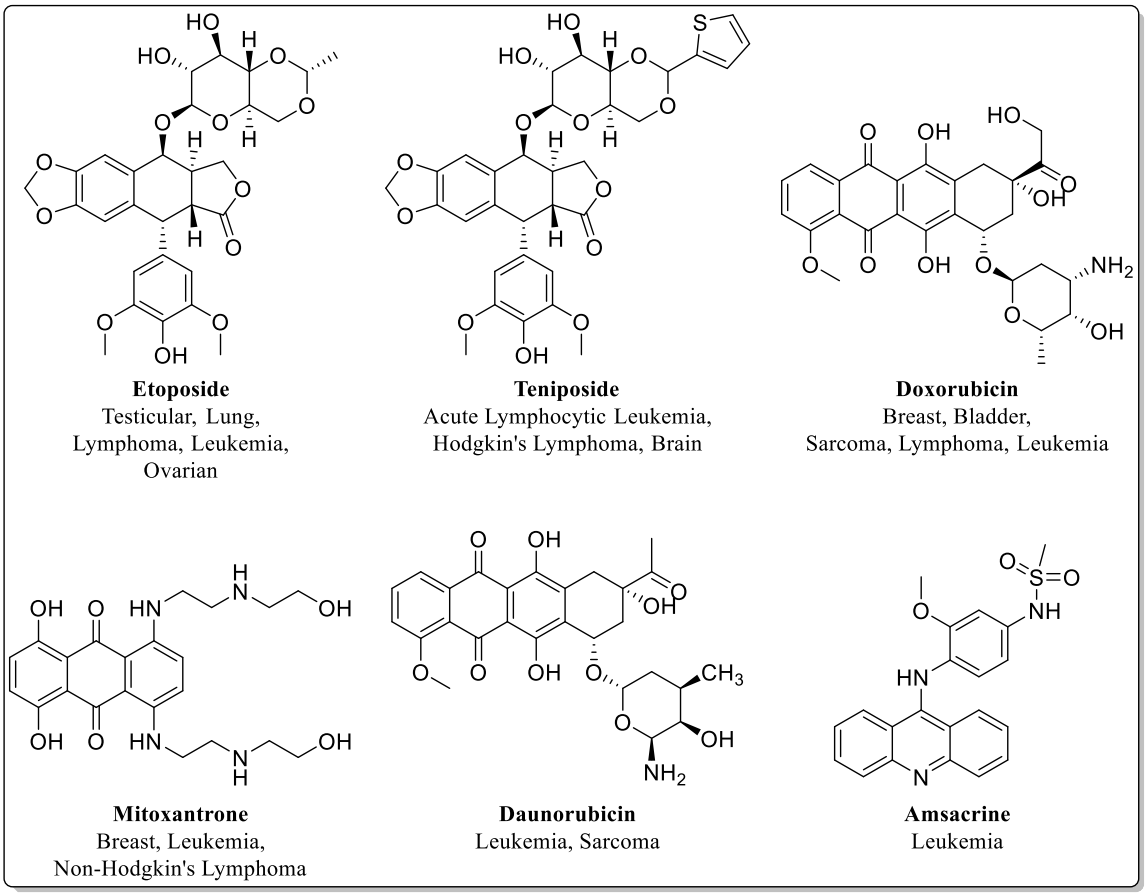

Figure 1.14: Examples of topoisomerase 2 inhibitors.

During DNA replication and transcription, DNA coding machinery causes an over-winding ahead of the replication fork that needs to be relaxed in order to release the torsional strain of the supercoiled DNA strand. Topoisomerase 1 and 2 are responsible for the unwinding of DNA by cutting either one or both strands respectively. Inhibitors of such action cause high levels of genomic instability due to high strain near DNA replication and transcription machinery, and further leading to DNA damage and cell death pathways. [47-48]

Introduction of above mentioned DNA alkylators and other DNA interacting agents has tremendously improved the therapeutic outcome for a wide variety of cancers.

However, due to their non-selectivity they suffer from significant side effects including teratogenicity, severe myelosuppression, and permanent damage to the immune system. Hence, the development of novel DNA alkylators with high structural tunability and different mode of action with fewer side effects are highly required. In this regard, we chose to explore the potential of an important C-C bond forming Baylis-Hillman (BH) reaction. This reaction is very simple to perform, and by mixing an aldehyde with electron withdrawing group substituted ethylenes such as methyl acrylate, methyl vinyl ketone, and acrylonitrile in the presence of a nucleophilic base 1,4-diazabicyclo[2.2.2]octane (DABCO) provides functionalized allyl alcohols in one step (**Scheme 1.1**). [49-58]

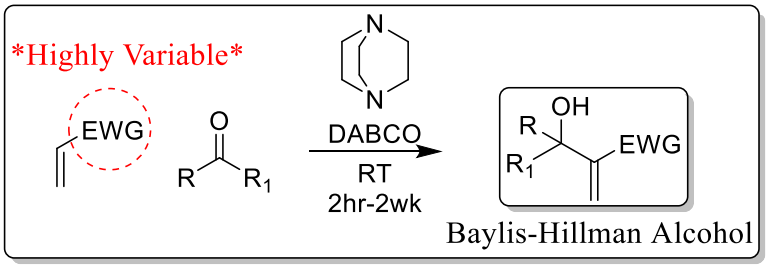

Scheme 1.1: Baylis-Hillman reaction.

This reaction is highly atom efficient and typically requires no solvent and can be performed at room temperature. The acetates of product BH alcohols can be isomerized with various nucleophiles in S_N2' fashion to provide further functionalized structural synthons (**Scheme 1.2**).

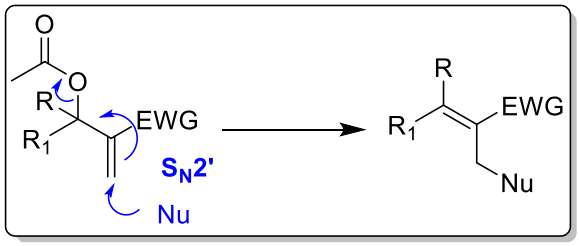

Scheme 1.2: S_N2' capability of BH acetates.

The BH alcohols can also be converted into allyl bromides by reacting them with HBr/H_2SO_4 or PBr_3 (**Scheme 1.3**).

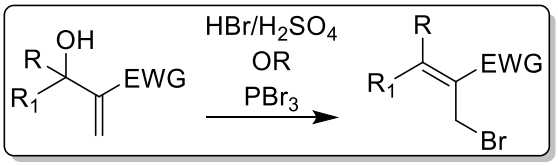

Scheme 1.3: Synthesis of BH-Bromide

The BH bromide **1** is an intriguing structural intermediate and provides three opportunities for nucleophilic substitutions. BH bromide **1** can undergo a direct nucleophilic substitution in S_N2 fashion, allylic rearrangement in S_N2' mode, and 1,4 addition reaction (**Figure 1.15**).

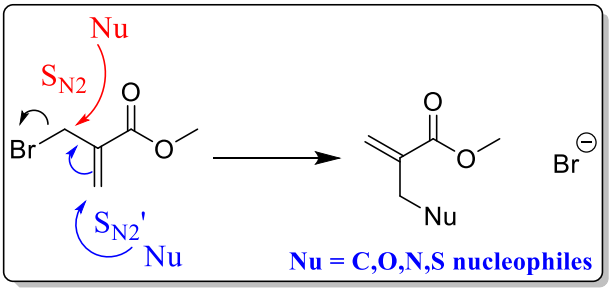

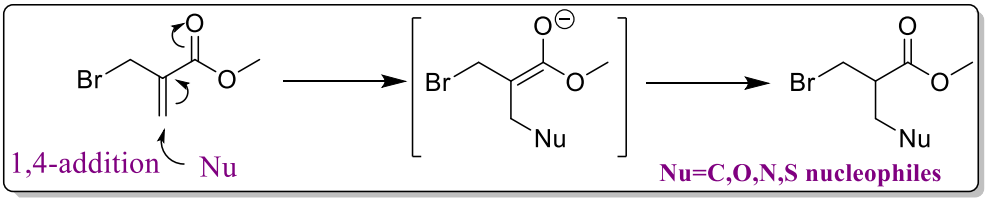

Figure 1.15: S_N2, S_N2', and 1,4 addition capabilities of BH bromide **1**.

1E. Utilization of BH bromides in organic synthesis

The formaldehyde derived BH bromide **1** and the benzaldehyde derived BH bromide **2** (**Figure 1.16**) have been extensively utilized for indium, zinc, and titanium and other metal based nucleophilic Barbier type allylation reactions to obtain allyl alcohol **3** (**Scheme 1.4**).[59-68]

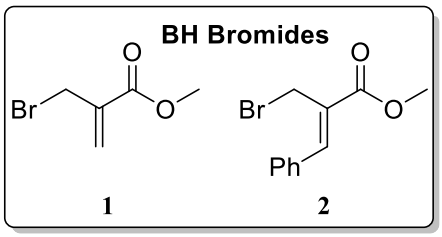

Figure 1.16: BH Bromides

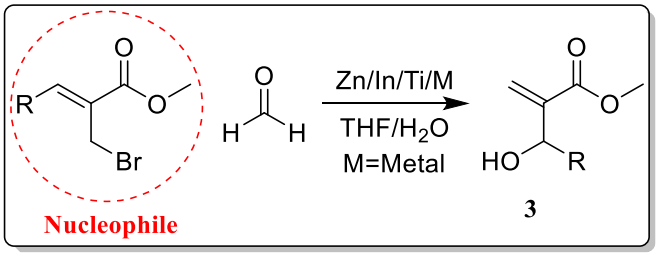

Scheme 1.4: Barbier allylation of carbonyl compounds with BH bromides.

Conversely, they have also been used as electrophiles for nucleophilic C, N, O and S alkylations for a wide variety of structurally interesting natural and unnatural products. They have also been explored for making a wide variety of medicinally important small molecules as anticancer, antibacterial, and pharmacological probes. Some of the applications of BH bromides **1** and **2** have been delineated below.

1E.1.Diastereoselective alkylation of aspartic acids with BH bromides

Hanessain *et al*. reported an anti-steroselective (85%) alkylation of N-CBz aspartic acid **4** using BH bromide **1** to provide the corresponding alkylated product **5** and **6** (85%:15%) in 87% yield (**Scheme 1.5**).[69]

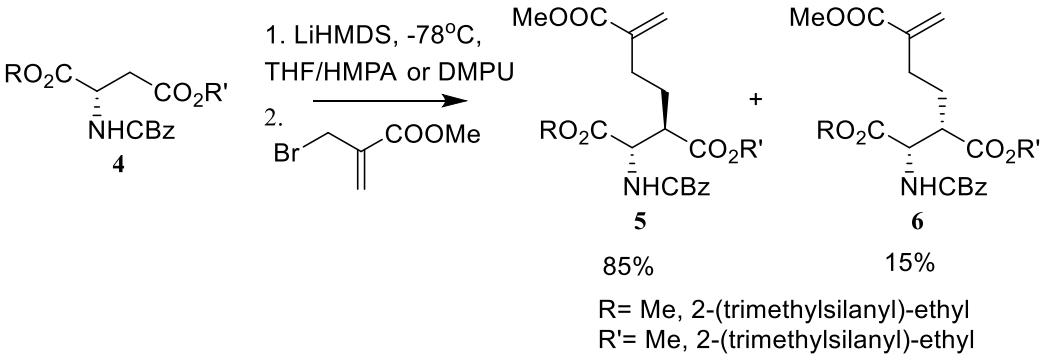

Scheme 1.5: Diastereoselective alkylation of aspartic acids with BH bromides

1E.2. Synthesis of BC-ring system of natural alkaloid tuberostemoninol using BH bromide

Williams and Jia reported the utilization of BH bromide **1** in the BC-ring system of natural alkaloid tuberostemoninol **6** (Figure 17). Alkylation of diphenyl morpholine **7** with BH bromide **1** in the presence of potassium bicarbonate in DMF provides the S_N2 substituted *N*-alkylated product **8**. Subsequently, **8** was converted into the BC-ring synthon of tuberostemoninol **9** in several steps (**Scheme 1.6**).[70]

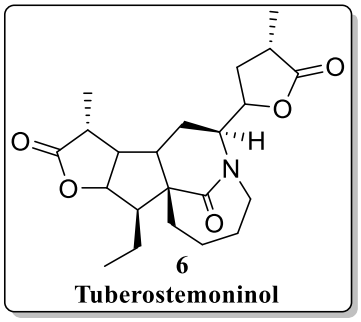

Figure 1.17: Structure of tuberstemoninol.

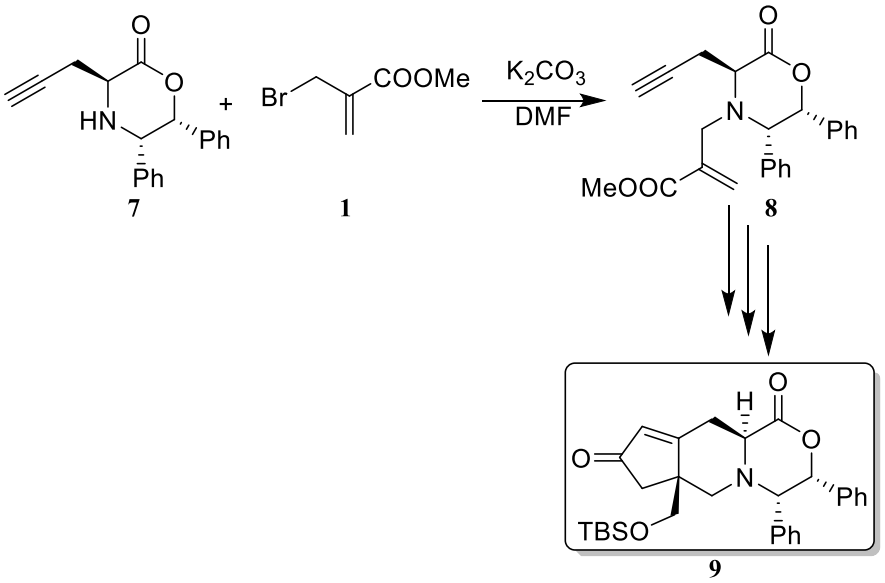

Scheme 1.6: Synthesis of BC-ring system of natural alkaloid tuberostemoninol using BH bromide **1**

1E.4. Synthesis of substituted quinoziline-4-ones with BH bromide

Spring *et al*. utilized BH bromide for N-alkylation of 6-bromo-2-pyridone to provide the N-alkylated product **11**. Bromide in **11** was coupled under Stille conditions using $Pd_2(dba)_3$ and allyl or methallyl tin reagents (**12** or **13**) to afford the diene products **14** or **15**. These products were cyclized using ring closing metathesis reaction with Grubb's second generation catalyst to obtain substituted quinoziline-4-ones **16** or **17** **(Scheme 1.7**).[71]

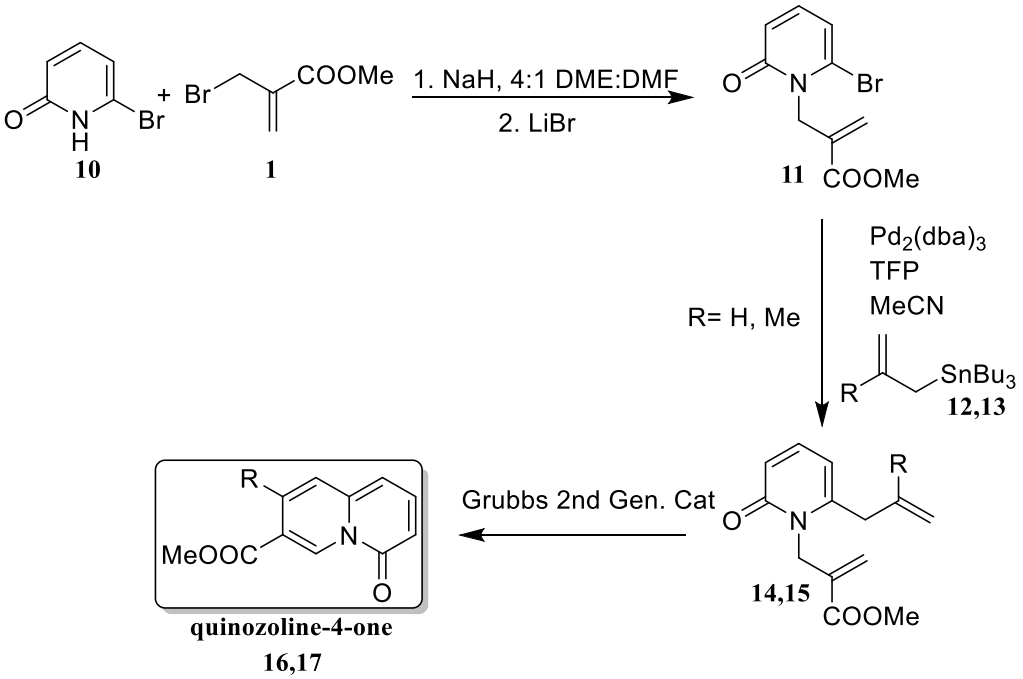

Scheme 1.7: Synthesis of substituted quinoziline-4-ones with BH bromide **1**.

1E.5. Synthesis of polycyclic γ-lactams utilizing BH bromide

Synthesis of polycyclic γ-lactams was achieved under metal free conditions via radical cyclization of 1,6-eneynes. The required eneynes were conveniently synthesized via alkylation of tosylamides with BH bromide followed by DCC mediated coupling with propargylic acids (**Scheme 1.8**). [72]

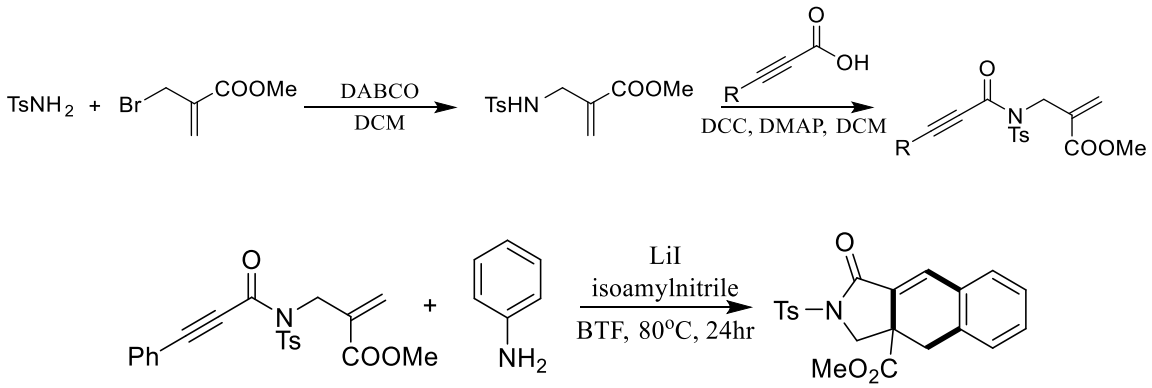

Scheme 1.8: Synthesis of polycyclic γ-lactams utilizing BH bromide **1**.

1E.6. Synthesis of (S)-(3-benzyl-3-methyl-2,3-dihydrobenzofuran-6-yl)-piperidin-1-yl-methanone utilizing BH bromide

Naguib and Luo synthesized piperidinyl methanone via *O*-alkylation of piperidine amide **18** with BH bromide **1** under basic conditions to obtain compound **19**. **19** was subsequently converted to (S)-(3-benzyl-3-methyl-2,3-dihydrobenzofuran-6-yl)-piperidin-1-yl-methanone **20** via a series of steps (**Scheme 1.9**).[73]

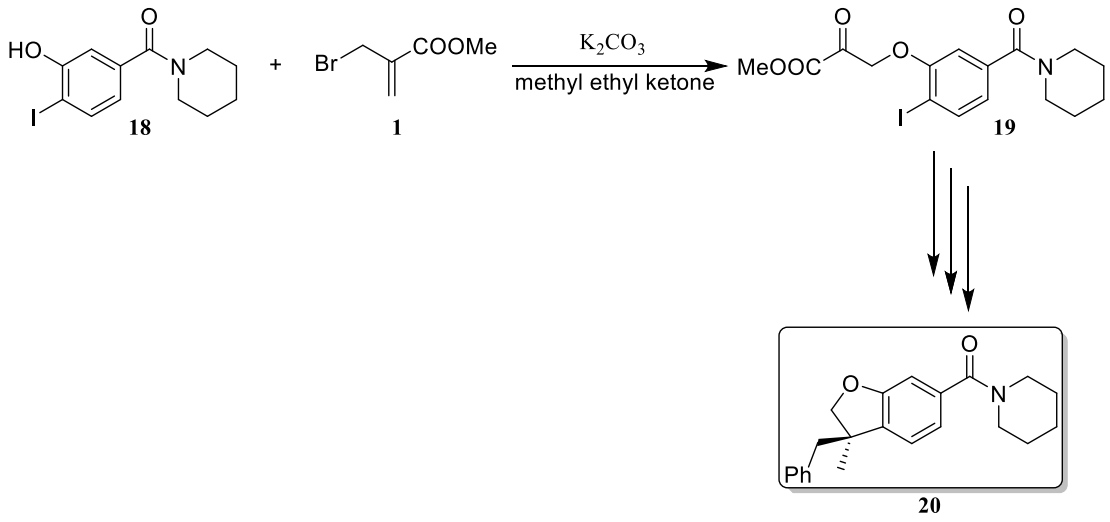

Scheme 1.9: Synthesis of (S)-(3-benzyl-3-methyl-2,3-dihydrobenzofuran-6-yl)-piperidin-1-yl-methanone using BH bromide **1**.

1E.7. Synthesis of BH bromide derived peptidomimetics

Ostaszewski *et al.* reported the synthesis of novel peptidomimetic inhibitors of thioredoxin−thioredoxin reductase system via *O*-alkylation of substituted cesium benzoates with BH bromide **1** and BH bromide derived peptidomimetic analogs **21** to provide BH product **22** and BH peptidomimetic product **23** (**Scheme 1.10**). [74]

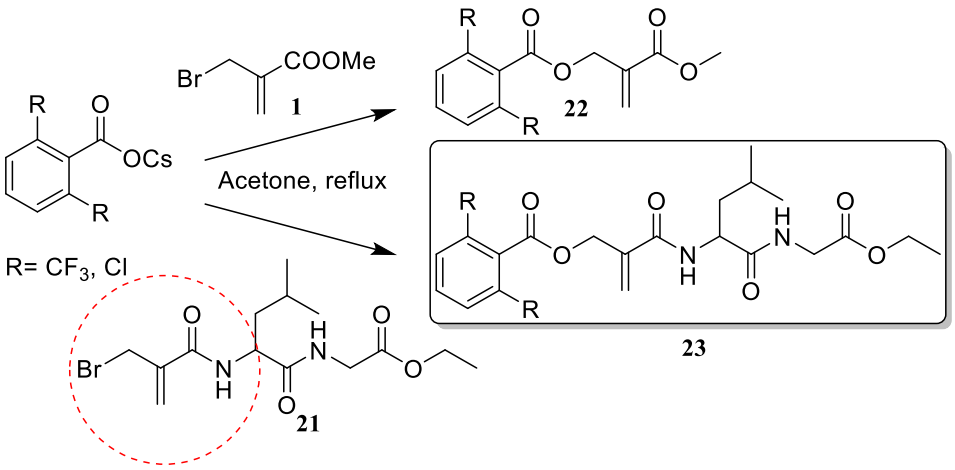

Scheme 1.10: Synthesis of BH bromide derived peptidomimetics.

1E.8. Synthesis of 3-benzylidene-pyrrolidine-2,5-dione using BH bromide

3-benzylidene-pyrrolidine-2,5-dione have been synthesized from BH bromide **2** via nucleophilic displacement of bromide with cyanide in S_N2 fashion to obtain compound **24.** followed by conversion of the corresponding nitriles to amide **25** and base promoted cyclization to obtain 3-benzylidene-pyrrolidine-2,5-dione product **26** (**Scheme 1.11**).[75]

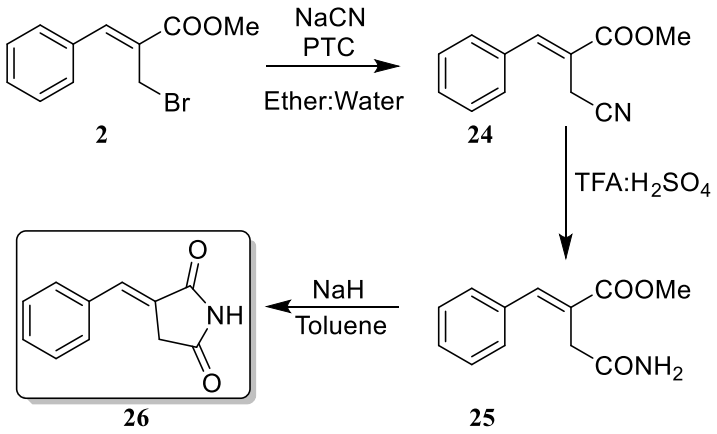

Scheme 1.11: Synthesis of 3-benzylidene-pyrrolidine-2,5-dione using BH bromide **2**.

1E.8. Synthesis of olefinic 1,5-dicarbonyl compounds with BH bromide

Kim *et al.* synthesized olefinic 1,5-dicarbonyl compounds via *C*-alkylation of BH bromide **2** with allyl substituted 1,3 dicarbonyl compound **27** followed by Pd-mediated decarboxylative protonation of compound **28** provided 1,5-dicarbonyl compound **29** (**Scheme 1.12**).[76]

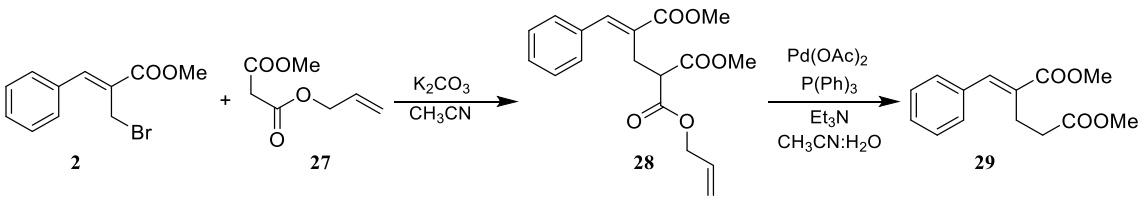

Scheme 1.12: Synthesis of olefinic 1,5-dicarbonyl compounds with BH bromide **2**.

1E.9. Synthesis of indoleazocines utilizing BH bromide

Batra *et al.* synthesized indoleazocine **32** starting with alkylation of trypatamine **30** with BH bromide **2** in the presence of trimethylamine . The corresponding *N*-alkylated product **31**was further converted into respective indoleazocine **32** by a series of steps (**Scheme 1.13**).[77]

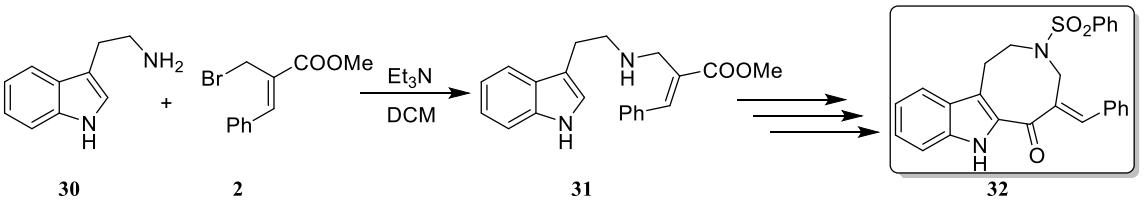

Scheme 1.13: Synthesis of indoleazocines utilizing BH bromide **2**.

1E.10. Synthesis of tricyclic tetrahydroquinoline using BH bromide

N-alkylation of *N*-tosylaminobenzaldehyde **33** with BH bromide **2** under basic conditions provided the product **34**. Treatment of **34** with hydroxyl amine afforded the aldoxime **35** which was directly treated with NCS and trimethylamine to obtain the tricyclic tetrahydroquinoline **36** via an intramolecular 1,3-dipolar nitrile oxide cycloaddition reaction. (**Scheme 1.14**).[78]

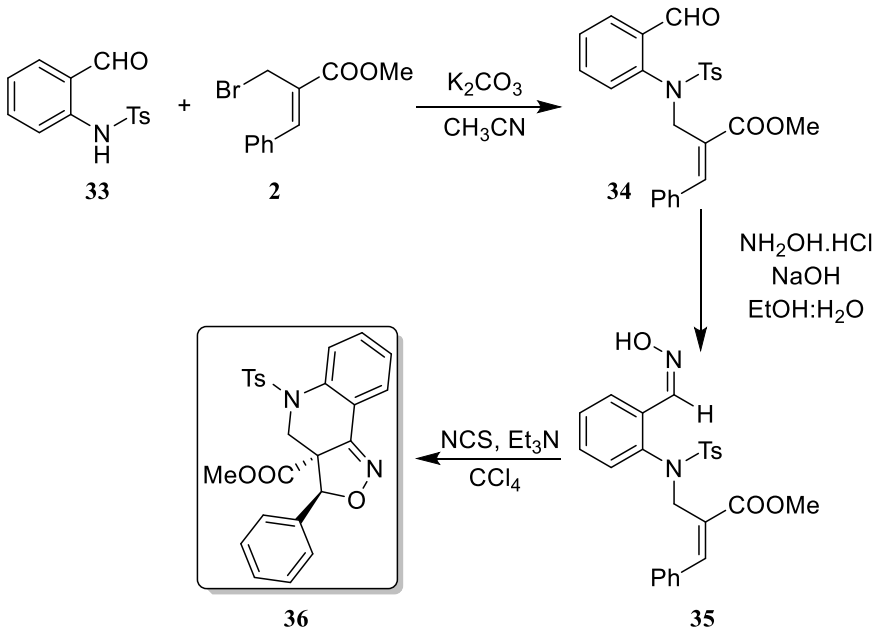

Scheme 1.14: Synthesis of tricyclic tetrahydroquinoline using BH bromide **2**.

1E.11. Synthesis of thiol-sensitive probes using BH bromide

BH-bromide **2** was *O*-alkylated with various phenols **36a-f** to afford corresponding phenacrylate derivatives **37a-f**. These were used as thiol sensitive probes for biological applications (**Scheme 1.15**).[79]

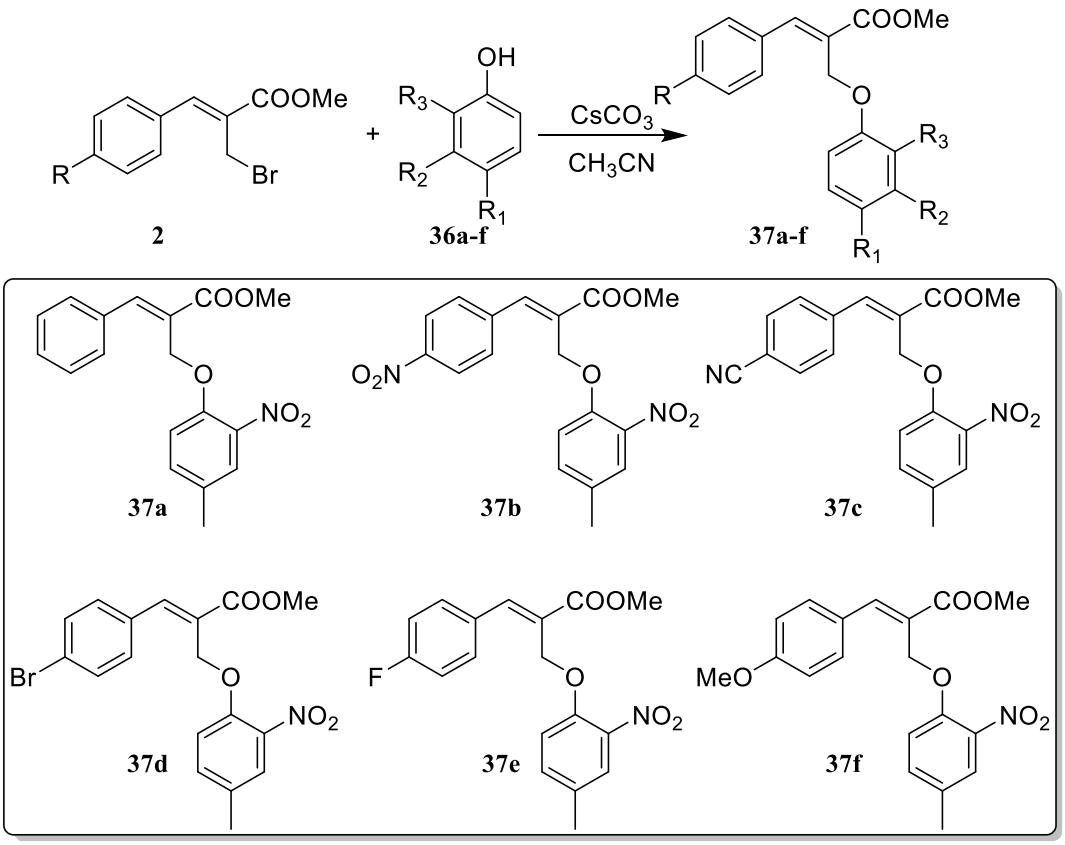

Scheme 1.15: Synthesis of thiol-sensitive probes using BH bromide **2**.

1E.12 Synthesis of dinapthyl chromanone utilizing BH bromide

Kankam *et al.* synthesized methylene-dinaphthyl bis-chromanones starting from **38** and BH bromide **2**. The esters in alkylated product **39** were hydrolyzed to corresponding carboxylic acids in **40** which were subsequently cyclized to corresponding dinapthyl chormanone **41** (**Scheme 1.16**). The product chomanone **41** was tested against several bacterial strains with good zone of inhibition.[80]

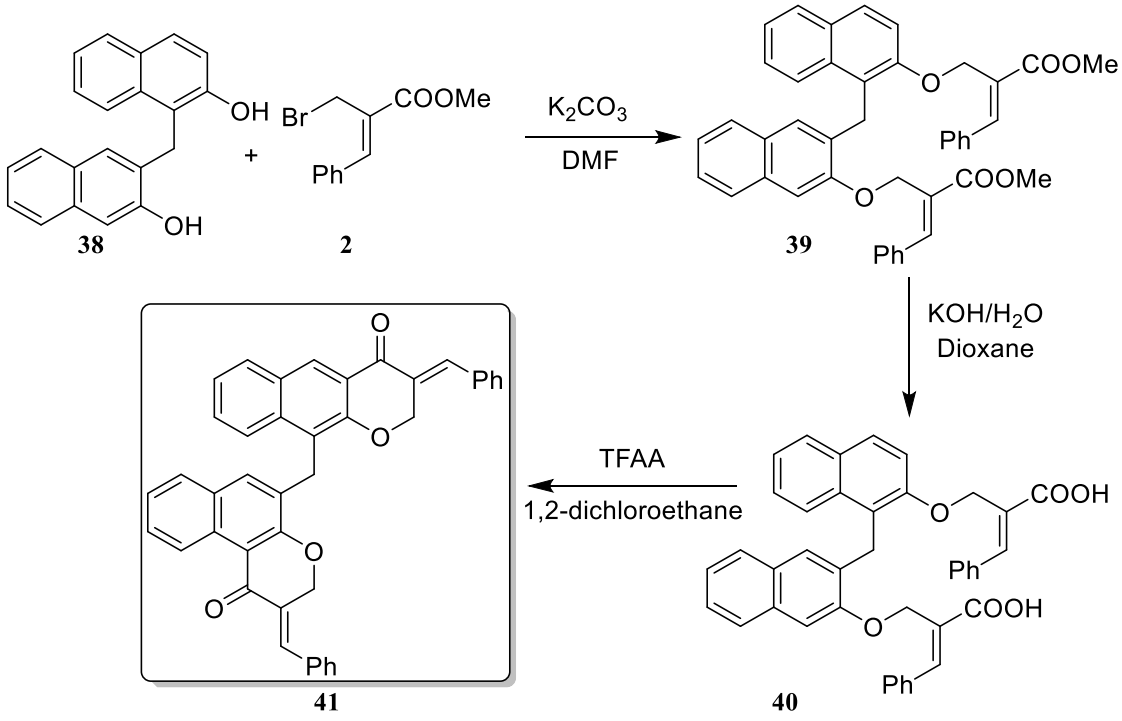

Scheme 1.16: Synthesis of dinapthyl chromanone utilizing BH bromide **2**.

1E.13 Synthesis of isothiouronium salts using BH bromide

Treatment of thiourea **42a** and alkyl/aryl substituted thioureas **42b-c** with BH bromide **2** provided *S*-allylic isothiouronium salts **43a-c** respectively. These thiourea salts were evaluated against a leukemia cancer cell line L1210 with moderate to good activity (**Scheme 1.17**).[81]

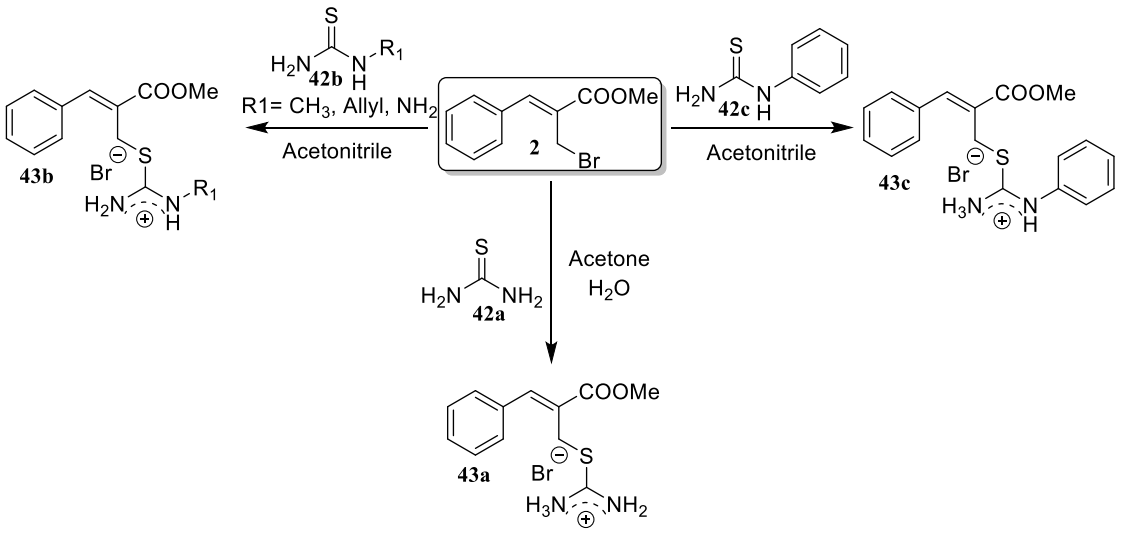

Scheme 1.17: Synthesis of isothiouronium salts using BH bromide **2**.

1E.13 Synthesis of allylic azides, thiocyanates, isothiouronium salts from BH bromide

Sa *et al.* utilized BH bromide **2** as a template to react N_3, SCN, and thiourea based nucleophiles in S_N2 fashion to obtain the corresponding allylic azides, thiocyanates, isothiouronium salts **44a-c** respectively. The isothiouronium salt **44c** was treated with acetic anhydride to obtain the acetylated product **45** (**Scheme 1.18**). These structurally diverse products were evaluated as antitubercular agents with MIC values ranging from low to high micromolar activity against mycobacterium tuberculosis strain Mtb H37Rv.[82]

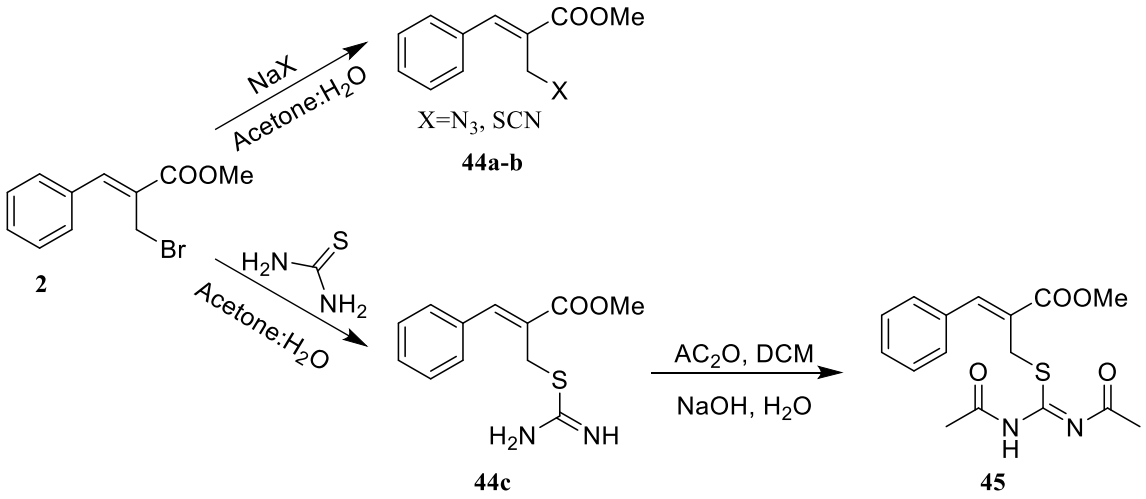

Scheme 1.18: Synthesis of allylic azides, thiocyanates, isothiouronium salts from BH bromide **2**.

We envision the utilization of BH bromides **1** and **2** to develop novel DNA based alkylators because of their versatility as electrophiles and nucleophiles, and their ability

to accept nucleophiles in S_N2, S_N2', and 1,4 addition fashion. The reactivity of bromides **1** and **2** to act as electrophiles for potential interaction with cellular components form the basis for the current thesis.

Results and Discussion

As described in the introduction, the BH bromides **1** and **2** (**Figure 2.1**) have been extensively utilized as nucleophiles in metal mediated Barbier type allylations and also as electrophiles for C, N, O and S alkylations for the synthesis of a wide variety of structurally and biologically interesting small molecules (**Figure 1.15 introduction**).[1-24] Mereddy's group has also been working on the utilization of BH bromides **1**, **2,** and **3** as nucleophiles and also as electrophiles for the synthesis of medicinally important small molecules (**Figure 2.1**).[25-27]

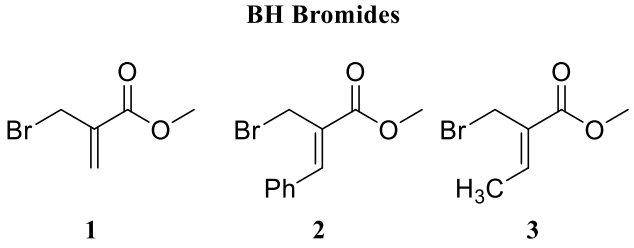

Figure 2.1: Baylis-Hillman (BH) bromides

Using BH bromides **1** and **3** as nucleophiles, Mereddy *et al.* carried out Zn based Barbier allylations on *o*-formyl phenyl boronic acids to synthesize functionalized benzoxaboroles **4** and **5** as potential antimicrobial agents.[25] The reaction took place in a highly diasteroselective (*syn*) manner with BH bromide **3** to obtain diastereometrically pure compound **5** (**Scheme 2.1**).

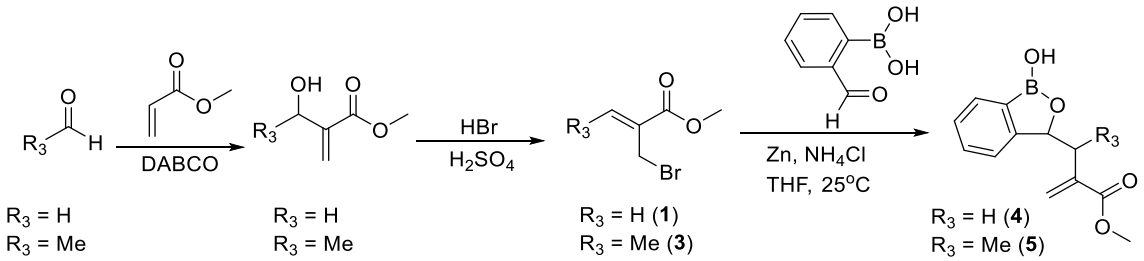

Scheme 2.1: Synthesis of functionalized benzoxaboroles from BH bromides.

BH bromides **1** and **3** was also utilized as electrophiles for the synthesis of α-methylene-β-substituted-γ-carboxy-γ-lactams. Here, the nucleophiles generated from α-amino ester based imines attacked the BH bromides **1** and **3** in S_N2' fashion to provide the functionalized pyroglutamates in a single step and in highly diastereoselctive fashion (**Scheme 2.2**). This methodology was applied for the synthesis of fused [3.2.0.] heterobicyclic γ-lactam-β-lactones and γ-lactam-γ-lactones (**Scheme 2.3**).[26]

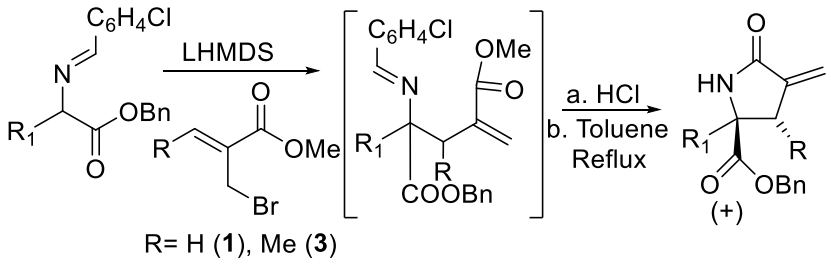

Scheme 2.2: Synthesis of α-methylene-β-substituted-γ-carboxy-γ-lactams

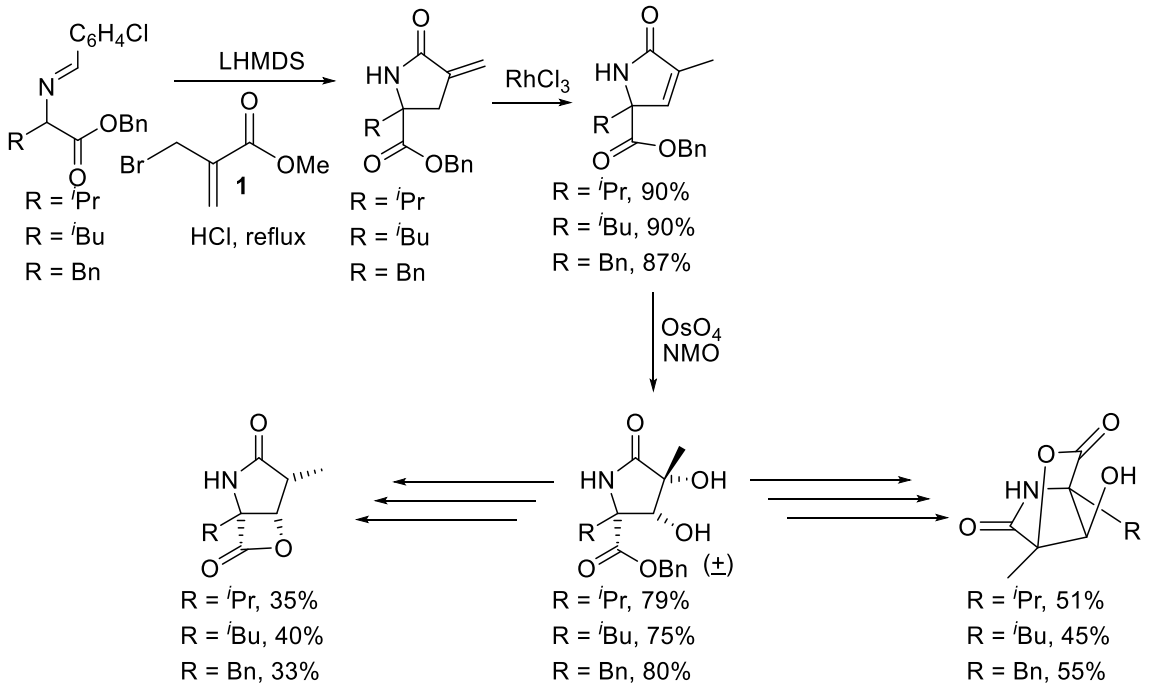

Scheme 2.3: Synthesis of fused [3.2.0.] heterobicyclic γ-lactam-β-lactones and γ-lactam-γ-lactones.

More recently, Mereddy's group exploited the S_N2/S_N2' nature of BH bromides **1** and **2** for the synthesis of quaternary ammonium curcuminoids as potential anticancer agents. The curcuminoids generated from piperizinyl benzaldehydes were treated with BH bromides **1** and **2** to provide quaternary ammonium curcuminoids **6** and **7** (**Scheme 2.4**). All the synthesized compounds were found to be highly water soluble and the BH derived quaternary ammonium salts acted as leaving groups and interacted as electrophiles with nucleophilic cellular components in S_N2/S_N2' fashion to provide moderate to good cell proliferation inhibition properties.[27] Further biological studies of these compounds revealed that they were well tolerated in healthy mice and good tumor growth inhibition properties were observed in a pancreatic cancer tumor model in athymic nude mice (**Figure 2.2** and **2.3**).

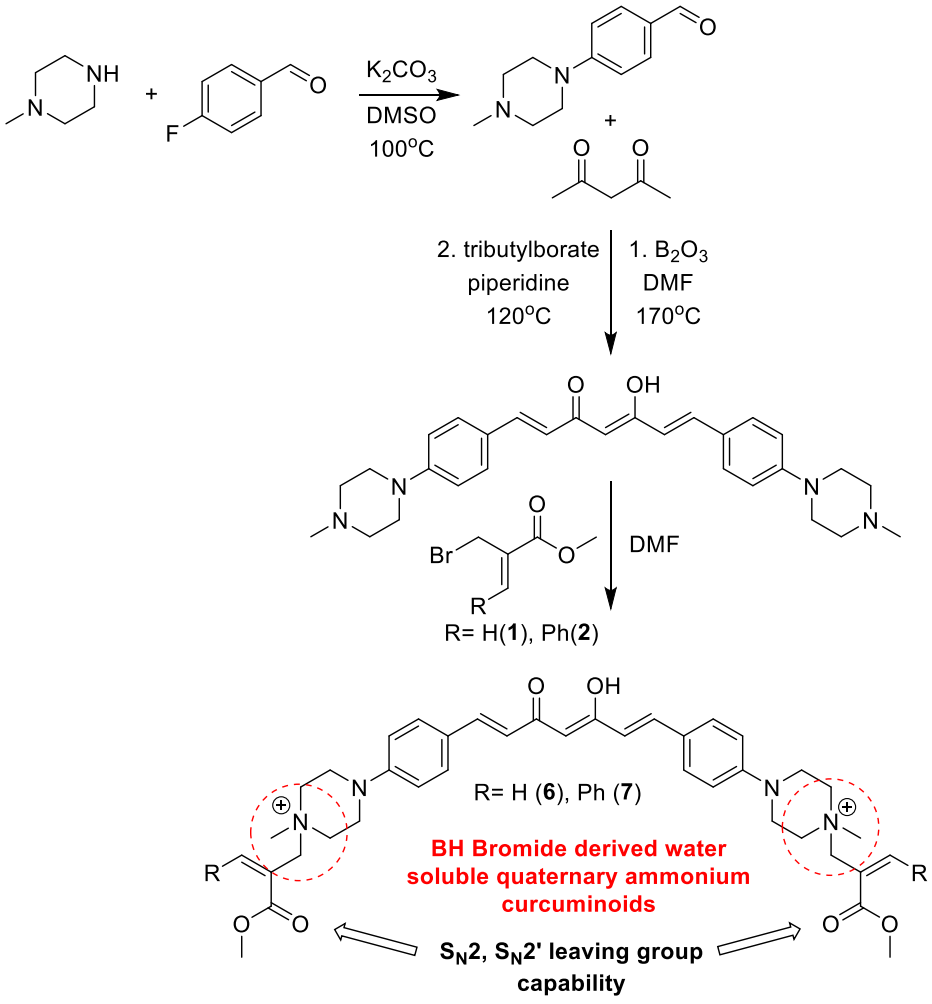

Scheme 2.4: Synthesis of BH bromide derived water soluble quaternary ammonium curcuminoids.

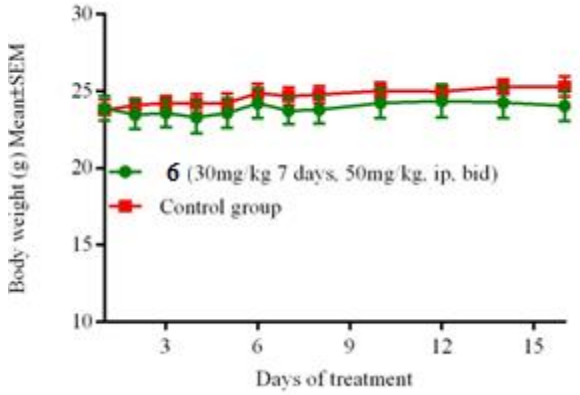

Figure 2.2: *In vivo* Systemic toxicity study of BH derived curcuminoid **6** in healthy CD-1 mice.

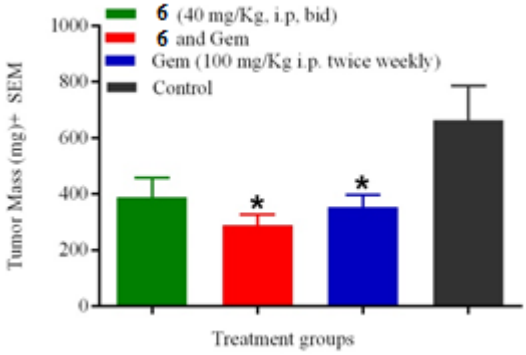

Figure 2.3: In vivo anticancer efficacy study of BH derived curcuminoid **6** in a MIAPaCa-2 xenograft model in athymic nude mice.

Fascinated by the highly electrophilic nature of BH bromides **1** and **2**, we sought to explore the potential of these bromides as alkylators of DNA and other nucleophilic cellular components for anticancer applications. *In vitro* cell proliferation inhibition studies of the bromides **1** and **2** against several cancer cell lines (MDA-MB-231, 4T1, MIAPaCa-2) using MTT assay indicated that these compounds exhibited moderate to good potency against all the cell lines tested. However, these compounds were found to be chemically not stable enough at room

temperature to be developed as potential anticancer agents. We also reasoned that the presence of very reactive allylic bromide system would be reactive with high metabolic vulnerability and this could potentially cause several side effects. In the present work, we envisaged to synthesize less reactive and more stable 2-(alkoxycarbonyl)-allyl esters from carboxylic acids and BH bromides to increase chemical and metabolic stability, and retain the intriguing S_N2, S_N2', and 1,4 addition capabilities for interaction with nucleophilic cellular components (**Schemes 2.5** and **2.6**). In these cases, the carboxylic acid group will act as a leaving group for either S_N2 or S_N2' interactions with nucleophiles.

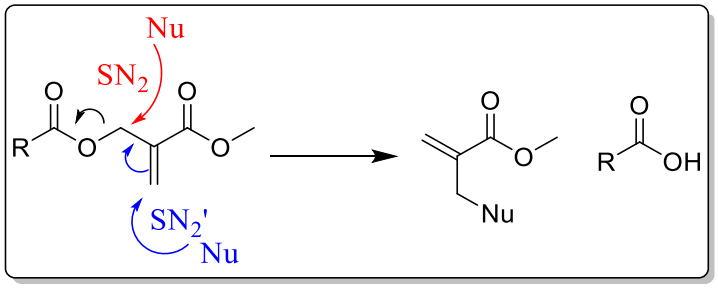

Scheme 2.5: S_N2/S_N2' capabilities of 2-(alkoxycarbonyl)-allyl esters.

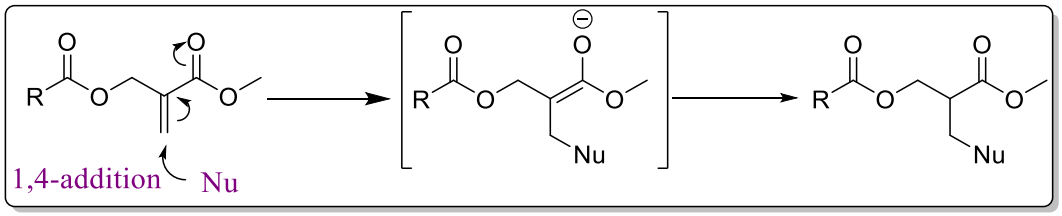

Scheme 2.6: 1,4-addition capability of 2-(alkoxycarbonyl)-allyl esters.

The 2-(alkoxycarbonyl)-allyl ester template provides high structural tunability and we envisioned three reactive sites for structural variations to improve the biological activity, targeted delivery to the reactive site, metabolic stability, water solubility, and other pharmaceutical and pharmacological properties. For example, attaching hydroxyethylpiperizine unit or a sugar unit at reactive carboxylic ester site should lead to high water solubility and reduce the metabolic

vulnerability of ester hydrolysis by plasma esterases. We can also attach some of the endogeneous molecules and metabolites such as cholesterol, amino acids, folic acid, α-tocopherol, fatty acids etc. This should lead to more targeted delivery to the tumor site due to the elevated requirement of these biosynthetic starting materials and cofactors for rapid cell proliferation of cancer cells (**Figure 2.4**).

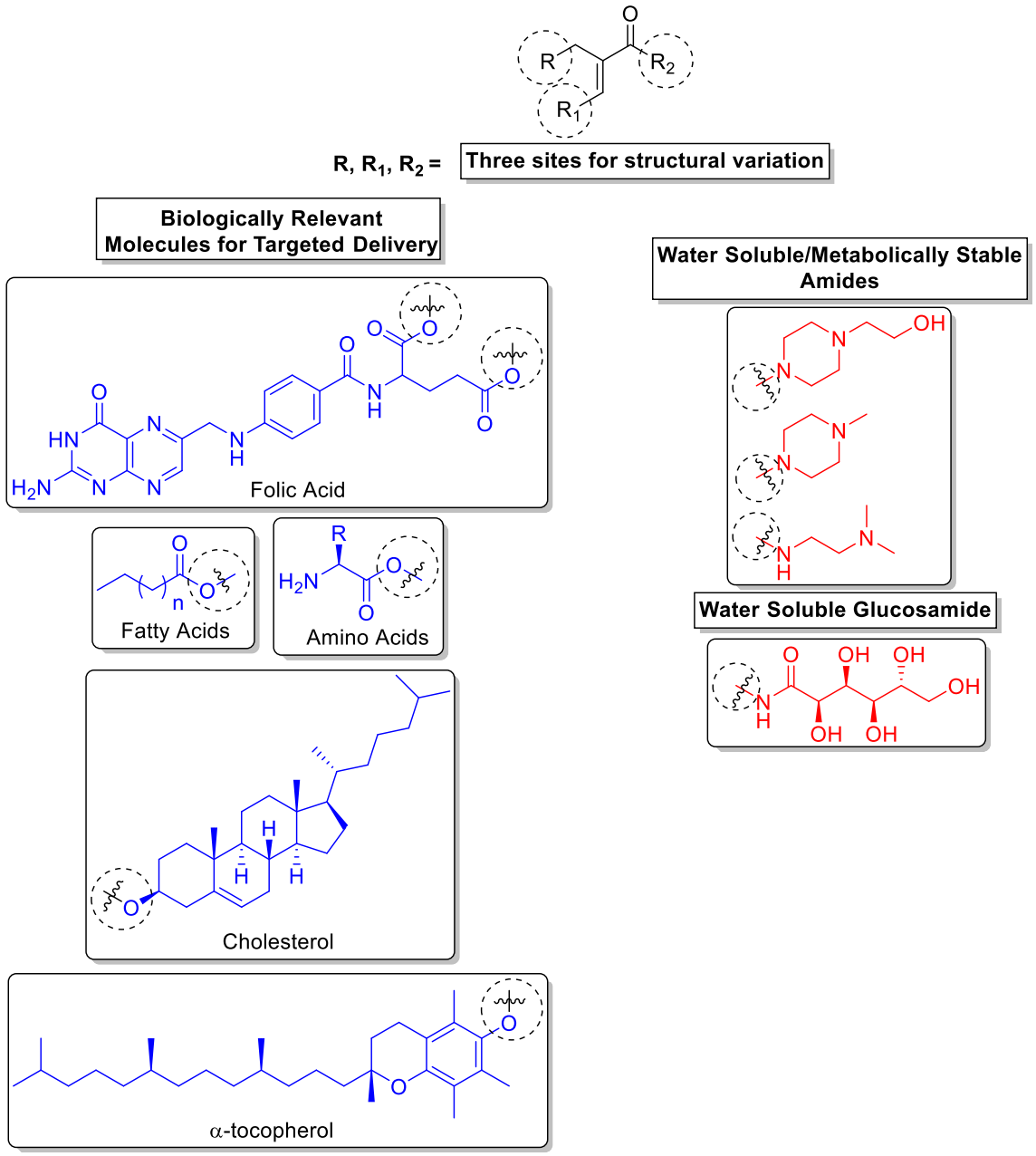

Figure 2.4: Structural tunability and potential of 2-(alkoxycarbonyl)-allyl template for improving water solubility, metabolic stability, and targeted delivery.

To test this hypothesis we first synthesized and evaluated the cancer cell proliferation inhibition properties of 2-(methoxycarbonyl)-allyl benzoate **8**. The required BH bromide **1** for the preparation of **8** was synthesized in two steps by BH reaction of formaldehyde and methyl acrylate in the presence of DABCO, and bromination of the resulting alcohol in HBr/H_2SO_4. The crude bromide was vacuum distilled to obtain the pure BH bromide **1**. The 2-(methoxycarbonyl)-

allyl benzoate **8** was synthesized by treating benzoic acid with BH bromide **1** in the presence of sodium carbonate in DMSO (**Scheme 2.7**). The crude product was extracted with ether and water, and the pure product was obtained upon purification with silica gel column chromatography with ethyl acetate:hexanes (2%:98%). Allyl benzoate **8** has excellent room temperature stability as evidenced by no observable decomposition at room temperature for one month according to ^{1}H NMR.

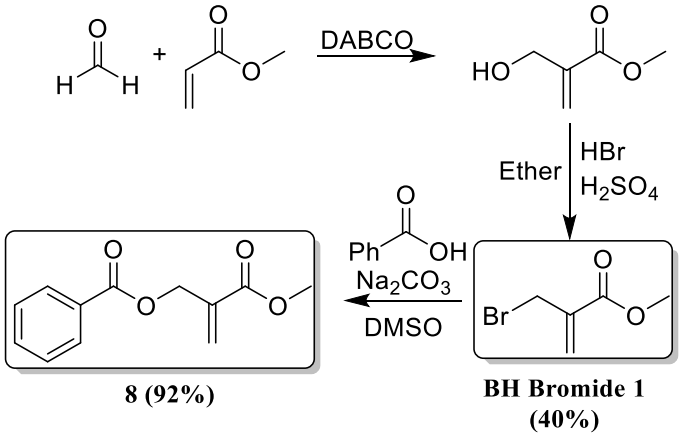

Scheme 2.7: Synthesis of 2-(methoxycarbonyl)-allyl benzoate.

Satisfied with the chemical stability, we then evaluated the *in vitro* cell proliferation inhibition on difficult to treat human triple-negative breast cancer cell line MDA-MB-231, murine metastatic breast cancer 4T1, and human pancreatic cancer cell line MIAPaCa-2 by utilizing the 3-(4,5-dimethylthiazol-2-yl)-2,5-diphenyltetrazolium bromide (MTT) cell viability assay. Cells cultured in 96-well plates were incubated with the test compounds for 72 h, and MTT values were expressed as percent of vehicle-only (control) wells. The IC_{50} value was calculated for each compound as the dose required to suppress the MTT signal to 50% of control values. Gratifyingly, compound **8** retained a comparable or higher biological potency to the parent bromo-congener **1** (**Figure 2.5**).

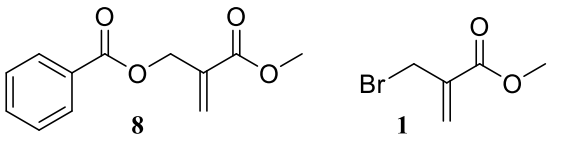

8

MDA-231: **12±1**
4T1: **19±2**
MIAPaCa-2: **34±5**

1

MDA-231: **39±6**
4T1: **22±1**
MIAPaCa-2: **12±1**

Figure 2.5: Cell proliferation inhibition (IC_{50}) values of **8** and **1** in micomolar concentration.

This encouraging biological activity and chemical stability led us to carry out a detailed structure activity relationship study (SAR) of 2-(alkoxycarbonyl)-allyl esters from various carboxylic acids and BH bromides. First, we utilized formaldehyde BH bromide **1** and reacted with various substituted aromatic carboxylic acids. Electron donating derived 2-(alkoxycarbonyl)-allyl ester examples included 4-*N*,*N*-dimethyl (**9**), 4-methoxy (**10**), 3,4,5-trimethoxy (**11**), and piperonyl (**12**) benzoic acid esters, and electron withdrawing examples included 4-nitro (**13**) and 4-cyano (**14**) carboxylic acid esters (**Scheme 2.8** and **2.9**). The corresponding product 2-(alkoxycarbonyl)-allyl esters were efficiently synthesized from the respective carboxylic acids and BH bromide **1** under basic conditions and purified via silica gel column chromatography in good to excellent yields (**Scheme 2.8** and **2.9**).

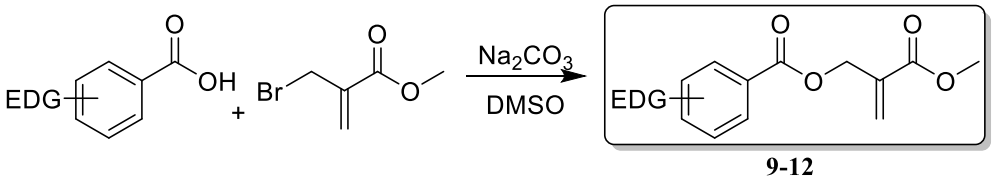

9-12

EDG= *N,N*-Dimethyl (**9,** 88%), 4-methoxy (**10,** 91%), 3,4,5-trimethoxy (**11,** 89%), piperonyl (**12,** 95%)

Scheme 2.8: Synthesis of 2-(alkoxycarbonyl)-allyl esters derived from EDG substituted benzoic acids.

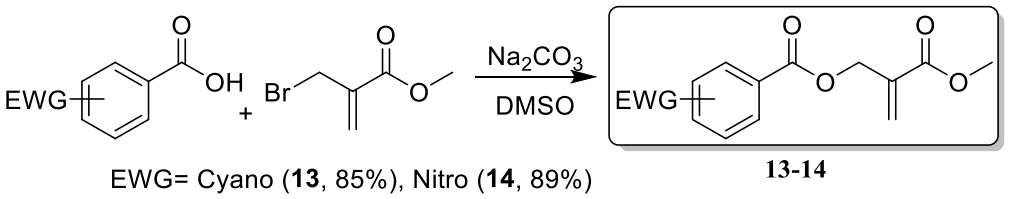

Scheme 2.9: Synthesis of 2-(alkoxycarbonyl)-allyl esters derived from EDG substituted benzoic acids.

We then carried out cell proliferation inhibition studies (MTT assay) on compounds **9-14** and found that both electron donating and electron withdrawing substituents on 2-(alkoxycarbonyl)-allyl esters **9-14** exhibited similar potency against all three cell lines (**Figure 2.6**).

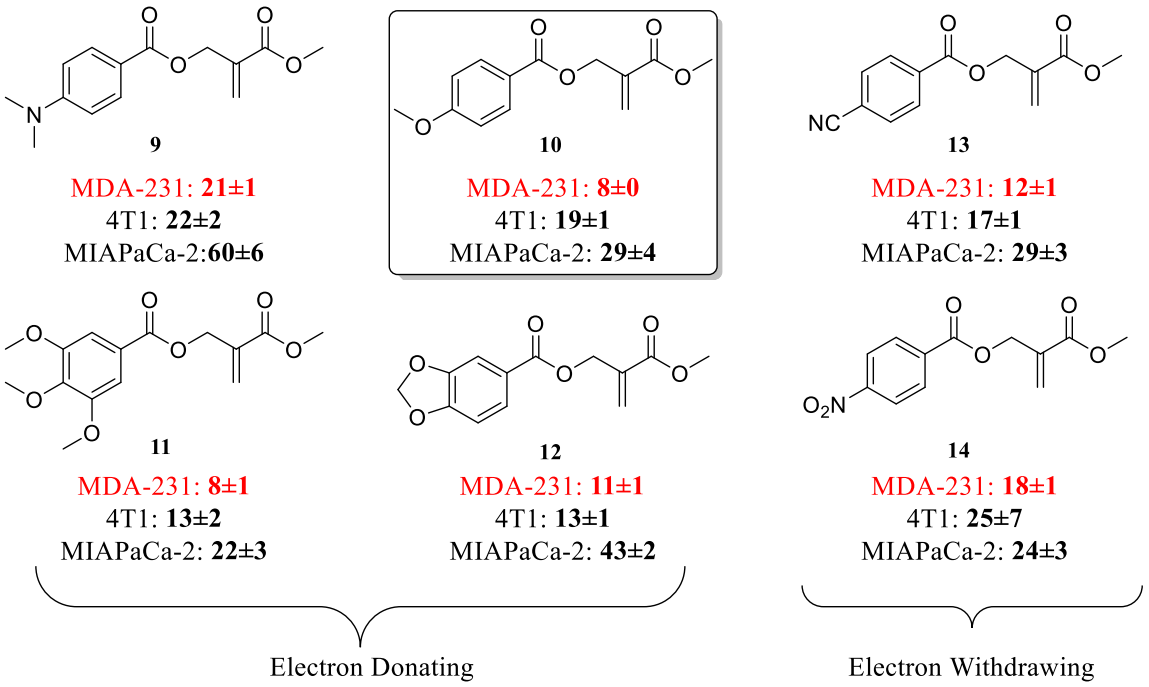

Figure 2.6: Cell proliferation inhibition (IC_{50}) values of **9-14** in micomolar concentration.

To further understand the SAR of the α-carboxy allyl ester unit, we took unsubstituted benzoic acid as a representative example. First, to understand the importance of the carboxy ester

group in providing biological activity, we synthesized simple allyl benzoate **15**. Compound **15** was readily obtained by treating sodium salt of benzoic acid with allyl bromide followed by purification by silica gel column chromatography (**Scheme 2.10**).

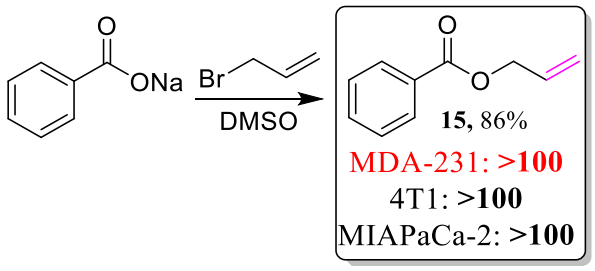

Scheme 2.10: Synthesis of allyl benzoate.

This compound is not capable of 1,4 addition and simple benzoate is a poor leaving group for S_N2 and S_N2' reactions in the absence of α-carboxy carbonyl group. As expected, compound **15** did not retain any biological activity even at 100μM concentration. This clearly exhibits the importance of the α-carboxy carbonyl group in providing S_N2/S_N2' capability for interaction with cellular components to provide biological activity. We then modified the alkoxy group in ester by replacing methyl with ethyl and butyl substituents. The corresponding BH bromides **16** and **17** were synthesized by performing BH reaction of ethyl and butyl acrylates with formaldehyde in the presence of DABCO, followed by bromination using HBr/H_2SO_4 to give corresponding BH bromides **16** and **17** (**Scheme 2.11**). The pure **16** and **17** were obtained via silica gel column chromatography using hexane as the elutant. The reaction of benzoic acid with BH bromides **16** and **17** under basic conditions followed by silica gel column chromatography gave the corresponding 2-(ethoxy/butoxycarbonyl)-allyl esters **18** and **19** respectively in good yield (**Scheme 2.11**).

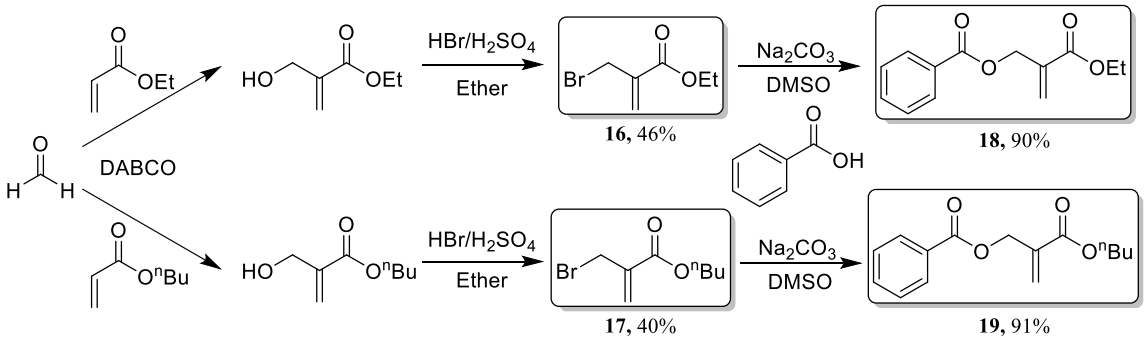

Scheme 2.11: Synthesis of 2-(ethoxy/butoxycarbonyl)-allyl esters **18** and **19**.

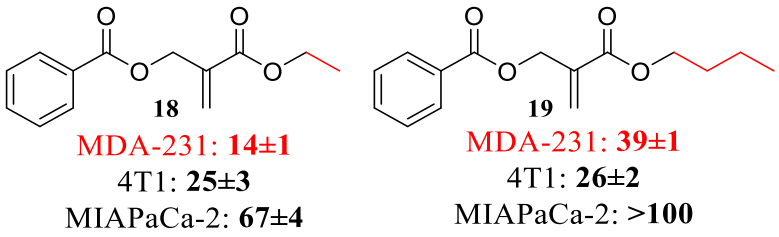

Figure 2.7: Cell proliferation inhibition (IC_{50}) values of **18** and **19** in micomolar concentration.

Cell proliferation inhibition studies of **18** and **19** did not lead to any enhanced activity, and the methyl substituent was found to be the optimal structural moiety for biological activity (**Figure 2.7**). Next, we sought to explore the importance of the double bond of 2-(alkoxycarbonyl)-allyl esters, since our hypothesis involved the reaction of nucleophilic cellular components in an S_N2' and/or 1,4 addition fashion for which the double bond was a critical component. Hence, we saturated the double bond in **8** by dihydroxylation using osmium tetroxide/NMO conditions to provide the corresponding diol **20** (**Scheme 2.12**).

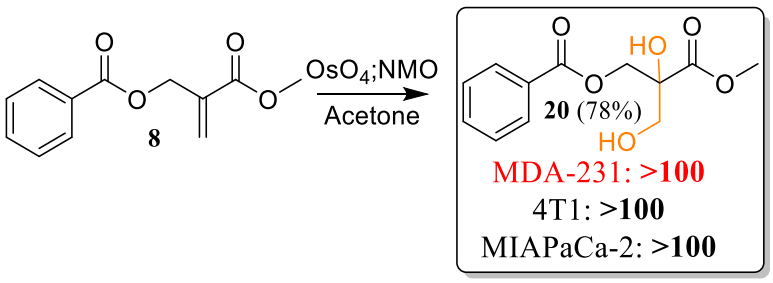

Scheme 2.12: Synthesis and cell proliferation inhibition (IC_{50}) values of **20** in micomolar concentration.

As anticipated, diol **20** did not retain any biological activity, illustrating the importance of the carboxycarbonyl double bond in its interaction with nucleophilic cellular components and subsequent S_N2, S_N2' and/or 1,4 addition for providing biological reactivity. We further investigated the SAR of 2-(alkoxycarbonyl)-allyl ester template by introducing β-substitution on double bond by placing a phenyl group. The required β-phenyl substituted derivative **22** was synthesized from benzoic acid and methyl (Z)-2-(bromomethyl)-3-phenylacrylate, BH bromide **2**. The corresponding BH bromide **2** was prepared by BH reaction of benzaldehyde with methyl acrylate in the presence of DABCO for one week. Crude allyl alcohol **21** was extracted with ethyl acetate and water and purified using silica gel column chromatography with ethyl acetate:hexanes (10%:90%) as the elutant. The allyl alcohol **21** was further brominated with HBr/H_2SO_4, and extracted with ether and water. The crude product was then purified via silica gel column chromatography using hexanes as elutant to obtain methyl (Z)-2-(bromomethyl)-3-phenylacrylate **2**. BH bromide **2** was then reacted with benzoic acid in the presence of Na_2CO_3 in DMSO and purified via silica gel column chromatography to obtain the β-substituted 2-(alkoxycarbonyl)-allyl ester **22** (**Scheme 2.13**). β-substitution resulted in a decrease in biological activity when compared to β-unsubstituted compound **8** (**Figure 2.8**).

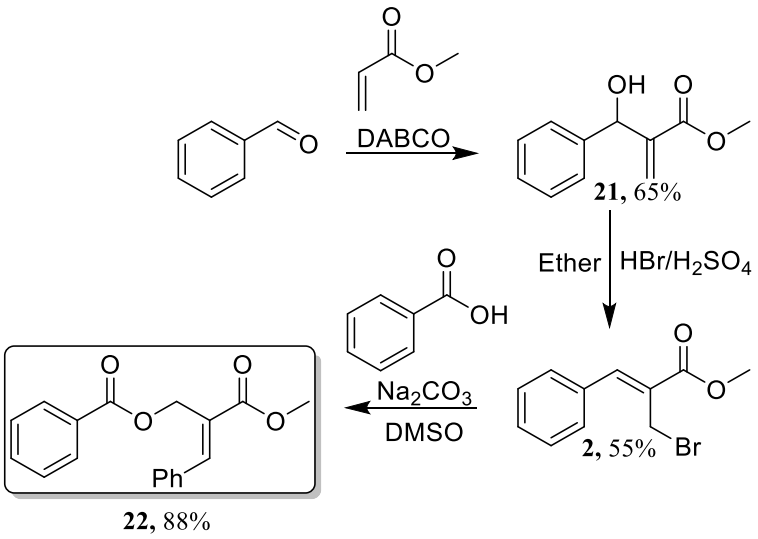

Scheme 2.13: Synthesis of β-substituted 2-(alkoxycarbonyl)-allyl ester **22**.

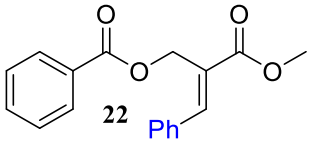

MDA-231: **18±1**
4T1: **30±4**
MIAPaCa-2: **>100**

Figure 2.8: Cell proliferation inhibition (IC_{50}) values of **22** in micomolar concentration

We then explored the SAR of expanded aromaticity of the carboxylic acid component by utilizing naphthalene and anthracene carboxylic acids. Reaction of 1-napthoic acid and 9-antharcenecarboxylic acid with BH bromide **1** under basic conditions efficiently provided corresponding 2-(alkoxycarbonyl)-allyl esters **23** and **24** in good yields (**Scheme 2.14**). Biological evaluation resulted in a decreased potency when compared to the monocyclic benzoic acid derivatives **8-14** (**Figure 2.9**).

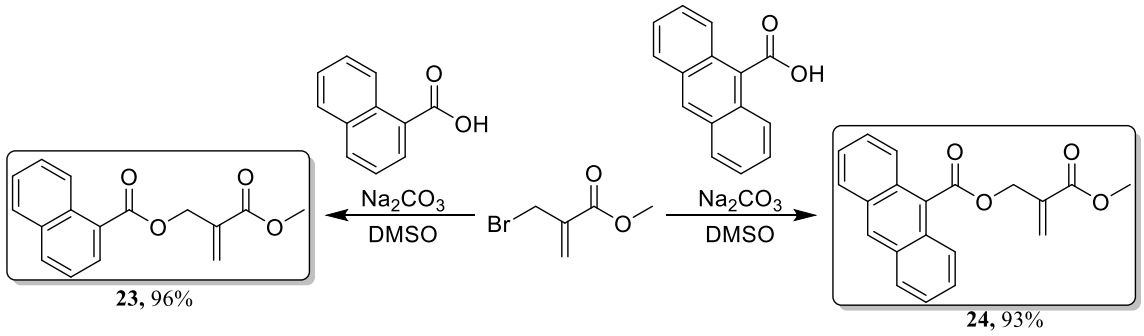

Scheme 2.14: Synthesis of 2-(alkoxycarbonyl)-allyl esters **23** and **24** from naphthalene and anthracene carboxylic acids.

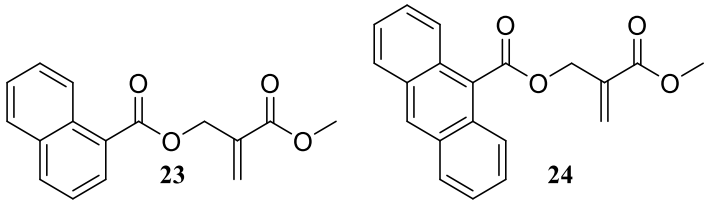

MDA-231: **29±2**
4T1: **43±12**
MIAPaCa-2: **73±8**

MDA-231: **30±4**
4T1: **23±3**
MIAPaCa-2: **73±3**

Figure 2.9: Cell proliferation inhibition (IC_{50}) values of **23** and **24** in micomolar concentration.

Structurally modified alkyl and alkenyl 2-(alkoxycarbonyl)-allyl esters **25** and **26** derived from cinnamic acid and 4-phenylbutyric acid were also synthesized to evaluate the effect alkyl and alkenyl spacers on biological activity. The required alkoxycarbonyl-allyl esters **25** and **26** were synthesized by treating cinnamic acid and 4-phenyl butyric acid with BH bromide **1** under basic conditions and purified via silica gel column chromatography to obtain **25** and **26** (**Scheme 2.15**).

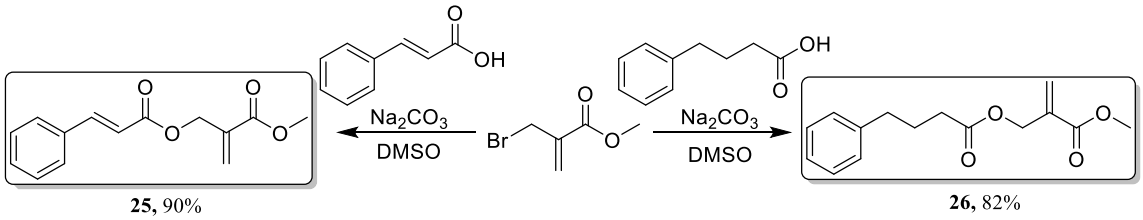

Scheme 2.15: Synthesis of 2-(alkoxycarbonyl)-allyl ester **25** and **26** from cinnamic and 4-phenyl butyric carboxylic acids.

Biological evaluation of **25** and **26** did not lead to decreased potency, illustrating the importance of aromatic carboxylic acid derived 2-(alkoxycarbonyl)-allyl esters for optimal biological activity (**Figure 2.10**).

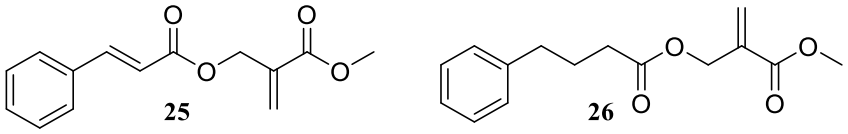

25

MDA-231:**41±4**
4T1:**36±4**
MIAPaCa-2:**64±4**

26

MDA-231: **45±1**
4T1: **52±2**
MIAPaCa-2: **>100**

Figure 2.10: Cell proliferation inhibition (IC_{50}) values of **25** and **26** in micomolar concentration.

To increase the functionalization, we utilized di- and tri-carboxylic acids to synthesize di- and tri-functionalized 2-(alkoxycarbonyl)-allyl esters. In this regard, derivatives **27-29** were synthesized using terephthalic acid, 2,6-pyridinedicarxoxylic acid, and trimesic acid respectively. These products **27-29** were conveniently synthesized by the reaction of stoichiometric equivalents BH bromide **1** with respective carboxylic acids **27-29** in the presence of Na_2CO_3 in DMSO, and were purified via silica gel column chromatography (**Scheme 2.16**).

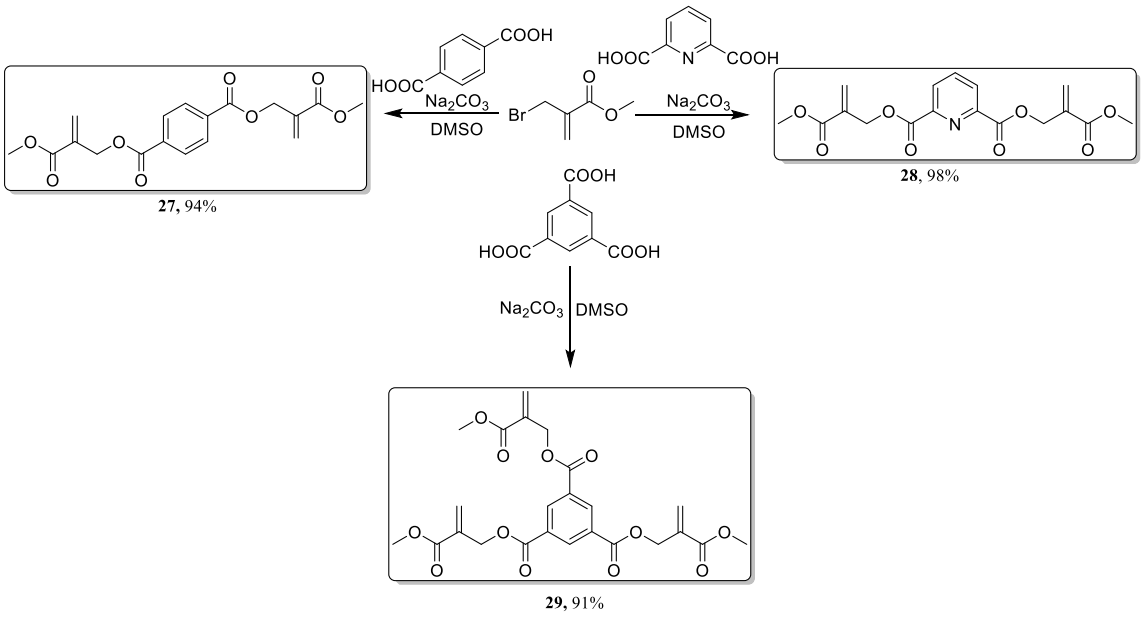

Scheme 2.16: Synthesis of 2-(alkoxycarbonyl)-allyl ester **27**, **28**, and **29** from terepthalic acid, 2,6-pyridinedicarboxylic acid, and trimesic acid.

Biological evaluation resulted in significantly enhanced cell proliferation inhibition properties when compared to the monoesters of aromatic carboxylic acids (**Figure 2.11**). For example, pyridine dicarboxylic acid derived 2-(alkoxycarbonyl)-allyl ester **28** exhibited cell proliferation inhibition IC_{50} values in the 3-6μM range when compared to mono allyl ester of benzoic acid derived **8** with IC_{50} values ranging from 12-35μM.

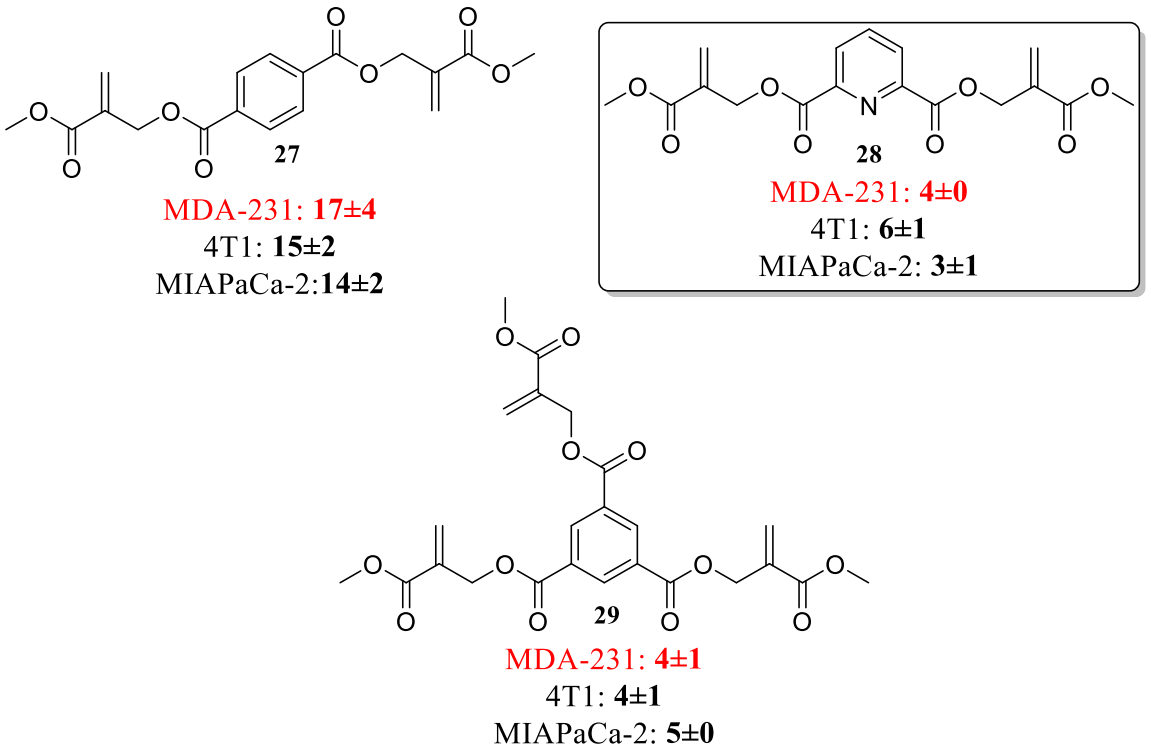

Figure 2.11: Cell proliferation inhibition (IC_{50}) values of **27**, **28**, and **29** in micomolar concentration.

To further expand the application of activity enhancing 2-(alkoxycarbonyl)-allyl esters, we employed clinically used chemotherapeutic agent chlorambucil **30** as a representative example. Chlorambucil is clinically utilized to treat chronic lymphatic leukemia, Hodgkin's disease, and other types of lymphomas.[28-30] Although chlorambucil has good activity against leukemia's and lymphomas, it does not exhibit any appreciable efficacy against solid tumor cell lines. For example, chlorambucil does not exhibit any cell proliferation inhibition properties up to 100μM against MDA-MB-231, 4T1, or MIAPaCa-2 cell lines. Reaction of chlorambucil carboxylic acid **30** with BH bromide **1** under basic conditions efficiently afforded compound **31**. Compound **31** showed enhanced biological activity when compared to parent chlorambucil **30**, with IC_{50} values in the range of 49-83μM against all three cell lines (**Figure 2.12**).

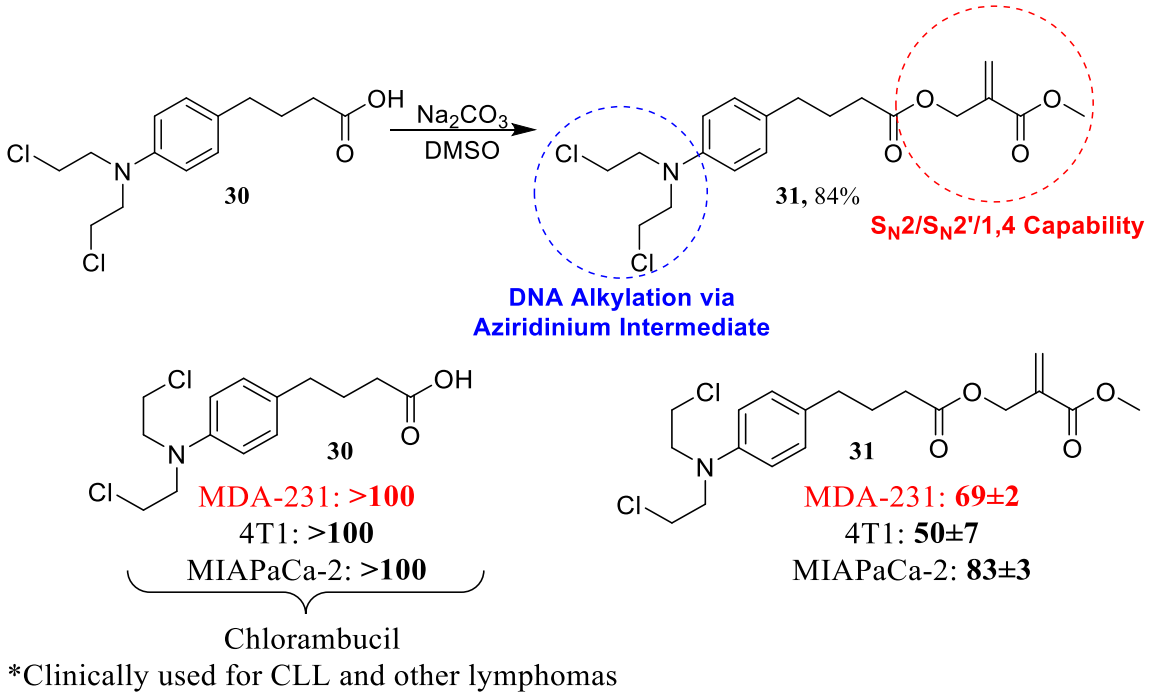

Figure 2.12: Synthesis and cell proliferation inhibition (IC_{50}) values of chlorambucil **30**, and compound **31** in micomolar concentration.

The chlorambucil alkoxy allyl ester **31** is highly interesting because it has dual reaction sites for interaction with cellular DNA with nitrogen mustard unit via aziridinium intermediate, and alkoxyester as $S_N2/S_N2'/1,4$ addition structural subunit (**Figure 2.12**).

It is interesting to note that parent BH alcohol **21** did not show any appreciable biological activity, but the corresponding acetate **32** derived from alcohol **21** and benzoyl chloride resulted in cell proliferation inhibition properties albeit at lower concentrations than the lead 2-(alkoxycarbonyl)-allyl esters. The biological activity of BH acetate **32** could be attributed to the leaving group capacity of allyl benzoate in the presence of cellular nucleophiles (**Figure 2.13**).

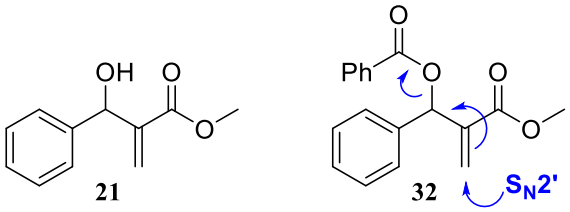

MDA-231:**>100**
4T1:**>100**
MIAPaCa-2:**75±9**

MDA-231:**41±4**
4T1:**36±4**
MIAPaCa-2:**64±4**

Figure 2.13: Cell proliferation inhibition (IC_{50}) values of **21** and **32** in micomolar concentration.

From these results, compounds **10** and **28** derived from 4-methoxybenzoic acid and 2,6-pyridine dicarboxylic acid were designated as lead compounds based on their potency in cell proliferation inhibition and mono-and di-functionalization. Further mechanistic studies of these two compounds were performed, starting first with the effect of compound treatment on cellular morphology based on phase contrast microscopy. MDA-MB-231 cells were plated on culture plates and exposed to compound **10** and **28** for 6 and 48 hours at concentrations equal to 1X, 2X, and 4X their IC_{50} values for cell proliferation inhibition; equating to 8, 16, and 32μM for compound **10**, and 4, 8, and 16μM for compound **28**, respectively. For both compounds, the 1X IC_{50} concentrations led to little to no morphological effects at either time point. However, for compound **10** cell rounding became evident at the 2X and 4X concentration after 6 hours of treatment which progressed to cell detachment and clustering after 48 hours (Figure 14). For compound **28**, noticeable cell rounding after 6 hours was apparent at the 4X concentration, which also advanced to clustering at the 48 hour time point (**Figure 2.14**). It was previously reported that rounding and clustering of cells were observed due to damage of cell integrins, cytoskeletal elements, and cadherins when treated with well characterized alkylating agents.[31]

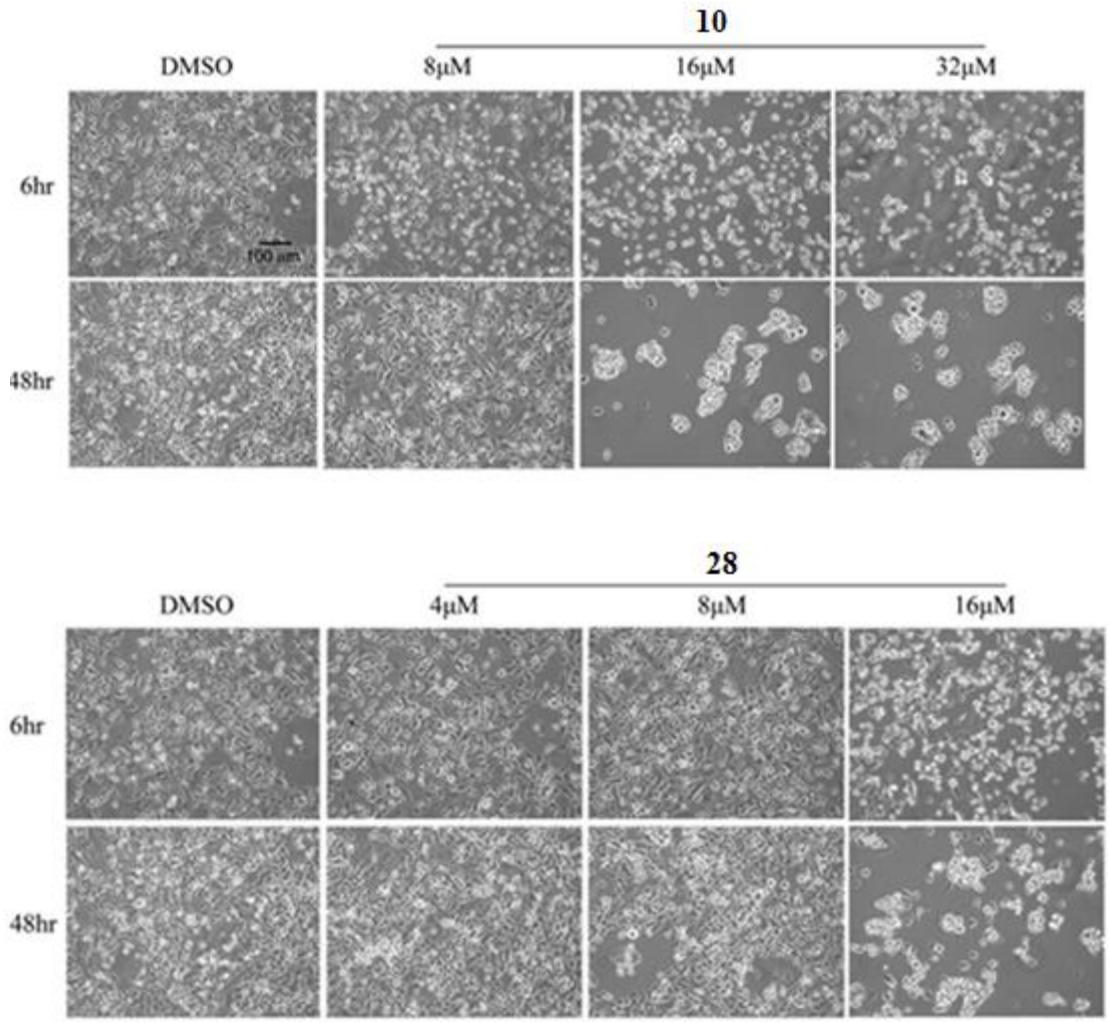

Figure 2.14: Phase contrast imaging of MDA-MB-231 cells after treatment with differing concentrations of compound **10** and **28**. All images were captured using the same magnification (see scale bar). Note cell rounding at the higher compound concentrations.

The make-up of DNA includes nucleophilic components that render the bio-macromolecule highly susceptible to alkylation by electrophilic agents. Such agents can react with nucleophilic ring nitrogens or exocyclic oxygens to produce a wide variety of DNA-adducts.[32] Both mono- and bifunctional alkylating agents can result in numerous complex cellular effects including DNA-strand breaks, cell cycle arrest and/or perturbation, and programmed cell death pathways.[33-34]

Due to the electrophilic nature of compounds **10** and **28**, the morphological effect of nuclear organization and cell cycle regulation were examined via immunofluorescent microscopy. MDA-MB-231 cells were plated on cover slips and treated with compound **10** and **28** at their IC_{50} value of cell proliferation inhibition. Cells were then fixed with 2% paraformaldehyde, and then labeled with Hochest dye to label nuclei. In some cases, cells were pulsed with bromodeoxyuridine (BrdU) to examine actively replicating nuclei of cells in S-phase. In control cultures, most nuclei exhibited a normal organized appearance, with a few nuclei exhibiting small micro nuclei. MDA-MB-231 exhibits a high level of genomic instability, and as a result has a small level of irregular nuclear bodies. In contrast, treatment with compound **28** for 24 hours resulted in a high percentage of nuclei exhibiting a large level of irregular nuclear bodies and micronucleation indicative of karyorrhexis (**Figure 2.15**). Compound **10** led to a more modest effect (data not shown). Well characterized and clinically used alkylating agents such as cisplatin, carboplatin, ifosfamide, carboplatin, thiotepa, and N-methyl-N-nitrosourea have also been shown to induce such nuclear fragmentation in numerous cell types.[34-35]

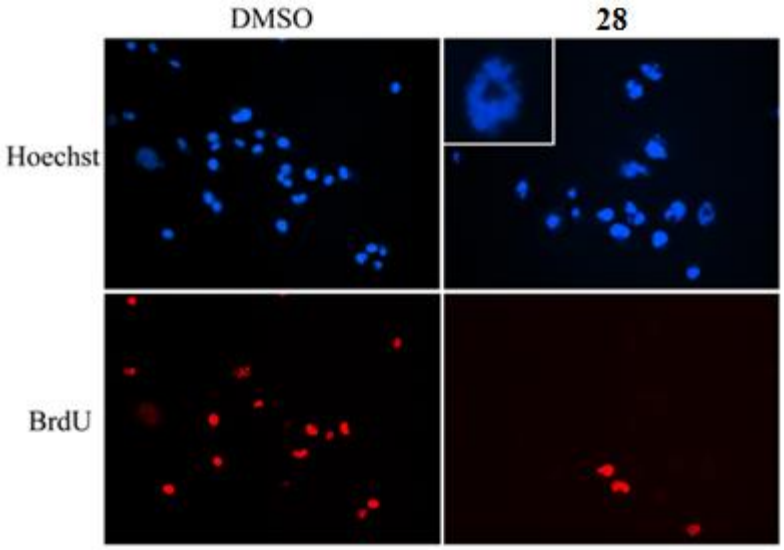

Figure 2.15: MDA-MB-231 cells treated with vehicle (DMSO) or compound **28** for 24 h, and subsequently pulsed with BrdU to identify replicating (S-phase) cells, and counterstained with Hoechst dye to label all nuclei. Hoechst fluorescence is shown in blue, and BrdU antibody

labeling is shown in red. Inset: higher magnification of fragmented nuclear bodies indicative of karyorrhexis in a cell treated with **28**.

Next, we sought to further understand the effect of compounds **10** and **28** on the molecular level by employing western blotting techniques. A widely used and established indication of DNA damage and repair pathway activation is histone H2AX phosphorylation, forming γ-H2AX. Histone H2AX plays major roles in the cells response to DNA damage, and is usually activated upon DNA single and double strand breaks.[36-37] The ability of compounds **10** and **28** to induce H2AX phosphorylation was evaluated by utilizing a phospho-specific antibody. MDA-MB-231 cells were treated with compound **10** and **28** for 6 hours at 1X, 2X and 4X their respective IC_{50} of cell proliferation inhibition and cells were harvested. Subsequently, the harvested cells were blotted for γ-H2AX using a phospho-specific antibody. High levels of genomic instability observed in MDA-MB-231 cells lead to a high level of intrinsic DNA damage, and hence a high level of H2AX phosphorylation. There was a clear increase in the γ-H2AX signal at the high end concentrations. Interestingly, the signal is comparable to that observed in MDA-MB-231 cells treated with well characterized alkylating agent mitomycin c (MC) (**Figure 2.16**).

Another important molecular response to DNA damage repair is the employment of enzyme poly (ADP-ribose) polymerase (PARP). Upon DNA damage, PARP is upregulated and recruited to the sites of damage and further initiates the DNA repair process.[38] Hence, PARP is activated by DNA alkylating agents. Depending on the extent of DNA damage, PARP activation can be followed by cell death pathways such as apoptosis or necrosis, and upon apoptosis activation, PARP is an early target for caspase induced cleavage.[39] In fact, cleavage of full length PARP is often used as an indication of caspase activation in apoptosis. Western blotting indicates an initial activation of PARP at low end concentrations of compound **10** and **28** at a similar extent as MC, followed by a decrease in the PARP signal at higher concentrations of **10** and **28**. These

results suggest initial activation upon alkylator induced DNA damage, followed by the activation of apoptosis at higher drug concentrations (**Figure 2.16**).

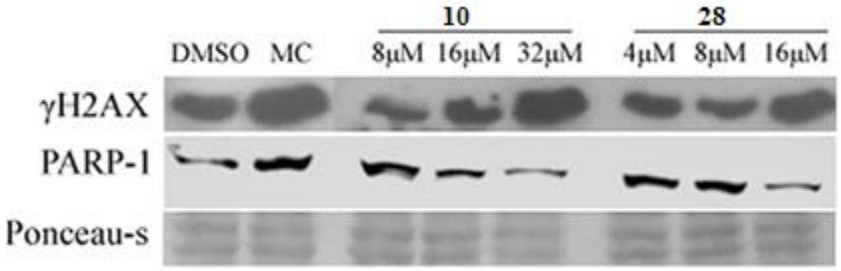

Figure 2.16: Western blot analysis of MDA-MB-231 whole cell lysates treated with differing concentrations of compounds **10**, **28**, DMSO (vehicle control) or Mitomycin C (MC) as an example of a well-characterized alkylating compound. γ-H2AX was probed after six hours whereas PARP-1 was probed after 48 h of treatment with **10** or **28.**

Cell cycle effects of compounds **10** and **28** were examined using BrdU uptake experiments and cyclin D1 expression changes. Cyclin D1 is an important regulating enzyme, and governs the cells G1 to S transition. Proteolytic degradation of cyclin D1 is an important mechanism of cell cycle regulation and hence, the quantity of the enzyme fluctuates throughout different phases of the cell cycle.[40-41] Western blotting indicated an initial increase in the expression of cyclin D1 at low to intermediate concentrations of **10** and **28**, followed by a decrease at higher concentrations (**Figure 2.17**).

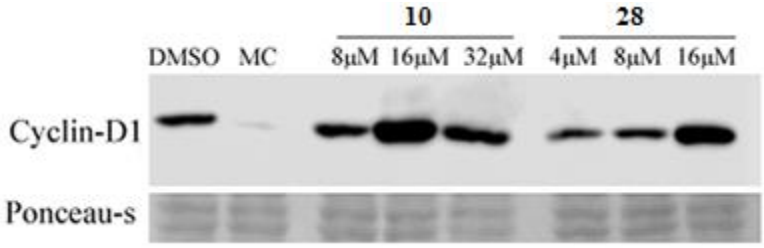

Figure 2.17: Western blot analysis of MDA-MB-231 whole cell lysates treated with differing concentrations of compounds **10**, **28**, DMSO (vehicle control) or Mitomycin C (MC) as an

example of a well-characterized alkylating compound. Cyclin D1 was probed after 48 h of treatment with **10** or **28**.

The increase in cyclin D1 expression could indicate cell cycle arrest at low levels of cyclin D1, and its following decrease may be indicative of an apoptotic response, which has also been supported by the decrease in PARP signal.

The effect of compounds **10** and **28** on DNA replication and synthesis was examined using BrdU uptake experiments through immunofluorescent microscopy. MDA-MB-231 cells were plated on cover slips, treated with compound **10** or **28** for 24 hours, pulsed with BrdU for one hour, and fixed for epifluorescent observation. At low concentrations of **10** or **28**, little change in BrdU positive (S-phase) cells was observed. At higher concentrations of **28**, however, there was a clear decrease in actively replicating cells. Interestingly, cells exhibiting high levels of nuclear fragmentation and karyorrhexis were BrdU negative, indicating karyorrhectic induced cell cycle cessation in the presence of compound **28** (**Figure 2.15**).

Based on these results, compound **28** has been designated as the lead candidate compound for further *in vivo* studies of systemic toxicity and chemotherapeutic efficacy based on its *in vitro* potency in the assays described above. Initially, compound **28** was examined for its systemic toxicity in CD-1 mice. 12 healthy CD-1 mice were divided into two groups (n=6): Group 1 was administered compound **28** (20mg/kg) and group 2 was administered vehicle only (control) intraperitoneally once daily six days a week for a total of 14 days. This study indicated that compound **28** was well tolerated with no apparent side effects at acceptable therapeutic dose regimens based on normal weight gains and behavior when compared to control group (**Figure 2.18**).

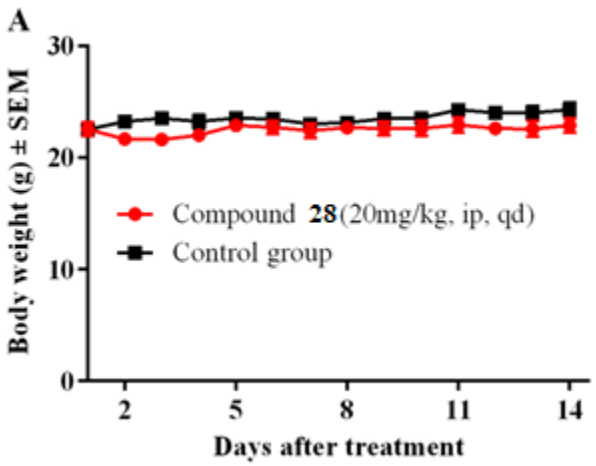

Figure 2.18: Systemic toxicity study of compound **28** in CD-1 mice

Compound **28** was then tested for its anticancer efficacy in a triple-negative breast cancer MDA-MB-231 xenograft model in NOD SCID mice. Cells were inoculated into the right flank of mice and treatment was initiated when the tumor volume reached ~150mm^3. Mice were randomly designated into three groups (n=7) based on average tumor volume. Group 1 was administered compound **28** (20mg/kg) three times a week, Group 2 was administered clinically used breast cancer drug doxorubicin (0.5mg/kg) five times a week, and Group 3 was administered vehicle. Tumor volumes and body weights were recorded every third day, and at the end of the study, mice were euthanized based on the institution of animal care and use committee (IACUC) guidelines. It was observed that compound **28** led to a statistically significant 55% decrease in tumor volume and a 41% decrease in tumor weight when compared to the control group. Comparatively, doxorubicin led to a 49% decrease in tumor volume and 28% decrease in tumor weight when compared to the control (**Figure 2.19**).

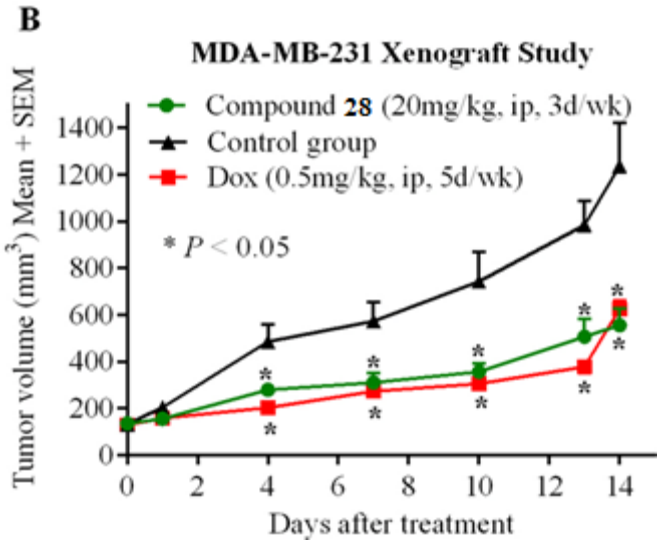

Figure 2.19: Tumor growth inhibition study of compound **28** in a MDA-MB-231; xenograft model.

Conclusion and Future Directions

In conclusion, several structurally diverse 2-alkoxycarbonyl-allyl esters were synthesized from BH bromides. SAR studies indicated that β-unsubstituted 2-(methoxycarbonyl)-allyl esters derived from aromatic carboxylic acids were optimal, the double bond was required for biological activity, and di- and tri-functionalized analogues had enhanced activity when compared to the mono esters. The cell proliferation inhibition properties were evaluated utilizing the MTT assay, with several derivatives exhibiting inhibition at low micromolar concentration. Preliminary *in vitro* studies indicated DNA damage and cell cycle effects that are consistent with alkylation. Finally, systemic toxicity studies indicated that compound **28** was well tolerated in healthy CD-1 mice, and exhibited statistically significant tumor growth inhibition properties in a MDA-MB-231 xenograoft model. Due to the ease of synthesis, potential for product diversity, structural tunability, novelty of the mechanism of action, and encouraging *in vitro* and *in vivo* activity, the compounds reported in this thesis are promising to be further developed as anticancer agents.

As a disclaimer, we do not discredit the ability of these molecules to interact with nucleophilic cellular components other than DNA. Several other nucleophilic biomolecules including amino acids such as cysteine, serine, threonine, and tyrosine can potentially react with 2-(alkoxycarbonyl)allyl esters in S_N2 or S_N2' fashion. Hence, molecules presented in this thesis have the potential to react with proteins in similar fashion as DNA. Further, mitochondrial DNA, although compartmentalized by the inner and outer mitochondrial membranes, is also susceptible to alkylation by electrophilic 2-(alkoxycarbonyl)-allyl esters in S_N2, S_N2', and 1,4 addition fashion. Also, glutathione and N-acetyl cysteine have the capability to react with electrophilic xenobiotics for protective mechanisms, and could potentially react with presented compounds in nucleophilic fashion. Although nuclear DNA is the most abundant nucleophile in the cell, and preliminary mechanisms of action support DNA alkylation, the intrinsic reactivity of molecules presented in this thesis may have cellular off-target effects.

Future directions of this project will involve attaching the BH-bromide template to biologically relevant molecules to achieve the targeted delivery to the tumor sites which would minimize the potential side effects expected from non-targeted therapeutic agents. Some of the other goals also involve improving the water solubility of the compounds by attaching piperizinyl, amino alkyl N,N-dialkyl groups etc. Some of these aspects have been described in **Figure 2.4**.

Experimental

Materials and Methods

Benzoic Acid (Fisher Scientific), trimesic Acid (Sigma-Aldrich), formaldehyde (Sigma-Aldrich), methyl acrylate (Sigma-Aldrich), phthalic acid (Sigma-Aldrich), 2, 6 pyridinedicarboxyllic acid (AKSci), cinnamic acid (Fisher Scientific), sodium carbonate (Fisher-Scientific), osmium tetroxide (Sigma-Aldrich), N-methyl morpholine N-Oxide (NMO, Sigma-Aldrich), 1-napthoic acid (AKSci), 9-anthracene carboxylic acid (AKSci), 4-phenylbutyric acid (Fischer Scientific). All other chemicals were of reagent grade quality and purchased from Sigma-Aldrich (St. Louis, MO). The ^{1}H- and ^{13}C-NMR spectra were plotted on a Varian Oxford-500 spectrometer. High-resolution mass spectra (HRMS) were recorded using a Bruker micrOTOF-Q III ESI mass spectrometer. Elemental analysis (CHN) results were obtained from Atlantic Microlab services.

Representative procedure for the synthesis of 2-(alkoxycarbonyl)allyl esters

To carboxylic acid (2 mmol) in DMSO (5 mL) was added Na_2CO_3 (6 mmol) and stirred for 15 min at room temperature. 2-(methoxycarbonyl) allyl bromide (2 mmol) was then added and reaction mixture was stirred for 2hr at room temperature. Upon completion (TLC), water (50 mL) was added and product was extracted with diethyl ether (3x50ml). Ether layer washed with saturated sodium bicarbonate (50 mL) to remove trace DMSO and unreacted acid. Organic layer was then dried using anhydrous $MgSO_4$ and filtered. Crude product was then concentrated under vacuum and pure compounds **5-14, 16-24** were obtained via column chromatography (1:20 EtOAc:Hexanes) (65-90%).

Synthesis of 2-hydroxy-2-(hydroxymethyl)-3-methoxy-3-oxopropyl benzoate

To compound **5** (2 mmol) in acetone (10 mL) was added N-methylmorpholine-N-oxide (NMO) (5 mmol) and catalytic osmium tetroxide (0.02 mmol). Reaction was stirred at room temperature for six hours. Upon completion (TLC), acetone was removed under reduced pressure and residue obtained was diluted with 50 mL of water and the crude product was extracted with ethyl acetate (3x25mL) and purified via column chromatography (1:5, EtOAc:Hexanes) to obtain compound **15** (70%).

Cell Culture

MDA-MB-231 cells (ATCC) were grown in DMEM supplemented with 10% FBS and penicillin-streptomycin (50U/ml-50µg/ml). MIAPaCa-2 cells (ATCC) were cultured in DMEM supplemented with 10% FBS, 2.5% Horse Serum and penicillin-streptomycin (50U/ml-50µg/ml). 4T1 cells (ATCC) were cultured in RPMI-1640 supplemented with 10% FBS and penicillin-streptomycin (50U/ml-50µg/ml).

Fluorescent Labeling

MDA-MB-231 cells ($5x10^4$cells/mL) were seeded on glass coverslips and cultured for 18-24hr. Cells were then treated with compound **7**, **22**, or DMSO (vehicle control) for 24 hours. After exposure, cells were pulsed with bromodeoxyuridine (BrdU, 4µg/mL) for 1 h. Media was then aspirated and cells were fixed with 2% paraformaldehyde in phosphate-buffered saline (PBS) for 15 min. Cells were rinsed with PBS containing 0.05% Tween-20 (PBST), and subsequently treated with 2N HCl for 20 min at room temperature and again rinsed with PBST. Cells were then blocked with normal goat serum (NGS) for 1 h at 37ºC and incubated in a 1:500 dilution of BrdU antibody (G3G4, Developmental Studies Hybridoma Bank, Iowa City, IA) in PBST/5% NGS at 4ºC

overnight. Following incubation, cells were rinsed with PBST and exposed to Texas Red conjugated secondary goat-anti-mouse antibody (Jackson Immunoresearch, Malvern, PA, 1:60 in PBST/5%NGS) and Hoechst (50μg/mL) for 1h at 37ºC. After three PBST washes, coverslips were mounted with anti-fade media (0.5M CAPS pH 9.8, 80% v/v glycerol, 0.1% w/v phenylene diamine, and 0.1% DABCO in PBS). Hoechst and BrdU labeled nuclei were then photographed using a Nikon TE2000 epifluorescent microscope; the images shown are representative of three separate experiments

Western Blot analysis

MDA-MB-231 cells ($5x10^4$ cells/mL) were treated with compound **7**, **22**, Mitomycin C (positive control) or DMSO (negative control) for 6 and 48 hours and whole cell lysates were collected. After denaturation at 95 °C for 10 min in a SDS sample buffer (5% w/v sodium dodecyl sulfate, 10% v/v glycerol, 60mM Tris, pH 6.8), protein concentration was determined using bicinchoninic acid (ThermoScientific) and equal amounts of protein (20 μg) separated by electrophoresis in 8% or 12% polyacrylamide gels. Proteins were electrophoretically transferred to nitrocellulose membranes for 90 min at 100 V, and subsequently stained with Ponceau to assess transfer quality and verify equal protein loading. After blocking the membranes with 10% w/v nonfat milk in PBST for 1 h at 35ºC, membranes were incubated overnight at 4 °C with rabbit anti-PARP (Santa Cruz H-250, 1:130), rabbit anti-Cyclin-D1 (Abcam AB16663, 1:260) or mouse anti-γH2AX (Upstate 05-636, 1:2500). Membranes were washed three times with PBST and incubated with the respective secondary goat anti-mouse IgG (1:2000) or goat anti-rabbit IgG (1:2000) horseradish peroxidase-conjugated antibodies (Jackson Immunoresearch). Membranes were again rinsed three times with PBST and were exposed to SuperSignal®

West Pico luminol enhancer solution and stable peroxide solution (ThermoScientific) for 2 minutes and visualized with a Licor imager. Images shown are representative of three separate experiments.

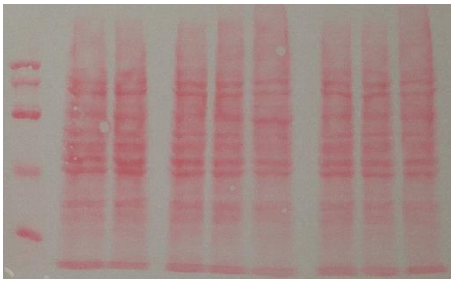

Ponceau-s stain of 8% SDS-PAGE of MDA-MB-231 cells exposed to compounds 7 and 22 used for PARP-1 and Cyclin-D1 antibodies.

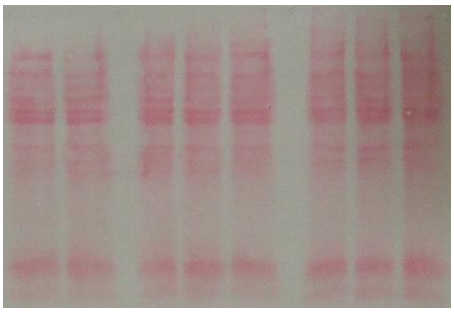

Ponceau-s stain of 12% SDS-PAGE of MDA-MB-231 cells exposed to compounds 7 and 22 used for γH2AX antibody.

Ethical Considerations

The experimental procedures involving animals that were conducted at the University of Minnesota Duluth was in compliance with the U.S. National Institutes of Health Guide for Care and Use of Laboratory Animals and approved by the Institutional Animal Care and Use Committee (IACUC). Studies with protocols 1311-31063A (systemic toxicity,

Figure 3A) and 1605-33796A (MDA-MB-231 xenograft, **Figure 3B**) were conducted at the University of Minnesota.

In vivo systemic toxicity in CD-1 mice

Five week old CD-1 mice (Charles River) were obtained and acclimatized for one week prior to treatment. Mice (n = 6) were grouped randomly based on average body weight. Group-1 was administered with compound 22 (20mg/kg) whereas group-2 was administered with vehicle intraperitoneally once daily, six days a week for a total of 14 days of treatment. Mice body weights were recorded daily, and euthanized according to IACUC guidelines at the end of the study. A graph of days of treatment versus body weight±SEM was generated using GraphPad software.

In vivo MDA-MB-231 xenograft model in SCID mice

$5x10^6$ cells MDA-MB-231 cells suspended in 1:1 matrigel-PBS were injected on right flank of female SCID mice (Jackson Laboratories). Treatment was initiated when the average tumor volume was ~$150mm^3$. The mice were randomly assigned into groups (n=7) based on average tumor volume and average body weight. Tumors were measured with calipers every two or three days and tumor volumes were calculated using the formula $V = (ab^2)/2$ where 'a' is the long diameter of the tumor and 'b' is the short diameter of the tumor. Mice were euthanized according to IACUC guidelines at the end of the study and tumors were isolated and weighed.

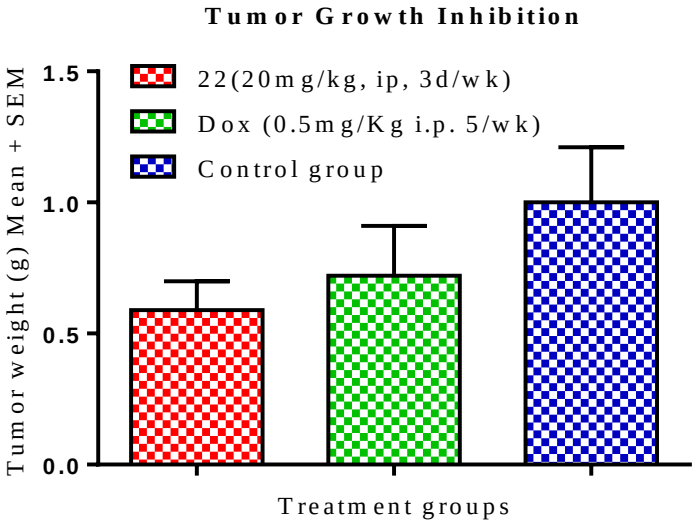

MDA-MB-231 Xenograft model. Graphical representation of average tumor mass (g) following 14 days of treatment.

Statistical Analysis

Statistics were computed using GraphPad Prism version 6.0. Mann-Whitney test was used to compare the compound-treated and control groups for *in vivo* tumor xenograft studies. A *P*-value of < 0.05 was considered significant.

Spectral Characterization

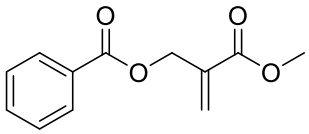

2-(methoxycarbonyl)allyl benzoate

^{1}H NMR (500MHz, $CDCl_3$): δ 8.07 (d, *J* = 8.5 Hz, 2H), 7.58 (t, *J* = 8.5 Hz, 1H), 7.45 (t, *J* = 8.0 Hz, 2H), 6.43 (s, 1H), 5.95 (s, 1H), 5.08 (s, 2H), 3.81 (s, 3H)

^{13}C NMR (125MHz, $CDCl_3$): δ 165.88, 165.62, 135.25, 133.11, 129.81, 129.62, 128.38, 127.38, 62.75, 52.02

Anal. Calcd for $C_{12}H_{12}O_4$ (220.22): C 65.45, H 5.49 **Found:** C 65.51. H 5.57

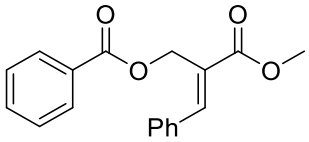

(E)-2-(methoxycarbonyl)-3-phenylallyl benzoate

^{1}H NMR (500MHz, $CDCl_3$): δ 8.07-8.05 (m, 3H), 7.57 (t, *J* = 7.5 Hz, 1H), 7.56-7.38 (m, 7H), 5.21 (s, 2H), 3.86 (s, 3H)

^{13}C NMR (125MHz, $CDCl_3$): δ 167.41, 166.32, 145.85, 134.25, 133.07, 130.05, 129.75, 129.67, 129.54, 128.82, 128.41, 126.66, 59.88, 52.38

Anal. Calcd for $C_{18}H_{16}O_4$ (296.32): C 72.96, H 5.44 **Found:** C 72.76. H 5.43

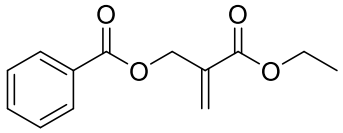

2-(ethoxycarbonyl)allyl benzoate

^{1}H NMR (500MHz, $CDCl_3$): δ 8.07 (d, *J* = 8.0 Hz, 2H), 7.60 (t, *J* = 7.5 Hz, 1H), 7.47 (t, *J* = 8.0 Hz, 2H), 6.42 (s, 1H), 5.94 (s, 1H), 5.08 (s, 2H), 4.30-4.25 (q, *J* = 7.5 Hz, 2H), 1.32 (t, *J* = 8.0 Hz, 3H)

^{13}C NMR (125MHz, $CDCl_3$): δ 165.95, 165.22, 135.61, 133.14, 129.91, 129.67, 128.43, 127.11, 62.86, 61.03, 14.17

Anal. Calcd for $C_{13}H_{14}O_4$ (234.25): C 66.66, H 6.02 **Found:** C 66.42. H 5.90

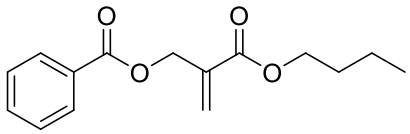

2-(butoxycarbonyl)allyl benzoate

^{1}H NMR (500MHz, $CDCl_3$): δ 8.07 (d, *J* = 7.5 Hz, 2H), 7.58 (t, *J* = 7.5 Hz, 1H), 7.46 (t, *J* = 8.0 Hz, 2H), 6.42 (s,1H), 5.93 (s,1H), 5.08 (s, 2H), 4.22 (t, *J* = 6.5 Hz, 2H), 1.70-1.64 (m, 2H), 1.45-1.37 (m, 2H), 0.93 (t, *J* = 7.5 Hz, 3H)

^{13}C NMR (125MHz, $CDCl_3$): δ 165.95, 165.30, 135.62, 133.14, 129.89, 129.67, 128.41, 127.22, 64.89, 62.90, 30.59, 19.16, 13.66

Anal. Calcd for $C_{15}H_{18}O_4$ (262.3): C 68.69, H 6.92 **Found:** C 68.45. H 6.97

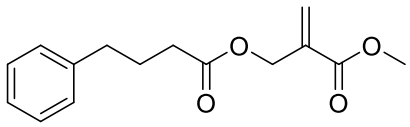

2-(methoxycarbonyl)allyl 4-phenylbutanoate

^{1}H NMR (500MHz, $CDCl_3$): δ 7.30-7.17 (m, 5H), 6.37 (s, 1H), 5.85 (s, 1H), 4.82 (s, 2H), 3.79 (s, 3H), 2.67 (t, *J* = 7.5Hz, 2H), 2.39 (t, *J* = 7.0Hz, 2H), 1.98 (quint, *J* =7.5Hz, 2H)

^{13}C NMR (125MHz, $CDCl_3$): δ 172.82, 165.67, 141.27, 135.30, 128.48, 128.40, 127.61, 126.02, 62.35, 52.04, 35.07, 33.48, 26.44

HRMS (ESI) m/z: calc'd for $C_{15}H_{18}O_4$ $[M+H]^+$: 263.1239, found 263.1306

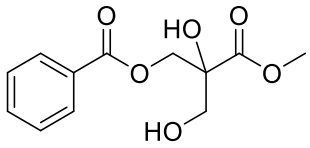

2-hydroxy-2-(hydroxymethyl)-3-methoxy-3-oxopropyl benzoate

^{1}H NMR (500MHz, $CDCl_3$): δ 8.00 (d, *J* = 8.0 Hz, 2H), 7.58 (t, *J* = 8.0 Hz, 1H), 7.45 (t, *J* = 7.8 Hz, 2H), 4.53-4.47 (dd, 2H), 3.93-3.78 (m, 6H), 2.22 (br s, 1H)

^{13}C NMR (125MHz, $CDCl_3$): δ 173.17, 166.01, 133.39, 129.69, 129.34, 128.50, 66.22, 64.69, 53.53, 42.67

Anal. Calcd for $C_{12}H_{14}O_6$ (254.08): C 56.69, H 5.55 **Found:** C 55.72, H 5.59

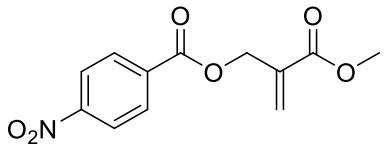

2-(methoxycarbonyl)allyl 4-nitrobenzoate

^{1}H NMR (500MHz, $CDCl_3$): δ 8.30 (d, *J* = 8.5 Hz, 2H), 8.23 (d, *J* = 8.0 Hz, 2H), 6.47 (s, 1H), 5.98 (s, 1H), 5.12 (s, 2H), 3.83 (s, 3H)

^{13}C NMR (125MHz, $CDCl_3$): δ 165.45, 164.09, 150.64, 135.21, 134.76, 130.80, 128.52, 123.58, 63.77, 52.18

HRMS (ESI) m/z: calc'd for $C_{12}H_{11}NO$ $[M+H]^+$: 266.0620, found 266.0659

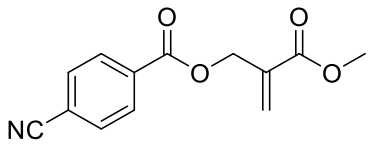

2-(methoxycarbonyl)allyl 4-cyanobenzoate

^{1}H NMR (500MHz, $CDCl_3$): δ 8.13 (d, *J* = 8.5 Hz, 2H), 7.74 (d, *J* = 8.5 Hz, 2H), 6.43 (s, 1H), 5.94 (s, 1H), 5.07 (s, 2H), 3.80 (s, 3H)

^{13}C NMR (125MHz, $CDCl_3$): δ 165.47, 164.34, 134.78, 133.64, 132.28, 130.18, 128.44, 117.89, 116.59, 63.64, 52.19

Anal. Calcd for $C_{13}H_{11}NO_4$ (245.23): C 63.67, H 4.52, N 5.71 **Found:** C 61.61, H 4.64, N 5.32

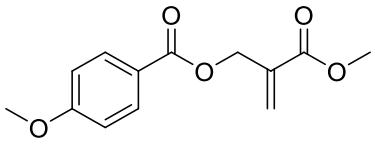

2-(methoxycarbonyl)allyl 4-methoxybenzoate

^{1}H NMR (500MHz, $CDCl_3$): δ 8.03 (d, *J* = Hz, 2H), 6.91 (d, *J* = Hz, 2H), 6.40 (s, 1H), 5.95 (s, 1H), 5.05 (s, 2H), 3.88 (s, 3H), 3.77 (s, 3H)

^{13}C NMR (125MHz, $CDCl_3$): δ 165.69, 165.62, 163.53, 135.48, 131.70, 127.13, 122.22, 113.67, 62.48, 55.41, 52.01

Anal. Calcd for $C_{13}H_{14}O_5$ (250.25): C 62.39, H 5.64 **Found:** C 62.21. H 5.62

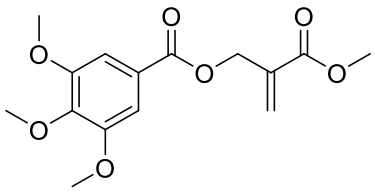

2-(methoxycarbonyl)allyl 3,4,5-trimethoxybenzoate

^{1}H NMR (500MHz, $CDCl_3$): δ 7.32 (s, 2H), 6.43 (s, 1H), 5.92 (s, 1H), 5.07 (s, 2H), 3.92-3.91(two singlets for two peaks, 9H), 3.82 (s, 3H)

^{13}C NMR (125MHz, $CDCl_3$): δ 165.63, 165.54, 152.97, 142.45, 135.32, 127.38, 124.79, 106.94, 62.86, 60.89, 56.24, 52.06

Anal. Calcd for $C_{15}H_{18}O_7$ (310.3): C 58.06, H 5.85 **Found:** C 57.53, H 5.81

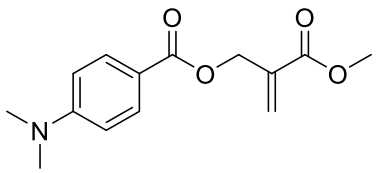

2-(methoxycarbonyl)allyl 4-(dimethylamino)benzoate

^{1}H NMR (500MHz, $CDCl_3$): δ 7.93 (d, *J* = 9Hz, 2H), 6.64 (d, *J* = 9Hz, 2H), 6.38 (s, 1H), 5.91 (s, 1H), 5.02 (s, 2H), 3.80 (s, 2H), 3.04 (s, 6H)

^{13}C NMR (125MHz, $CDCl_3$): δ 166.24, 165.86, 153.45, 135.82, 131.40, 126.65, 116.49, 110.70, 61.98, 51.97, 40.03

Anal. Calcd for $C_{14}H_{17}NO_4$ (263.29): C 63.87, H 6.51, N 5.32 **Found:** C 63.64. H 6.48, N 5.24

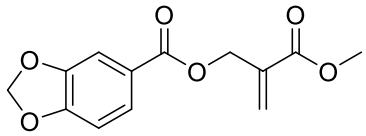

2-(methoxycarbonyl)allyl benzo[d][1,3]dioxole-5-carboxylate

^{1}H NMR (500MHz, $CDCl_3$): δ 7.70 (d, *J* = Hz, 1H), 7.49 (s, 1H), 6.87 (d, *J* = Hz, 1H), 6.40 (s, 1H), 6.05 (s, 2H), 5.93 (s, 1H), 5.04 (s, 2H), 3.80 (s, 3H)

^{13}C NMR (125MHz, $CDCl_3$): δ 165.66, 165.24, 151.79, 147.76, 135.36, 127.33, 125.51, 123.80, 109.53, 108.01, 101.84, 62.73, 52.05

Anal. Calcd for $C_{13}H_{12}O_6$ (264.23): C 59.09, H 4.58 **Found:** C 58.97. H 4.62

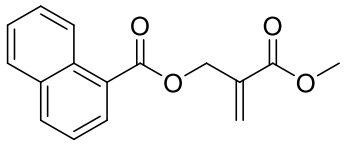

2-(methoxycarbonyl)allyl 1-naphthoate

^{1}H NMR (500MHz, $CDCl_3$): δ 8.94 (d, *J* = 8.5 Hz, 1H), 8.22 (d, *J* = 7.0 Hz, 1H), 8.02 (d, *J* = 7.5 Hz, 1H), 7.88 (d, *J* = 8.0 Hz, 1H), 7.62 (t, *J* = 7.5 Hz, 1H), 7.55-7.48 (m, 2H), 6.46 (s, 1H), 6.00 (s, 1H), 5.17 (s, 2H), 3.83 (s, 3H)

^{13}C NMR (125MHz, $CDCl_3$): δ 166.73, 165.69, 135.32, 133.81, 133.59, 131.37, 130.31, 128.54, 127.84, 127.77, 126.65, 126.24, 125.69, 124.46, 63.00, 52.06

Anal. Calcd for $C_{16}H_{14}O_4$ (270.28): C 71.10, H 5.22 **Found:** C 70.44, H 5.22

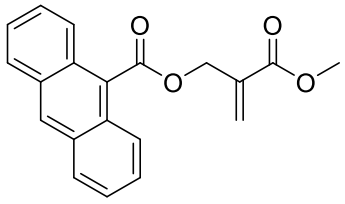

2-(methoxycarbonyl)allyl anthracene-9-carboxylate

^{1}H NMR (500MHz, $CDCl_3$): δ 8.55 (s, 1H), 8.08-8.03 (m, 4H), 7.56-7.49 (m, 4H), 6.48 (s, 1H), 6.03 (s, 1H), 5.36 (s, 2H), 3.85 (s, 3H)

^{13}C NMR (125MHz, $CDCl_3$): δ 164.31, 160.93, 130.27, 126.21, 124.88, 124.23, 123.90, 123.83, 122.58, 122.32, 120.75, 120.23, 59.06, 47.44

Anal. Calcd for $C_{20}H_{16}O_4$ (320.34): C 74.99, H 5.03 **Found:** C 74.71, H 5.10

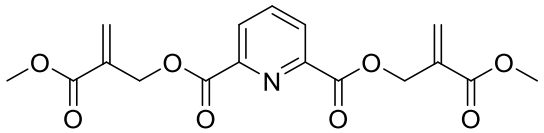

bis(2-(methoxycarbonyl)allyl) pyridine-2,6-dicarboxylate

^{1}H NMR (500MHz, $CDCl_3$): δ 8.30 (d, *J* = 8.0 Hz, 2H), 8.04 (t, *J* = 8.0 Hz, 1H), 6.46 (s, 2H), 6.06 (s, 2H), 5.16 (s, 4H), 3.82 (s, 6H)

^{13}C NMR (125MHz, $CDCl_3$): δ 165.50, 163.90, 148.22, 138.29, 134.68, 128.09, 127.89, 63.66, 52.10

HRMS (ESI) m/z: calc'd for $C_{17}H_{17}O_8$ $[M+H]^+$: 364.0988, found 364.1065

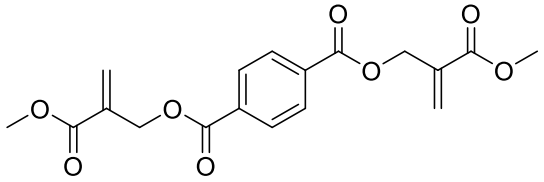

bis(2-(methoxycarbonyl)allyl) terephthalate

^{1}H NMR (500MHz, $CDCl_3$): δ 8.12 (s, 4H), 6.44 (s, 2H), 5.96 (s, 2H), 5.09 (s, 4H), 3.81 (s, 6H)

^{13}C NMR (125MHz, $CDCl_3$): δ 165.58, 165.11, 135.02, 133.85, 129.71, 127.98, 63.30, 52.14

HRMS (ESI) m/z: calc'd for $C_{18}H_{18}O_8$ $[M+H]^+$: 363.1035, found 363.1115

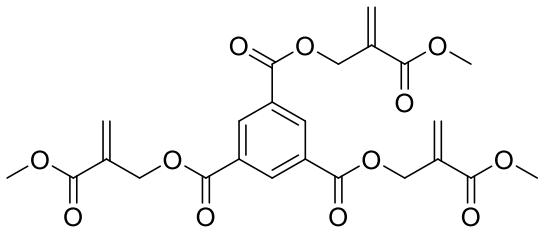

tris(2-(methoxycarbonyl)allyl) benzene-1,3,5-tricarboxylate

^{1}H NMR (500MHz, $CDCl_3$): δ 8.88 (s, 3H), 6.46 (s, 3H), 5.97 (s, 3H), 5.12 (s, 6H), 3.82 (s, 9H)

^{13}C NMR (125MHz, $CDCl_3$): δ 165.50, 164.24, 134.90, 134.82, 131.13, 128.27, 63.59, 52.18

Anal. Calcd for $C_{24}H_{24}O_{12}$ (504.44): C 57.14, H 4.80 **Found:** C 57.41, H 4.84

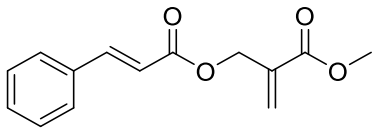

2-(methoxycarbonyl)allyl cinnamate

^{1}H NMR (500MHz, $CDCl_3$): δ 7.73 (d, *J* = 16Hz, 1H), 7.54-7.52 (m, 2H), 7.39-7.38 (m, 3H), 6.48 (d, *J* = 16Hz, 1H), 6.40 (s, 1H), 5.91 (s, 1H), 4.96 (s, 2H), 3.80 (s, 3H)

^{13}C NMR (125MHz, $CDCl_3$): δ 166.27, 165.69, 145.43, 135.32, 134.25, 130.44, 128.91, 128.14, 127.51, 117.52, 62.45, 52.04

HRMS (ESI) m/z: calc'd for $C_{12}H_{11}NO$ $[M+Na]^+$: 269.2518, found 269.0784

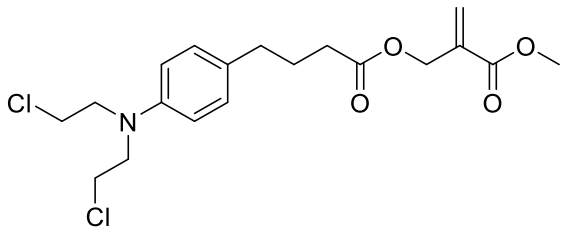

2-(methoxycarbonyl)allyl 4-(4-(bis(2-chloroethyl)amino)phenyl)butanoate

^{1}H NMR (500MHz, $CDCl_3$): δ 7.00 (d, *J* = 8Hz, 2H), 6.56 (d, *J* = 8Hz, 2H), 6.30 (s, 1H), 5.77 (s, 1H), 4.74 (s, 2H), 3.72 (s, 3H), 3.65-3.62 (m, 4H), 3.57-3.54 (m, 4H), 2.50 (t, *J* = 7.5Hz, 2H), 2.30 (t, *J* = 7Hz, 2H), 1.86 (quintet, *J* = 7.5Hz 2H)

^{13}C NMR (125MHz, $CDCl_3$): δ 172.90, 165.66, 144.37, 135.32, 130.45, 129.69, 127.55, 112.18, 62.31, 53.59, 52.04, 40.53, 33.93, 33.49, 26.69

Anal. Calcd for $C_{19}H_{25}Cl_2NO_4$ (402.31): C 56.72, H 6.26, N 3.48 **Found:** C 56.64, H 6.22, N 3.44

References (Introduction)

1. American Cancer Society. Cancer Facts and Figures. *Am. Cancer Soc.* (2017). doi:10.1101/gad.1593107

2. Weinmann, H. Cancer Immunotherapy: Selected Targets and Small-Molecule Modulators. *ChemMedChem* **11,** 450–466 (2016).

3. Tong, X. P. *et al.* Key autophagic targets and relevant small-molecule compounds in cancer therapy. *Cell Prolif.* **48,** 7–16 (2015).

4. Zhao, Y., Aguilar, A., Bernard, D. & Wang, S. Small-molecule inhibitors of the MDM2 − p53 protein − protein interaction (MDM2 inhibitors) in clinical trials for cancer treatment. *J. Med. Chem.* **58,** 1038–1052 (2015).

5. Maschinot, C. a, Pace, J. R. & Hadden, M. K. Synthetic Small Molecule Inhibitors of Hh Signaling As Anti-Cancer Chemotherapeutics. *Curr. Med. Chem.* **22,** 4033–57 (2015).

6. Monroig, P. D. C., Chen, L., Zhang, S. & Calin, G. a. Small molecule compounds targeting miRNAs for cancer therapy. *Adv. Drug Deliv. Rev.* **81,** 104–116 (2015).

7. Belmar, J. & Fesik, S. W. Small molecule Mcl-1 inhibitors for the treatment of cancer. *Pharmacol. Ther.* **145,** 76–84 (2014).

8. Bai, L., Smith, D. C. & Wang, S. Small-molecule SMAC mimetics as new cancer therapeutics. *Pharmacol. Ther.* **144,** 82–95 (2014).

9. Su, Y. *et al.* Small molecule with big role: MicroRNAs in cancer metastatic microenvironments. *Cancer Lett.* **344,** 147–156 (2014).

10. Van de Donk, N. W. C. J. *et al.* Monoclonal antibodies targeting CD38 in hematological malignancies and beyond. *Immunol. Rev.* **270,** 95–112 (2016).

11. Henricks, L. M., Schellens, J. H. M., Huitema, A. D. R. & Beijnen, J. H. The use of combinations of monoclonal antibodies in clinical oncology. *Cancer Treat. Rev.* **41,** 859–867 (2015).

12. Moussavou, G., Ko, K., Lee, J.-H. & Choo, Y.-K. Production of monoclonal antibodies in plants for cancer immunotherapy. *Biomed Res. Int.* **2015,** 306164 (2015).

13. Li, G., Wang, S., Xue, X., Qu, X. & Liu, H. Monoclonal antibody-related drugs for cancer therapy. *Drug Discov. Ther.* **7,** 178–184 (2013).

14. Melssen, M. & Slingluff, C. L. Vaccines targeting helper T cells for cancer immunotherapy. *Curr. Opin. Immunol.* **47,** 85–92 (2017).

15. Holay, N., Kim, Y., Lee, P. & Gujar, S. Sharpening the Edge for Precision Cancer Immunotherapy: Targeting Tumor Antigens through Oncolytic Vaccines. *Front. Immunol.* **8,** 800 (2017).

16. Lichtenegger, F. S., Krupka, C., Haubner, S., Köhnke, T. & Subklewe, M. Recent developments in immunotherapy of acute myeloid leukemia. *J. Hematol. Oncol.* **10,** 142 (2017).

17. Grierson, P., Lim, K.-H. & Amin, M. Immunotherapy in gastrointestinal cancers. *J. Gastrointest. Oncol.* **8,** 474–484 (2017).

18. Kumai, T., Fan, A., Harabuchi, Y. & Celis, E. Cancer immunotherapy: moving forward with peptide T cell vaccines. *Curr. Opin. Immunol.* **47,** 57–63 (2017).

19. Gao, X. *et al.* Cytokine-Induced Killer Cells As Pharmacological Tools for Cancer Immunotherapy. *Front. Immunol.* **8,** 774 (2017).

20. Yang, K. Inhibitors of the PD-1 / PD-L1 axis for the treatment of head and neck cancer : current status and future perspectives. 2007–2014 (2017). doi:10.2147/DDDT.S140687

21. Wu, L. & de Perrot, M. Radio-immunotherapy and chemo-immunotherapy as a novel treatment paradigm in malignant pleural mesothelioma. *Transl. Lung Cancer Res.* **6,** 325–334 (2017).

22. Dozier, J., Zheng, H. & Adusumilli, P. S. Immunotherapy for malignant pleural mesothelioma: current status and future directions. *Transl. Lung Cancer Res.* **6,** 315–324 (2017).

23. Hamid, O., Hoffner, B., Gasal, E., Hong, J. & Carvajal, R. D. Oncolytic immunotherapy: unlocking the potential of viruses to help target cancer. *Cancer Immunol. Immunother.* (2017). doi:10.1007/s00262-017-2025-8

24. Parp, T. & Cancer, P. Targeting PARP in Prostate Cancer: Novelty, Pitfalls, and Promise. 1–7 (2016).

25. Puigvert, J. C., Sanjiv, K. & Helleday, T. Targeting DNA repair, DNA metabolism and replication stress as anti-cancer strategies. *FEBS J.* **283,** 232–245 (2016).

26. O'Connor, M. J. Targeting the DNA Damage Response in Cancer. *Mol. Cell* **60,** 547–560 (2015).

27. Erdmann, A., Halby, L., Fahy, J. & Arimondo, P. B. Targeting DNA Methylation with Small Molecules: What ' s Next? (2014). doi:10.1021/jm500843d

28. Ali, A. & Bhattacharya, S. DNA binders in clinical trials and chemotherapy. *Bioorganic Med. Chem.* **22,** 4506–4521 (2014).

29. Hosoya, N. & Miyagawa, K. Targeting DNA damage response in cancer therapy. *Cancer Sci.* **105,** 370–388 (2014).

30. Furgason, J. M. & Bahassi, E. M. Targeting DNA repair mechanisms in cancer. *Pharmacol. Ther.* **137,** 298–308 (2013).

31. Zhang, D., Wang, H. B., Brinkman, K. L., Han, S. X. & Xu, B. Strategies for targeting the DNA damage response for cancer therapeutics. *Chin J Cancer* **31,** 359–363 (2012).

32. Hurley, L. H. DNA and its associated processes as targets for cancer therapy. *Nat. Rev. Cancer* **2,** 188–200 (2002).

33. Povirk, L. F. & Shuker, D. E. DNA damage and mutagenesis induced by nitrogen mustards. *Mutat. Res. Genet. Toxicol.* **318,** 205–226 (1994).

34. Musser, S. M., Pan, S. S., Egorin, M. J., Kyle, D. J. & Callery, P. S. Alkylation of Dna With Aziridine Produced During the Hydrolysis of N,N',N"-Triethylenethiophosphoramide. *Chem. Res. Toxicol.* **5,** 95–99 (1992).

35. Gates, K. S., Nooner, T. & Dutta, S. N7-Alkylguanine Residues in DNA. **17,** (2004).

36. Nejad, M. I., Johnson, K. M., Price, N. E. & Gates, K. S. A New Cross-Link for an Old Cross-Linking Drug: The Nitrogen Mustard Anticancer Agent Mechlorethamine Generates Cross-Links Derived from Abasic Sites in Addition to the Expected Drug-Bridged Cross-Links. *Biochemistry* **55,** 7033–7041 (2016).

37. Agarwal, S., Jangir, D. K., Mehrotra, R., Lohani, N. & Rajeswari, M. R. A structural insight into major groove directed binding of nitrosourea derivative nimustine with DNA: A spectroscopic study. *PLoS One* **9,** 2–9 (2014).

38. Drabløs, F. *et al.* Alkylation damage in DNA and RNA - Repair mechanisms and medical significance. *DNA Repair (Amst).* **3,** 1389–1407 (2004).

39. Boose, R. B. 2-Clioroethanol Formation as Evidence for a 2-Chloroethyl Alkylating Intermediate during Chemical Degradation of. **35,** 568–576 (1975).

40. Hartley, J. a., O'Hare, C. C. & Baumgart, J. DNA alkylation and interstrand cross-linking by treosulfan. *Br. J. Cancer* **79,** 264–266 (1999).

41. Iwamoto, T. *et al.* DNA intrastrand cross-link at the 5′-GA-3′ sequence formed by busulfan and its role in the cytotoxic effect. *Cancer Sci.* **95,** 454–458 (2004).

42. Streeper, R. T., Cotter, R. J., Colvin, M. E., Hilton, J. & Michael Colvin, O. Molecular Pharmacology of Hepsulfam, NSC 3296801: Identification of Alkylated Nucleosides, Alkylation Site, and Site of DNA Cross-Linking. *Cancer Res.* **55,** 1491–1498 (1995).

43. Ponti, M., Souhami, R. L., Fox, B. W. & Hartley, J. a. DNA interstrand crosslinking and sequence selectivity of dimethanesulphonates. *Br. J. Cancer* **63,** 743–7 (1991).

44. Shaloam, D. & Tchounwou, P. B. Cisplatin in cancer therapy: Molecular mechanisms of action. *Eur. J. Pharmacol.* **740,** 364–378 (2014).

45. Gescher, A. & Threadgill, M. D. The Metabolism of Triazene Antitumor Drugs. *Pharmacol. Ther.* **32,** 191–205 (1987).

46. Marchesi, F. *et al.* Triazene compounds: Mechanism of action and related DNA repair systems. *Pharmacol. Res.* **56,** 275–287 (2007).

47. Xu, Y. & Her, C. Inhibition of topoisomerase (DNA) I (TOP1): DNA damage repair and anticancer therapy. *Biomolecules* **5,** 1652–1670 (2015).

48. Pommier, Y. Topoisomerase I inhibitors: camptothecins and beyond. *Nat. Rev. Cancer* **6,** 789–802 (2006).

49. Chandra Bharadwaj, K. Intramolecular Morita–Baylis–Hillman and Rauhut–Currier reactions. A catalytic and atom economic route for carbocycles and heterocycles. *RSC Adv.* **5,** 75923–75946 (2015).

50. Wei, Y. & Shi, M. Recent advances in organocatalytic asymmetric Morita-Baylis-Hillman/aza-Morita-Baylis-Hillman Reactions. *Am. Chem. Soc.* **2,** 42–53 (2012).

51. Ma, G.-N., Jiang, J.-J., Shi, M. & Wei, Y. Recent extensions of the Morita-Baylis-Hillman reaction. *Chem. Commun. (Camb).* 5496–5514 (2009). doi:10.1039/b909405a

52. Basavaiah, D., Venkateswara Rao, K. & Jannapu Reddy, R. The Baylis–Hillman reaction: a novel source of attraction, opportunities, and challenges in synthetic chemistry. *Chem. Soc. Rev.* **36,** 1581 (2007).

53. Basavaiah, D. & Roy, S. Derivatives Using the Baylis # Hillman Bromides Dimethyl Sulfide Induced [3 + 2] Annulation Strategy : An Efficient Synthesis of Functionalized Dihydropyrazole Derivatives Using the Baylis - Hillman Bromides. 2–5 (2008). doi:10.1021/ol800424v

54. Basavaiah, D. & Veeraraghavaiah, G. The Baylis–Hillman reaction: a novel concept for creativity in chemistry. *Chem. Soc. Rev.* **41,** 68–78 (2012).

55. Basavaiah, D., Badsara, S. S. & Sahu, B. C. Baylis-Hillman Bromides as a Source of 1,3-Dipoles: Sterically Directed Synthesis of Oxindole-Fused Spirooxirane and Spirodihydrofuran Frameworks. *Chem. - A Eur. J.* **19,** 2961–2965 (2013).

56. Basavaiah, D., Reddy, B. S. & Badsara, S. S. Recent contributions from the Baylis-Hillman reaction to organic chemistry. *Chem. Rev.* **110,** 5447–5674 (2010).

57. Basavaiah, D., Reddy, K. R. & Kumaragurubaran, N. An expedient, facile and simple one-pot synthesis of 2-methylenealkanoates and alkanenitriles from the Baylis-Hillman bromides in aqueous media. *Nat. Protoc.* **2,** 2665–76 (2007).

58. Basavaiah, D., Sharada, D. S. & Kumaragurubaran, N. The Baylis - Hillman Reaction : One-Pot Facile Synthesis of 2 , 4-Functionalized 1 , 4-Pentadienes The Baylis - Hillman reaction is a three-component reaction involving the construction of the carbon - carbon bond between the R -position of activated alke. 7135–7137 (2002).

59. Frlan, R., Sova, M., Gobec, S., Stavber, G. & Asar, Z. Cobalt-Catalyzed Cross-Coupling of Grignards with Allylic and Vinylic Bromides: Use of Sarcosine as a Natural Ligand. *J. Org. Chem.* **80,** 7803–7809 (2015).

60. Bai, X., Lv, L. & Li, Z. Copper-catalyzed tandem trifluoromethylation–cyclization of olefinic carbonyls: synthesis of trifluoromethylated 2,3-dihydrofurans and 3,4-dihydropyrans. *Org. Chem. Front.* **3,** 804–808 (2016).

61. Sova, M., Frlan, R., Gobec, S., Stavber, G. & Asar, Z. D-Glucosamine in iron-catalysed cross-coupling reactions of Grignards with allylic and vinylic bromides: Application to the synthesis of a key sitagliptin precursor. *Appl. Organomet. Chem.* **29,** 528–535 (2015).

62. Zhu, Z. *et al.* Discovery of Novel Hydroxamates as Highly Potent Tumor Necrosis Factor-α Converting Enzyme Inhibitors: Part I-Discovery of Two Binding Modes. *J. Med. Chem.* **51,** 725–736 (2008).

63. Enz, A. *et al.* Gamma-lactams—A novel scaffold for highly potent and selective α7 nicotinic acetylcholine receptor agonists. *Bioorg. Med. Chem. Lett.* **19,** 1287–1291 (2009).

64. Grim, J. C., Garber, K. C. a & Kiessling, L. L. Glycomimetic building blocks: A divergent synthesis of epimers of shikimic acid. *Org. Lett.* **13,** 3790–3793 (2011).

65. Casey, T. C. *et al.* Stereoselective α, α'-annelation reactions of 1,3-dioxan-5-ones. *J. Org. Chem.* **75,** 7461–7464 (2010).

66. Maezaki, N., Sawamoto, H., Suzuki, T., Yoshigami, R. & Tanaka, T. Highly stereoselective synthesis of functionalized β,β-di- and trisubstituted vinylic sulfoxides by cu-catalyzed conjugate addition of organozinc reagents. *J. Org. Chem.* **69,** 8387–8393 (2004).

67. Teng, H. L., Huang, H. & Wang, C. J. Catalytic asymmetric construction of spiro(γ-butyrolactam-γ- butyrolactone) moieties through sequential reactions of cyclic imino esters with Morita-Baylis-Hillman bromides. *Chem. - A Eur. J.* **18,** 12614–12618 (2012).

68. Singh, D. *et al.* Natural Product Inspired Designing and Synthesis of β-Carboline and γ-Lactones Based Molecular Hybrids. *Org. Biomol. Chem.* 8154–8166 (2016). doi:10.1039/C6OB01216G

69. Hanessian, S. & Margarita, R. 1,3-Asymmetric induction in dianionic allylation reactions of amino acid derivatives-synthesis of functionally useful enantiopure glutamates, pipecolates and pyroglutamates. *Tetrahedron Lett.* **39,** 5887–5890 (1998).

70. Jia, ., Williams, R. A Diastereoselective Intramolecular Pauson-Khand Approach to the Construction of the BC Ring System in Tuberostemoninol. *Tetrahedron Asymmetry* **19,** 2901–2906 (2008).

71. Alanine, T. A., Galloway, W. R. J. D., McGuire, T. M. & Spring, D. R. Concise synthesis of substituted quinolizin-4-ones by ring-closing metathesis. *European J. Org. Chem.* **2014,** 5767–5776 (2014).

72. Xuan, J., Daniliuc, C. G. & Studer, A. Construction of Polycyclic γ-Lactams and Related Heterocycles via Electron Catalysis. *Org. Lett.* **18,** 6372–6375 (2016).

73. Luo, Z. & Naguib, M. A synthetic approach for (S)-(3-benzyl-3-methyl-2,3-dihydro-benzofuran-6-yl)-piperidin-1-yl-methanone, a selective CB2 receptor agonist. *Tetrahedron Lett.* **53,** 3316–3318 (2012).

74. Kłossowski, S., Muchowicz, A., Firczuk, M., Marta, S. & Redzej, A. Studies toward Novel Peptidomimetic Inhibitors of Thioredoxin − Thioredoxin Reductase System. 97–99 (2012).

75. Singh, V., Pathak, R. & Batra, S. Significant yield improvement in the stereoselective synthesis of allyl cyanides from Baylis-Hillman derivatives in aqueous medium under the influence of the phase-transfer catalyst. *Catal. Commun.* **8,** 2048–2052 (2007).

76. Gowrisankar, S., Kim, K. H., Kim, S. H. & Kim, J. N. Synthesis of 1,5-dicarbonyl and related compounds from Baylis-Hillman adducts via Pd-mediated decarboxylative protonation protocol. *Tetrahedron Lett.* **49,** 6241–6244 (2008).

77. Pandey, G., Kant, R. & Batra, S. A general route to the synthesis of indoloazocines using allyl bromides prepared from Morita-Baylis-Hillman adducts. *Tetrahedron Lett.* **56,** 930–933 (2015).

78. Bakthadoss, M. . B. & Vinayagam, V. . A novel protocol for the facile construction of tetrahydroquinoline fused tricyclic frameworks via an intramolecular 1,3-dipolar nitrile oxide cycloaddition reaction. *Org. Biomol. Chem.* **13,** 10007–10014 (2015).

79. Sankar, R. K., Kumbhare, R. S., Dharmaraja, A. T. & Chakrapani, H. A phenacrylate scaffold for tunable thiol activation and release. *Chem. Commun. (Camb).* **50,** 15323–6 (2014).

80. Rajan, Y. C., Kanakam, C. C., Selvam, S. P. & Murugesan, K. A study on the synthesis and biological and optical properties of methylene-dinaphthyl bis-chromanones: the utility of Baylis-Hillman adducts. *Tetrahedron Lett.* **48,** 8562–8565 (2007).

81. Ferreira, M. *et al.* Allylic isothiouronium salts: The discovery of a novel class of thiourea analogues with antitumor activity. *Eur. J. Med. Chem.* **129,** 151–158 (2017).

82. Silveira, G. P. *et al.* Allylic thiocyanates as a new class of antitubercular agents. *Bioorganic Med. Chem. Lett.* **22,** 6486–6489 (2012).

References (Results and Discussion)

1. Frlan, R., Sova, M., Gobec, S., Stavber, G. & Asar, Z. Cobalt-Catalyzed Cross-Coupling of Grignards with Allylic and Vinylic Bromides: Use of Sarcosine as a Natural Ligand. *J. Org. Chem.* **80,** 7803–7809 (2015).

2. Bai, X., Lv, L. & Li, Z. Copper-catalyzed tandem trifluoromethylation–cyclization of olefinic carbonyls: synthesis of trifluoromethylated 2,3-dihydrofurans and 3,4-dihydropyrans. *Org. Chem. Front.* **3,** 804–808 (2016).

3. Sova, M., Frlan, R., Gobec, S., Stavber, G. & Asar, Z. D-Glucosamine in iron-catalysed cross-coupling reactions of Grignards with allylic and vinylic bromides: Application to the synthesis of a key sitagliptin precursor. *Appl. Organomet. Chem.* **29,** 528–535 (2015).

4. Zhu, Z. *et al.* Discovery of Novel Hydroxamates as Highly Potent Tumor Necrosis Factor-α Converting Enzyme Inhibitors: Part I-Discovery of Two Binding Modes. *J. Med. Chem.* **51,** 725–736 (2008).

5. Enz, A. *et al.* Gamma-lactams—A novel scaffold for highly potent and selective α7 nicotinic acetylcholine receptor agonists. *Bioorg. Med. Chem. Lett.* **19,** 1287–1291 (2009).

6. Grim, J. C., Garber, K. C. a & Kiessling, L. L. Glycomimetic building blocks: A divergent synthesis of epimers of shikimic acid. *Org. Lett.* **13,** 3790–3793 (2011).

7. Casey, T. C. *et al.* Stereoselective-annelation reactions of 1,3-dioxan-5-ones. *J. Org. Chem.* **75,** 7461–7464 (2010).

8. Maezaki, N., Sawamoto, H., Suzuki, T., Yoshigami, R. & Tanaka, T. Highly stereoselective synthesis of functionalized β,β-di- and trisubstituted vinylic sulfoxides by cu-catalyzed conjugate addition of organozinc reagents. *J. Org. Chem.* **69,** 8387–8393 (2004).

9. Teng, H. L., Huang, H. & Wang, C. J. Catalytic asymmetric construction of spiro(γ-butyrolactam-γ- butyrolactone) moieties through sequential reactions of cyclic imino esters with Morita-Baylis-Hillman bromides. *Chem. - A Eur. J.* **18,** 12614–12618 (2012).

10. Singh, D. *et al.* Natural Product Inspired Designing and Synthesis of β-Carboline and γ-Lactones Based Molecular Hybrids. *Org. Biomol. Chem.* 8154–8166 (2016). doi:10.1039/C6OB01216G

11. Hanessian, S. & Margarita, R. 1,3-Asymmetric induction in dianionic allylation reactions of amino acid derivatives-synthesis of functionally useful enantiopure glutamates, pipecolates and pyroglutamates. *Tetrahedron Lett.* **39,** 5887–5890 (1998).

12. Jia, ., Williams, R. A Diastereoselective Intramolecular Pauson-Khand Approach to the Construction of the BC Ring System in Tuberostemoninol. *Tetrahedron Asymmetry* **19,** 2901–2906 (2008).

13. Alanine, T. A., Galloway, W. R. J. D., McGuire, T. M. & Spring, D. R. Concise synthesis of substituted quinolizin-4-ones by ring-closing metathesis. *European J. Org. Chem.* **2014,** 5767–5776 (2014).

14. Xuan, J., Daniliuc, C. G. & Studer, A. Construction of Polycyclic γ-Lactams and Related Heterocycles via Electron Catalysis. *Org. Lett.* **18,** 6372–6375 (2016).

15. Luo, Z. & Naguib, M. A synthetic approach for (S)-(3-benzyl-3-methyl-2,3-dihydro-benzofuran-6-yl)-piperidin-1-yl-methanone, a selective CB2 receptor agonist. *Tetrahedron Lett.* **53,** 3316–3318 (2012).

16. Kłossowski, S., Muchowicz, A., Firczuk, M., Marta, S. & Redzej, A. Studies toward Novel Peptidomimetic Inhibitors of Thioredoxin − Thioredoxin Reductase System. 97–99 (2012).

17. Singh, V., Pathak, R. & Batra, S. Significant yield improvement in the stereoselective synthesis of allyl cyanides from Baylis-Hillman derivatives in aqueous medium under the influence of the phase-transfer catalyst. *Catal. Commun.* **8,** 2048–2052 (2007).

18. Gowrisankar, S., Kim, K. H., Kim, S. H. & Kim, J. N. Synthesis of 1,5-dicarbonyl and related compounds from Baylis-Hillman adducts via Pd-mediated decarboxylative protonation protocol. *Tetrahedron Lett.* **49,** 6241–6244 (2008).

19. Pandey, G., Kant, R. & Batra, S. A general route to the synthesis of indoloazocines using allyl bromides prepared from Morita-Baylis-Hillman adducts. *Tetrahedron Lett.* **56,** 930–933 (2015).

20. Bakthadoss, M. . B. & Vinayagam, V. . A novel protocol for the facile construction of tetrahydroquinoline fused tricyclic frameworks via an intramolecular 1,3-dipolar nitrile oxide cycloaddition reaction. *Org. Biomol. Chem.* **13,** 10007–10014 (2015).

21. Sankar, R. K., Kumbhare, R. S., Dharmaraja, A. T. & Chakrapani, H. A phenacrylate scaffold for tunable thiol activation and release. *Chem. Commun. (Camb).* **50,** 15323–6 (2014).

22. Rajan, Y. C., Kanakam, C. C., Selvam, S. P. & Murugesan, K. A study on the synthesis and biological and optical properties of methylene-dinaphthyl bis-chromanones: the utility of Baylis-Hillman adducts. *Tetrahedron Lett.* **48,** 8562–8565 (2007).

23. Ferreira, M. *et al.* Allylic isothiouronium salts: The discovery of a novel class of thiourea analogues with antitumor activity. *Eur. J. Med. Chem.* **129,** 151–158 (2017).

24. Silveira, G. P. *et al.* Allylic thiocyanates as a new class of antitubercular agents. *Bioorganic Med. Chem. Lett.* **22,** 6486–6489 (2012).

25. J. Sravan Kumar, M. A. Alam, Shirisha Gurrapu, Grady Nelson, Michael Williams, M. A. C. & Joseph L. Johnson, Subash Jonnalagadda, and V. R. M. Synthesis and Biological Evaluation of Novel Benzoxaboroles as Potential Antimicrobial and Anticancer Agents. *J. Heterocycl. Chem.* **50,** 814–820 (2012).

26. Tekkam, S., Alam, MA., Just, MJ., Berry, SM., Johnson, JL., Jonnalagadda, SC., and Mereddy, V. Stereoselective Synthesis of Pyroglutamate Natural Product Analogs from α-Aminoacids and their Anti-Cancer Evaluation. *Anticancer Agents Med Chem* **13,** 1514–1530 (2013).

27. Solano, L. N. *et al.* Synthesis, in vitro, and in vivo evaluation of novel functionalized quaternary ammonium curcuminoids as potential anti-cancer agents. *Bioorganic Med. Chem. Lett.* **25,** 5777–5780 (2015).

28. Goede V, Eichhorst B, Fischer K, Wendtner CM, H. M. Past, present and future role of chlorambucil in the treatment of chronic lymphocytic leukemia. *Leuk Lymphoma* **56,** doi: 10.3109/10428194.2014.963077 (2015).

29. Lepretre S, Dartigeas C, Feugier P, Marty M, S. G. Systematic review of the recent evidence for the efficacy and safety of chlorambucil in the treatment of B-cell malignancies. *Leuk Lymphoma* **57,** doi: 10.3109/10428194.2015 (2016).

30. Hallek, M. Chronic lymphocytic leukemia: 2015 Update on diagnosis, risk stratification, and treatment. *Am. J. Hematol.* **90,** 446 – 60 (2015).

31. Sourdeval M, Boisvieux-Ulrich E, Gendron MC, M. F. Mitochondrial Inside-Out Signalling During Alkylating Agent-Induced Anoikis. *Front. Biosci.* **14,** 1917–1931 (2009).

32. Beranek, D. T. Distribution of methyl and ethyl adducts following alkylation with monofunctional alkylating agents. *Mutat. Res. - Fundam. Mol. Mech. Mutagen.* **231,** 11–30 (1990).

33. Drabløs, F. *et al.* Alkylation damage in DNA and RNA - Repair mechanisms and medical significance. *DNA Repair (Amst).* **3,** 1389–1407 (2004).

34. Rasmussen, K., Peterson, B.L., Jacobo, E., Penick, G.D., Sall, J. Cytologic effects of thiotepa and adriamycin and normal canine urothelium. *Acta Cytol.* **3,** 237–243 (1980).

35. Kinoshita, J. *et al.* N-methyl-N-nitrosourea induced acute alteration of retinal function and morphology in monkeys. *Investig. Ophthalmol. Vis. Sci.* **56,** 7146–7158 (2015).

36. Rogakou, E. P., Pilch, D. R., Orr, a. H., Ivanova, V. S. & Bonner, W. M. Double-stranded Brekas Induce Histone H2AX phosphorylation on Serine 139. *J. Biol. Chem.* **273,** 5858–5868 (1998).

37. Meador, J. a *et al.* Histone H2AX is a critical factor for cellular protection against DNA alkylating agents. *Oncogene* **27,** 5662–71 (2008).

38. Debiak, M., Kehe, K. & Bürkle, A. Role of poly(ADP-ribose) polymerase in sulfur mustard toxicity. *Toxicology* **263,** 20–25 (2009).

39. Baptiste-Okoh, N., Barsotti, A. M. & Prives, C. A role for caspase 2 and PIDD in the process of p53-mediated apoptosis. *Proc. Natl. Acad. Sci. U. S. A.* **105,** 1937–42 (2008).

40. Yang, K., Hitomi, M. & Stacey, D. W. Variations in cyclin D1 levels through the cell cycle determine the proliferative fate of a cell. *Cell Div.* **1,** 32 (2006).

41. Daniell, H. F-box proteins FBXO31 and FBX4 in regulation of cyclin D1 degradation upon DNA damage. *Pigment Cell Melanoma Res.* **22,** 518–519 (2009).

Appendix

8.0
7.5
7.0
6.5
6.0
5.5
5.0
4.5
4.0
3.5
3.0
ppm
1.93
2.02
1.01
1.01
1.04
2.07
3.00

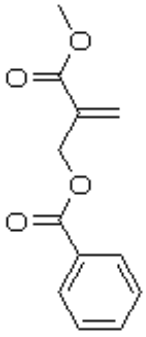

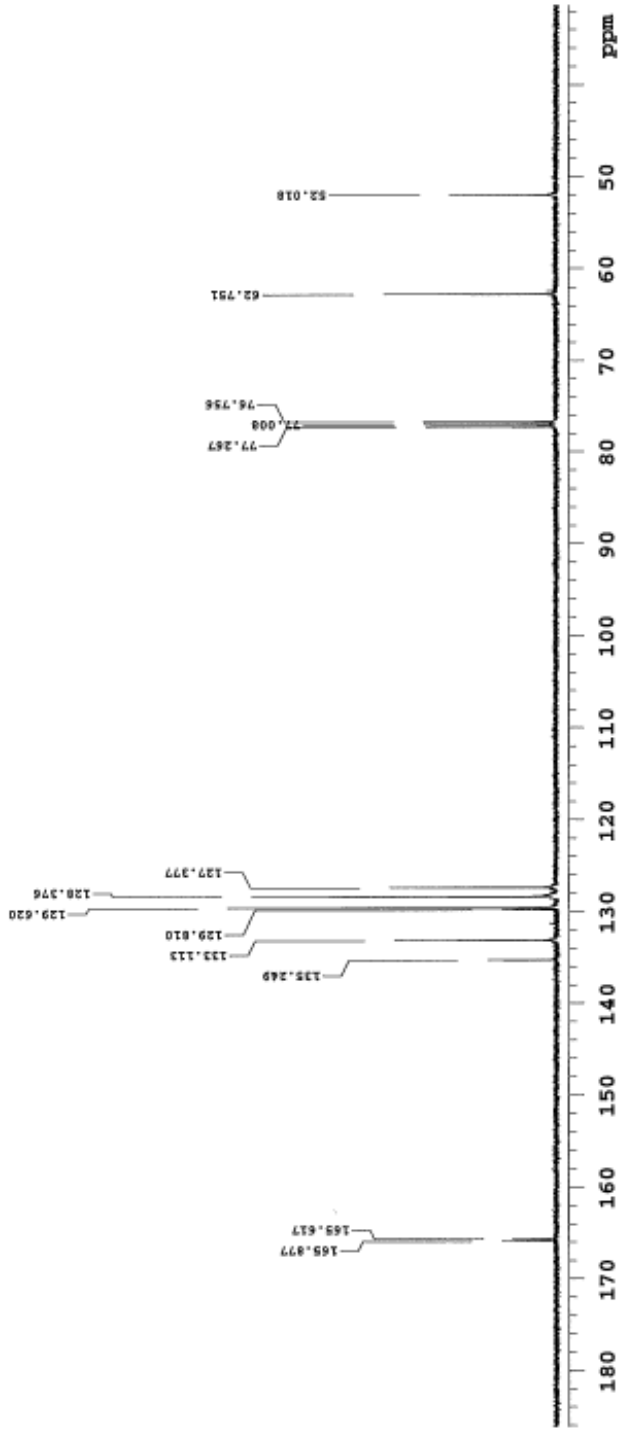
ppm
50
60
70
80
90
100
110
120
130
140
150
160
170
180
53.018
62.751
77.267
77.008
76.756
127.377
128.376
129.630
129.810
133.113
135.249
165.617
165.877

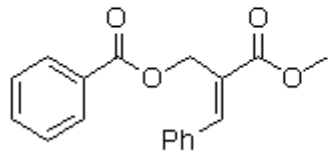
O
O
O
O
Ph

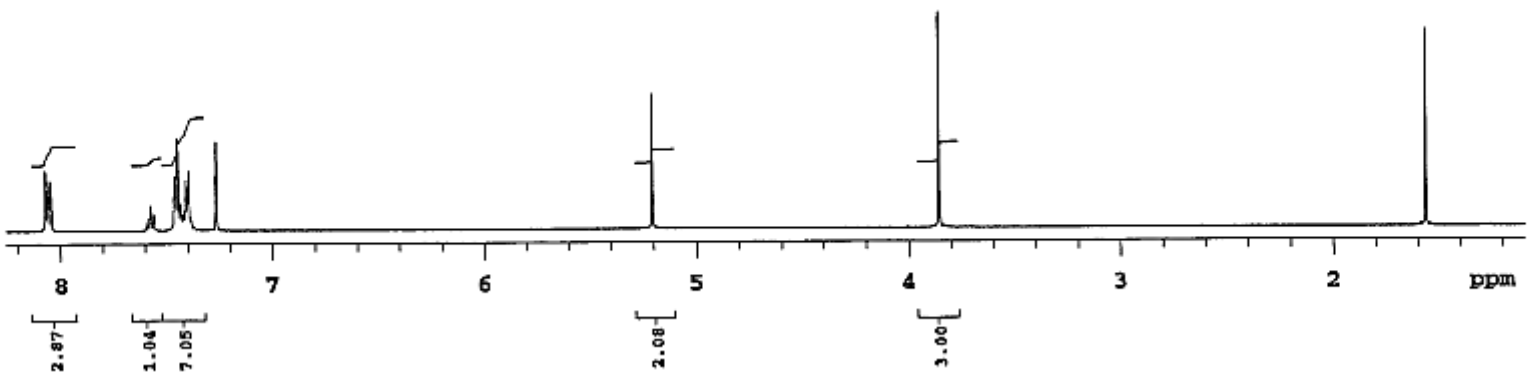
8
7
6
5
4
3
2
ppm
2.87
1.04
7.05
2.08
3.00

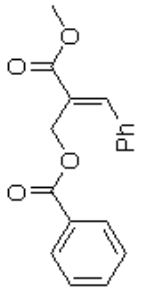
O
O
O
O
Ph

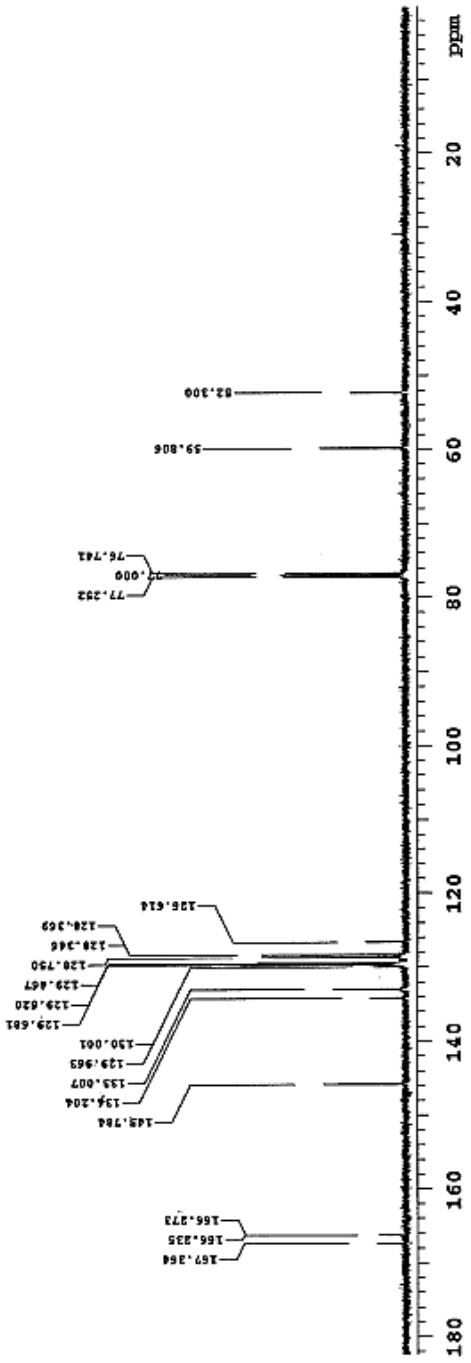
ppm
20
40
60
80
100
120
140
160
180
82.300
59.806
77.252
77.000
76.743
136.614
128.369
128.366
128.750
129.467
129.620
129.681
130.061
129.963
133.007
134.204
148.764
166.273
166.335
167.364

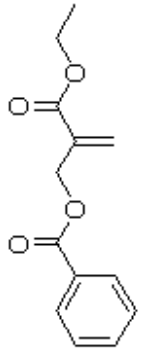

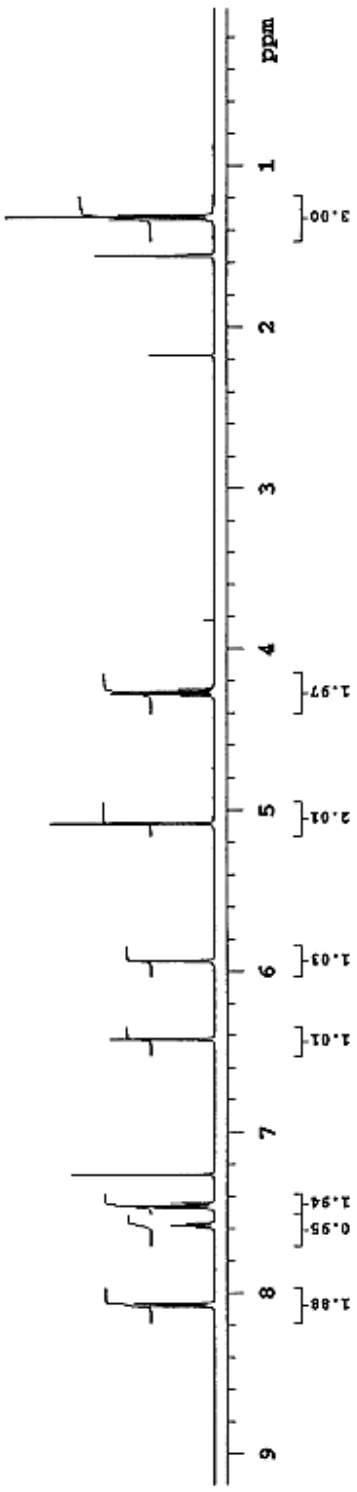
ppm
1
2
3
4
5
6
7
8
9
3.00
1.97
2.01
1.03
1.01
1.94
0.95
1.88

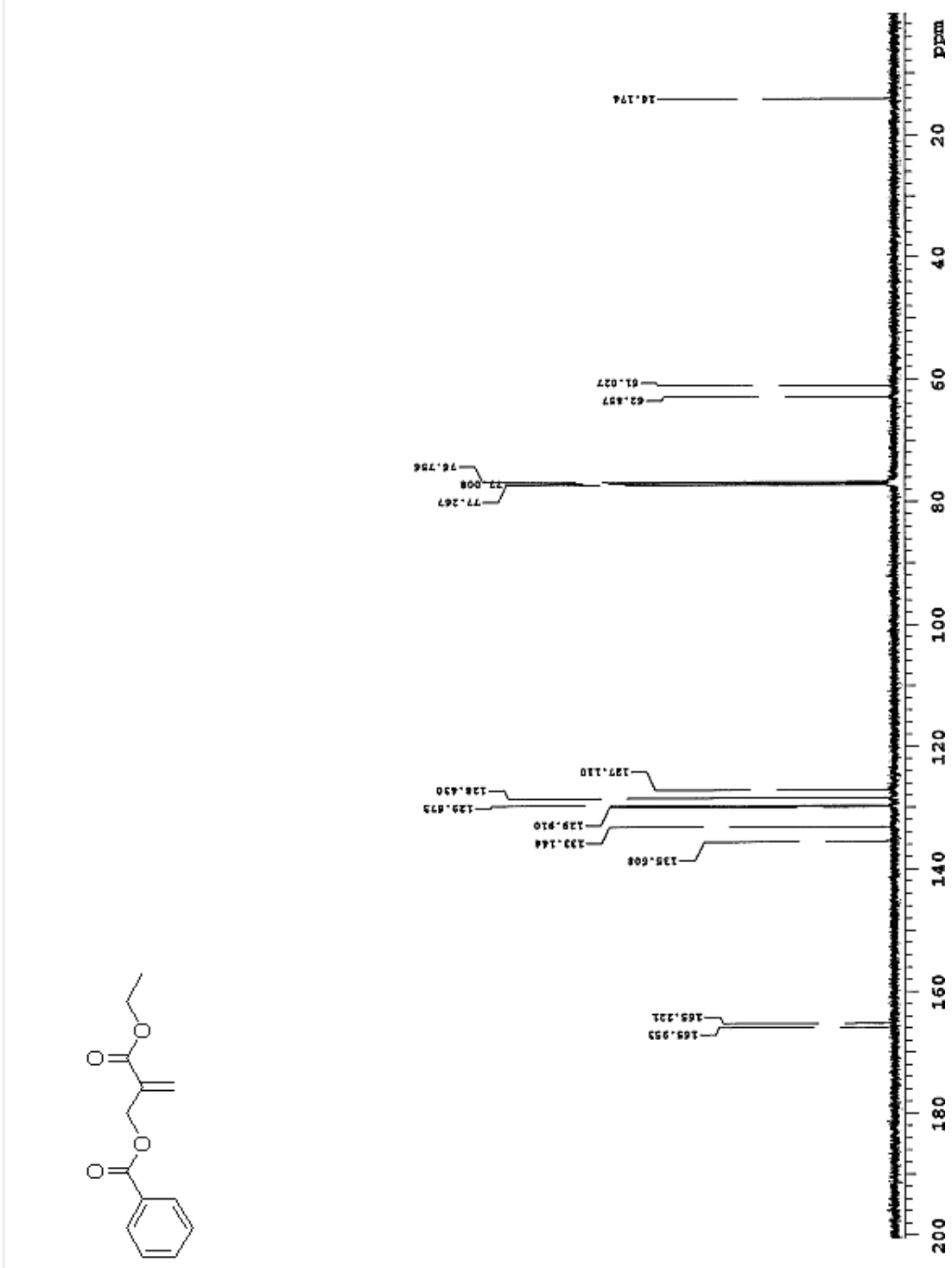
14.174
61.027
62.857
76.756
77.008
77.267
127.110
128.430
129.673
129.910
133.144
135.608
165.953
165.331
ppm
20
40
60
80
100
120
140
160
180
200

ppm
3.00
2.07
2.06
1.94
1.93
0.97
0.95
1.88
0.90
1.75

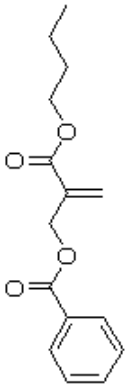

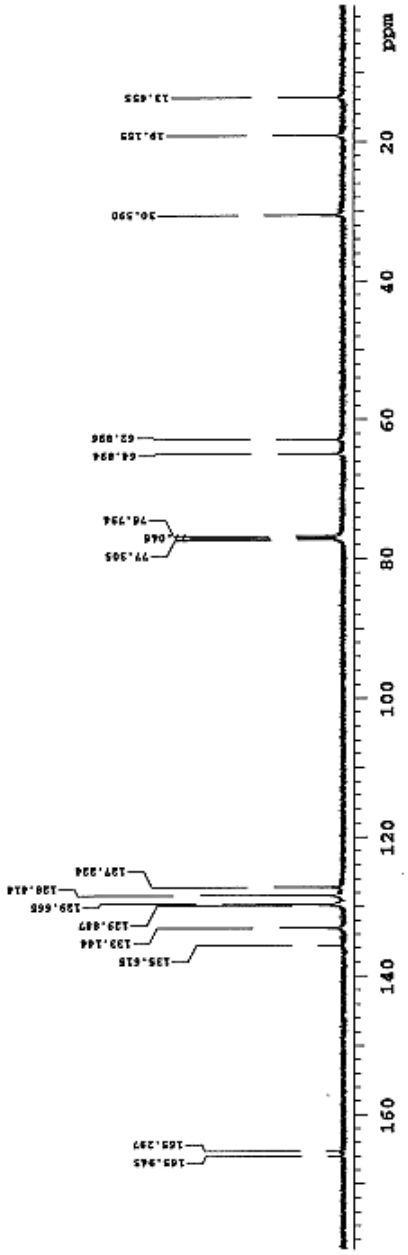
13.655
19.159
30.590
62.886
64.894
74.394
77.365
139.334
139.668
139.887
133.144
135.618
165.945
165.297
ppm

O
O
O
O
O2N

ppm
1
2
3
4
5
6
7
8
9
0.61
2.95
2.03
1.03
1.00
0.58
1.83
1.90

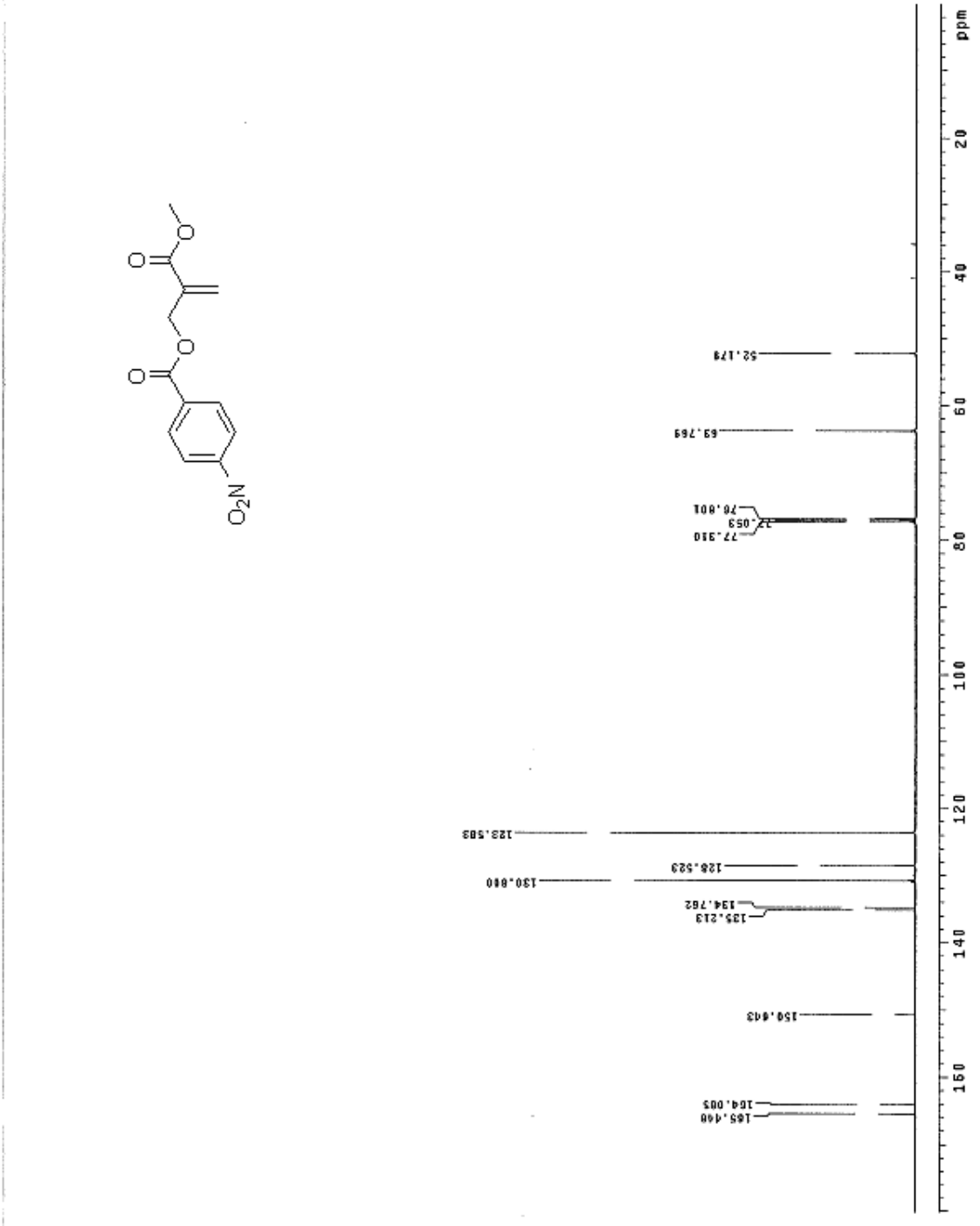
O
O
O
O
O_2N
52.179
63.769
76.801
77.059
77.310
123.583
126.529
130.080
134.762
135.213
150.443
164.005
165.460
ppm

O
O
O
O
NC

ppm
2
3
4
5
6
7
8

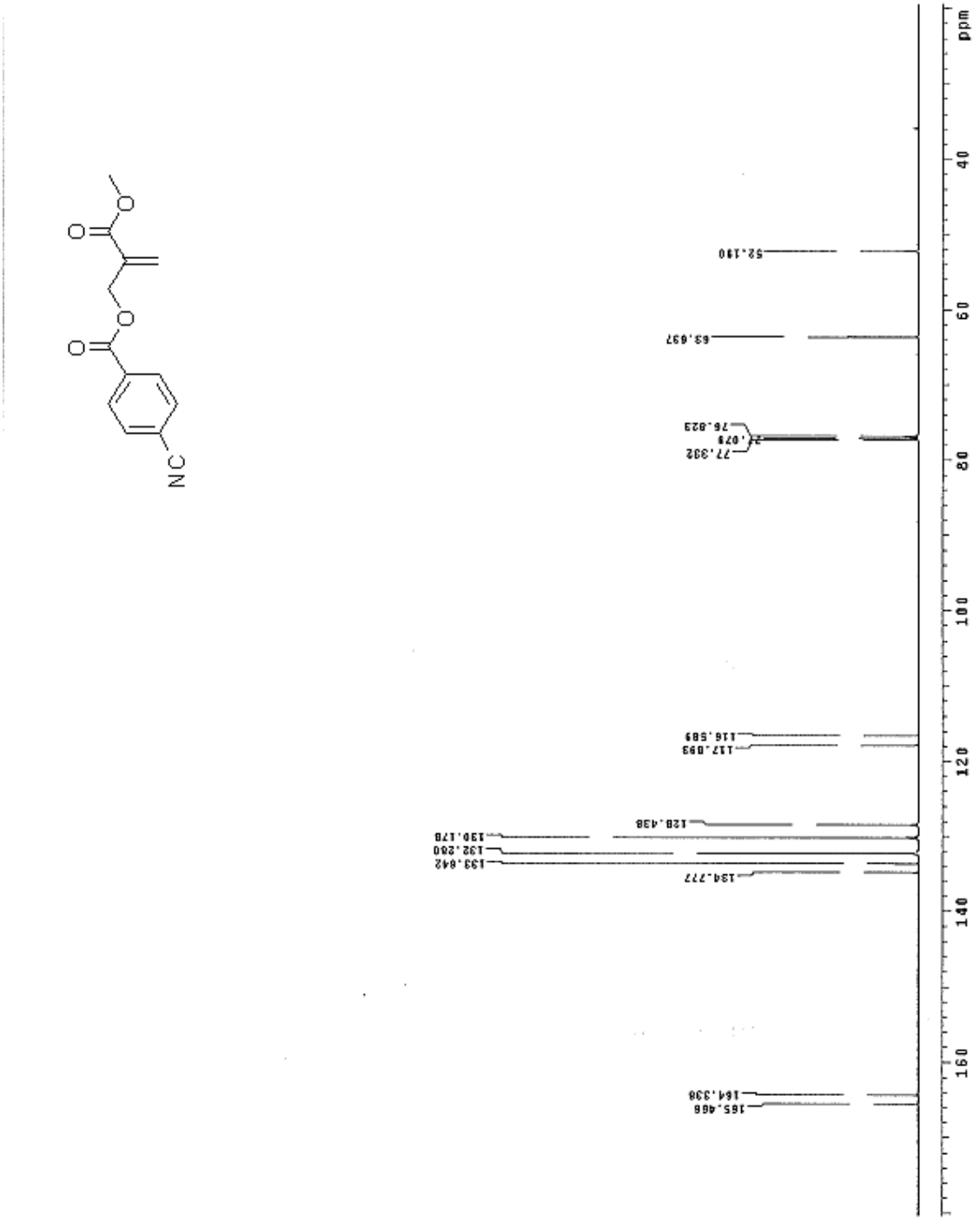
O
O
O
O
N
52.190
63.697
76.823
77.079
77.302
116.589
117.093
128.438
130.178
132.260
133.842
154.777
164.336
165.468
ppm
40
60
80
100
120
140
160

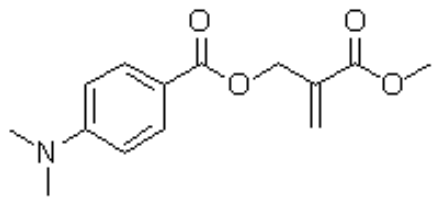
O
O
O
O
N

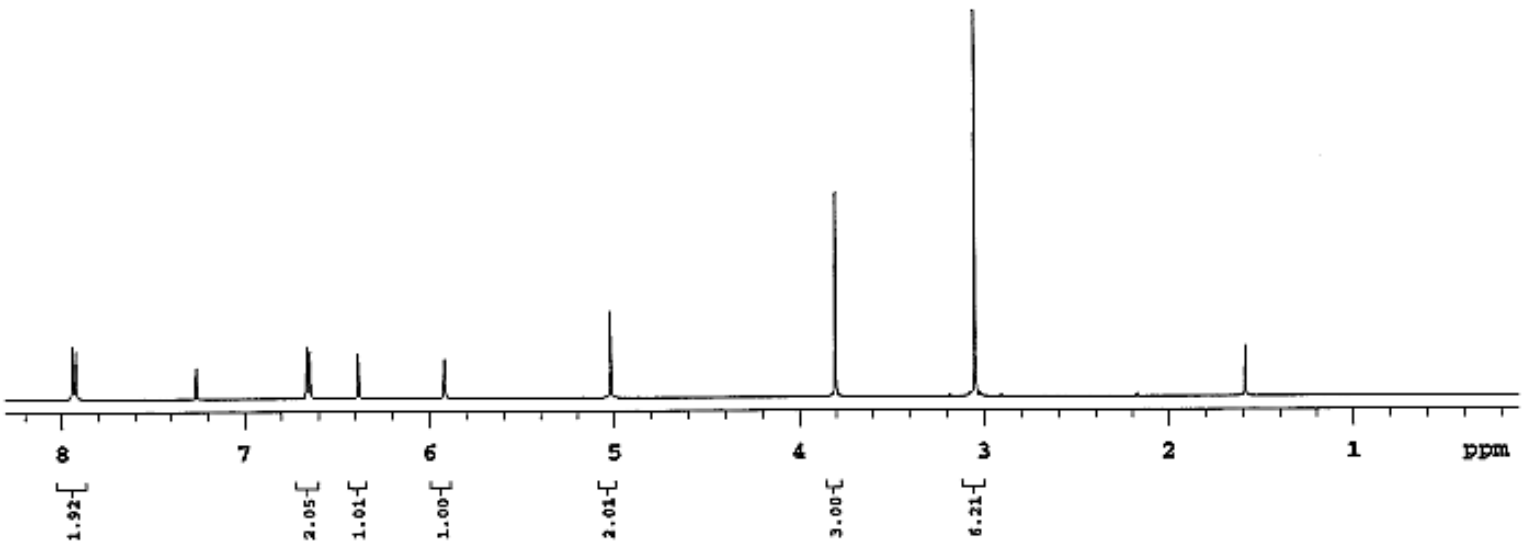
8
7
6
5
4
3
2
1
ppm
1.92
2.05
1.01
1.00
2.01
3.00
6.21

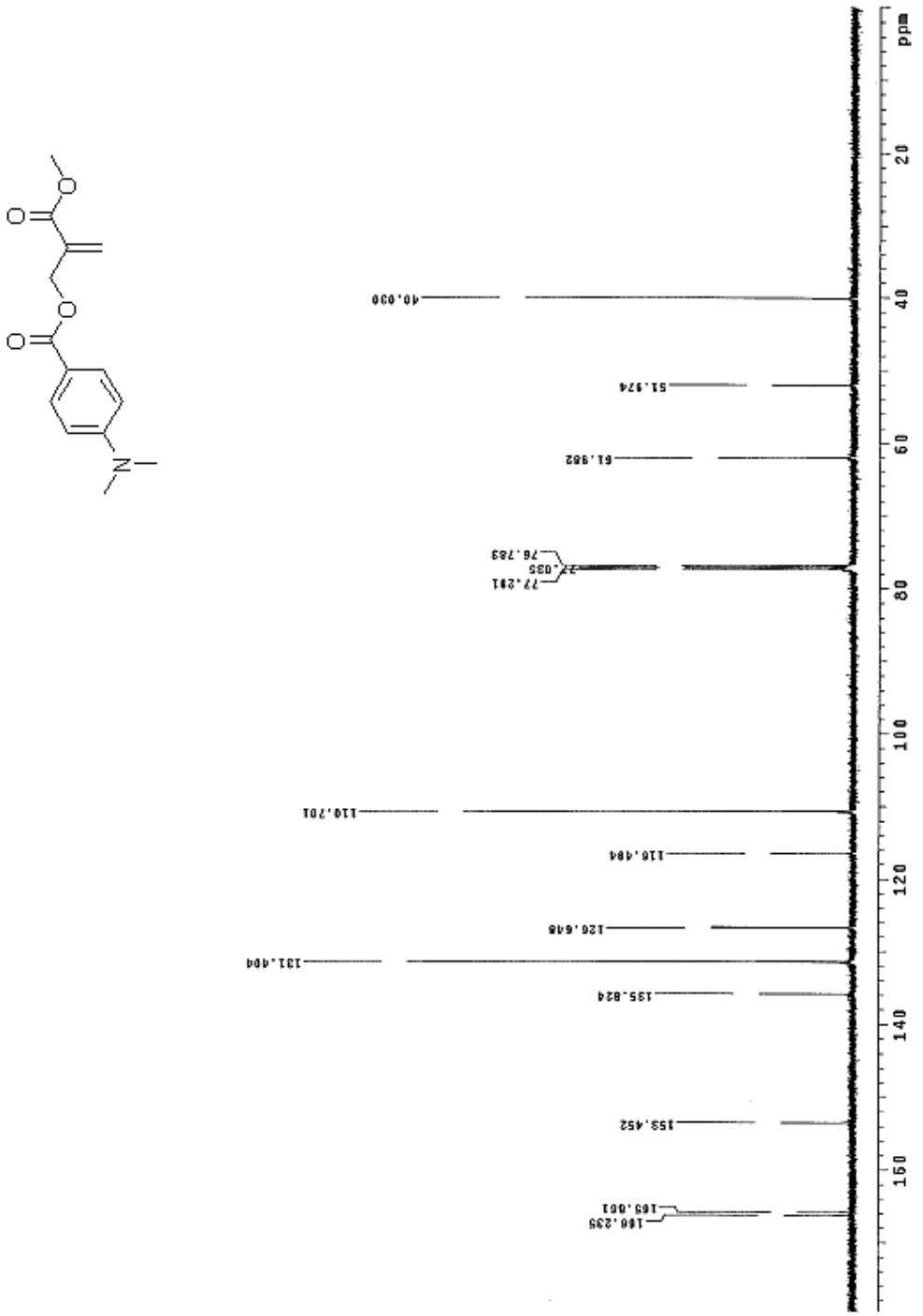
ppm
20
40
60
80
100
120
140
160
40.030
51.974
61.982
77.281
77.035
78.783
110.701
116.484
126.648
131.404
155.824
155.452
165.061
166.235

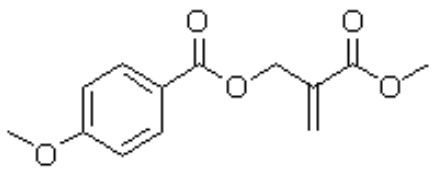
O
O
O
O
O

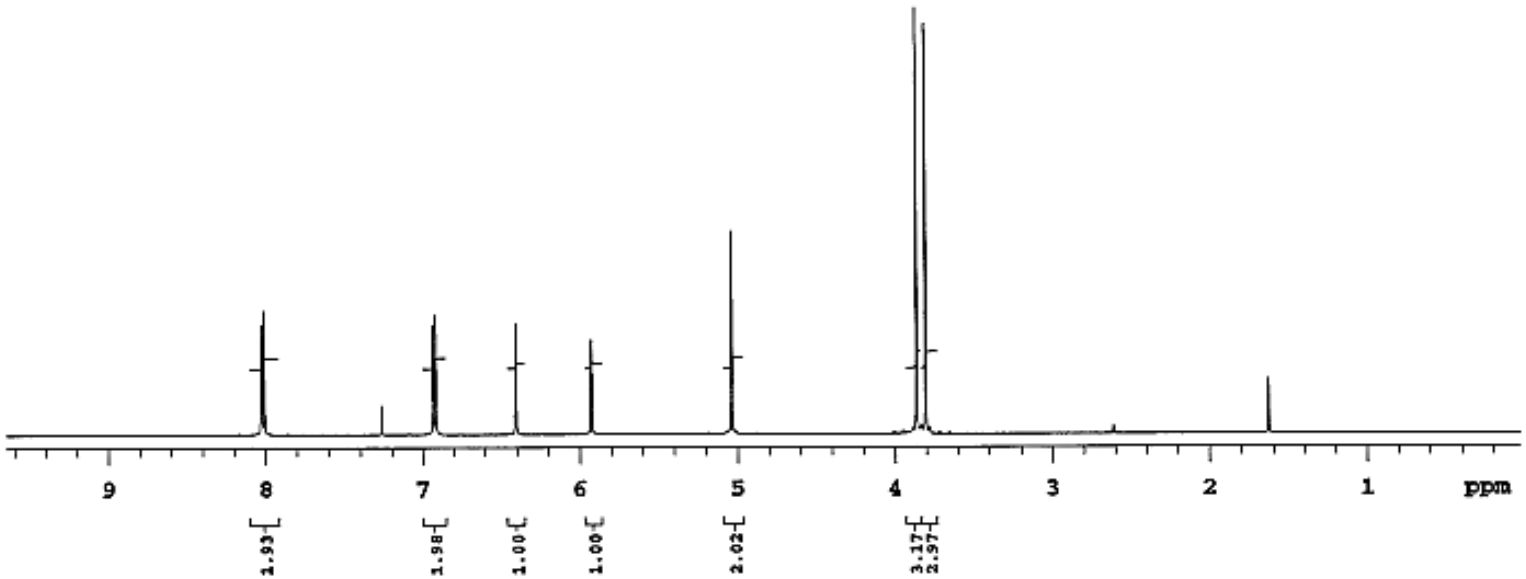
9
8
7
6
5
4
3
2
1
ppm
1.93
1.98
1.00
1.00
2.02
3.17
2.97

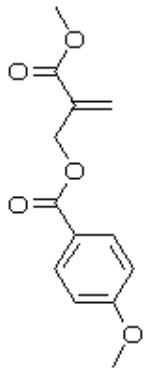

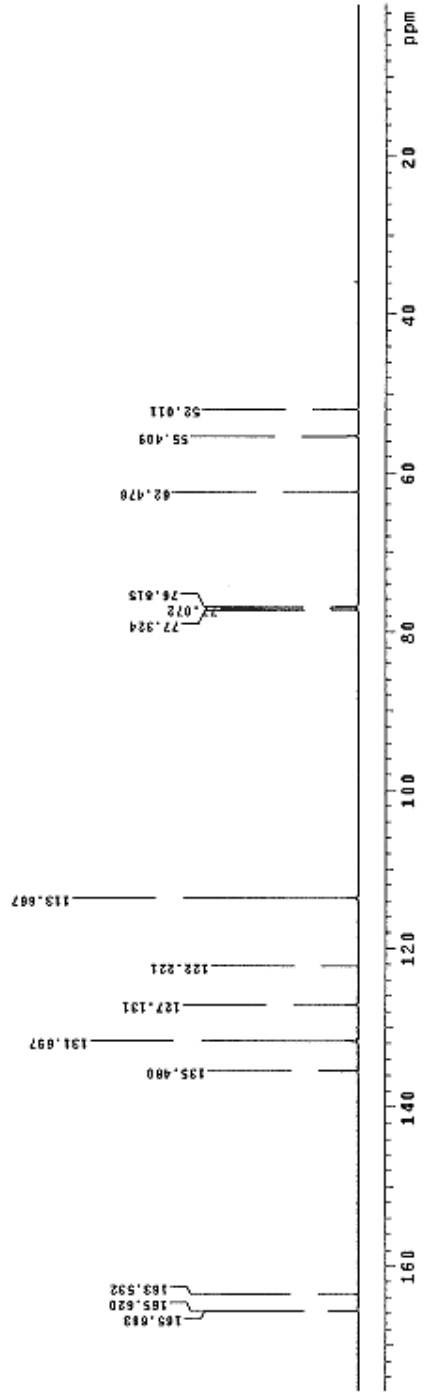
52.011
55.409
62.478
76.615
77.072
77.324
113.687
122.221
127.131
131.697
135.480
163.592
165.620
165.683
ppm

O
O
O
O
O
O
O
O

ppm
1
2
3
4
5
6
7
3.00
8.86
1.96
0.99
0.98
1.88
1.48

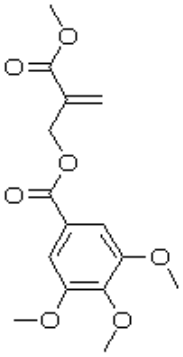

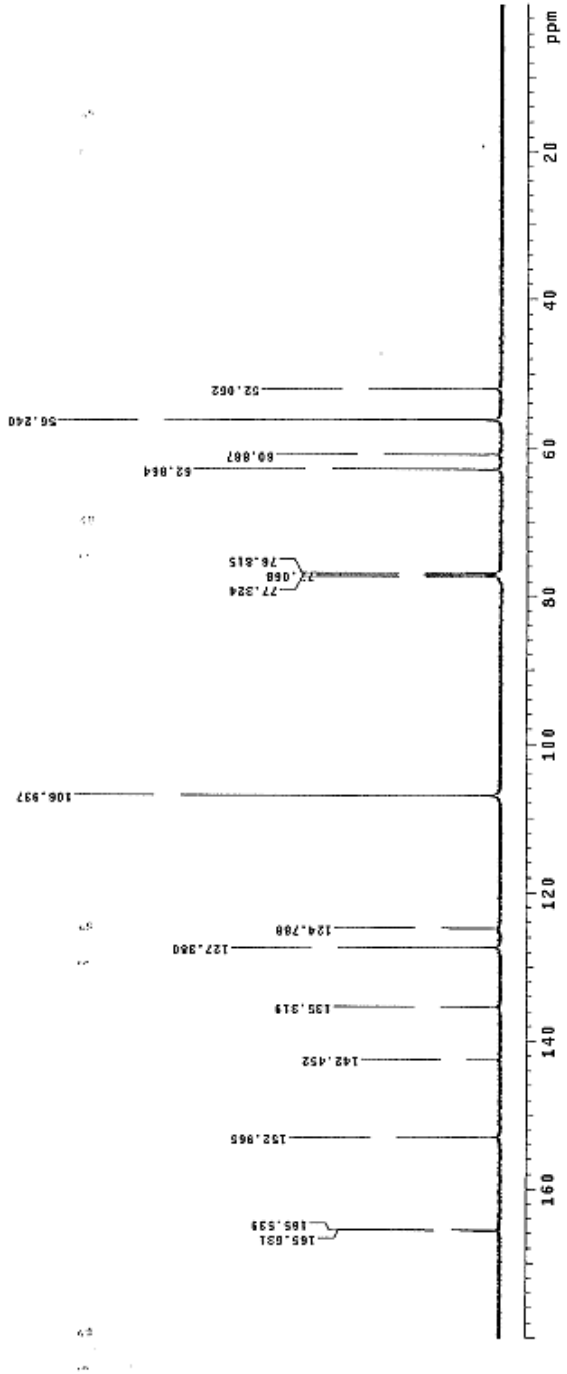
ppm
20
40
60
80
100
120
140
160
52.062
56.240
60.887
62.864
77.068
77.324
78.815
106.937
124.788
127.360
135.319
142.452
152.865
165.531
165.539

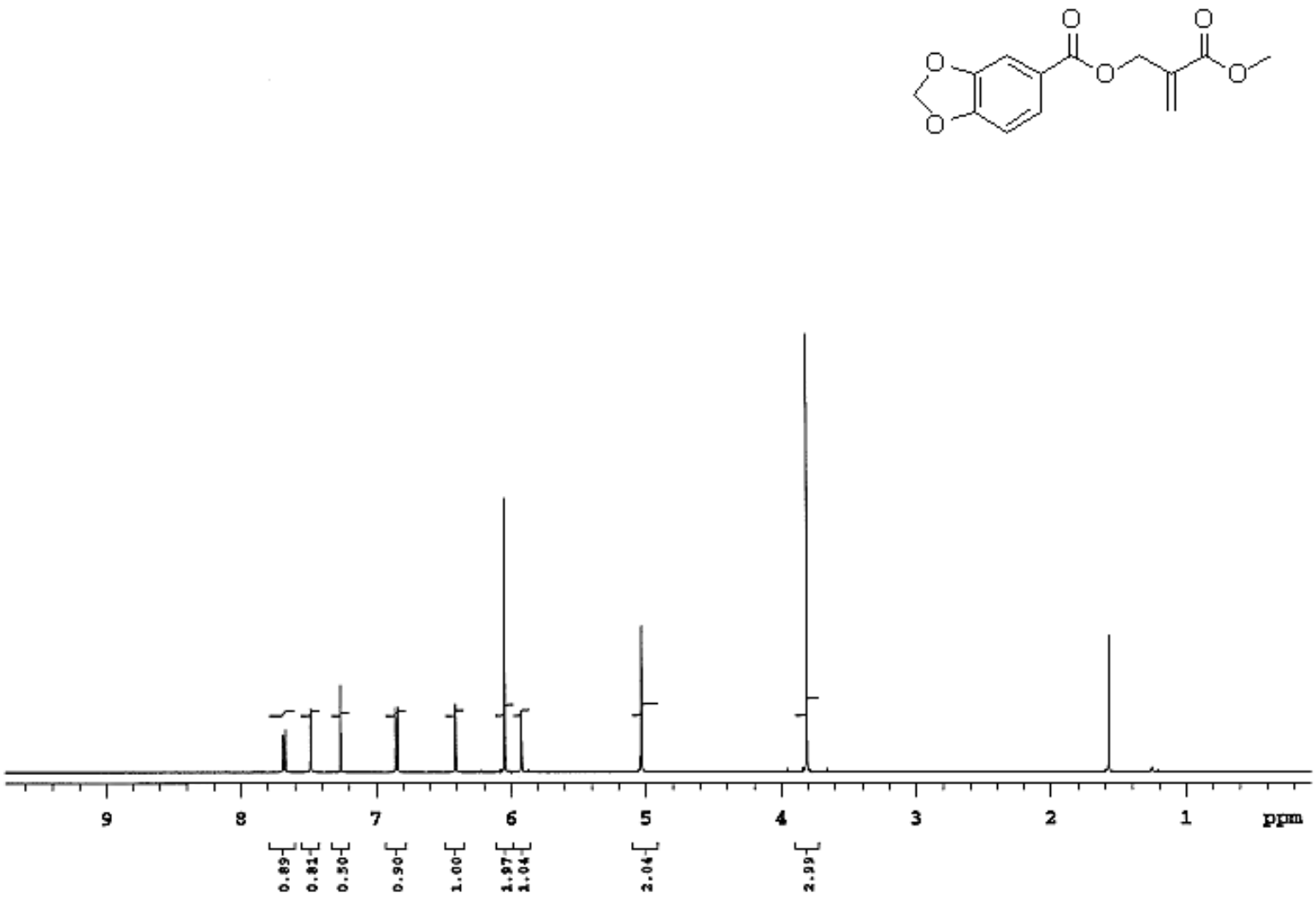
9
8
7
6
5
4
3
2
1
ppm
0.89
0.81
0.50
0.90
1.00
1.97
1.04
2.04
2.99

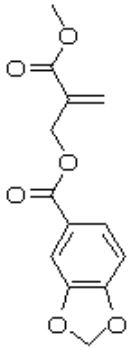

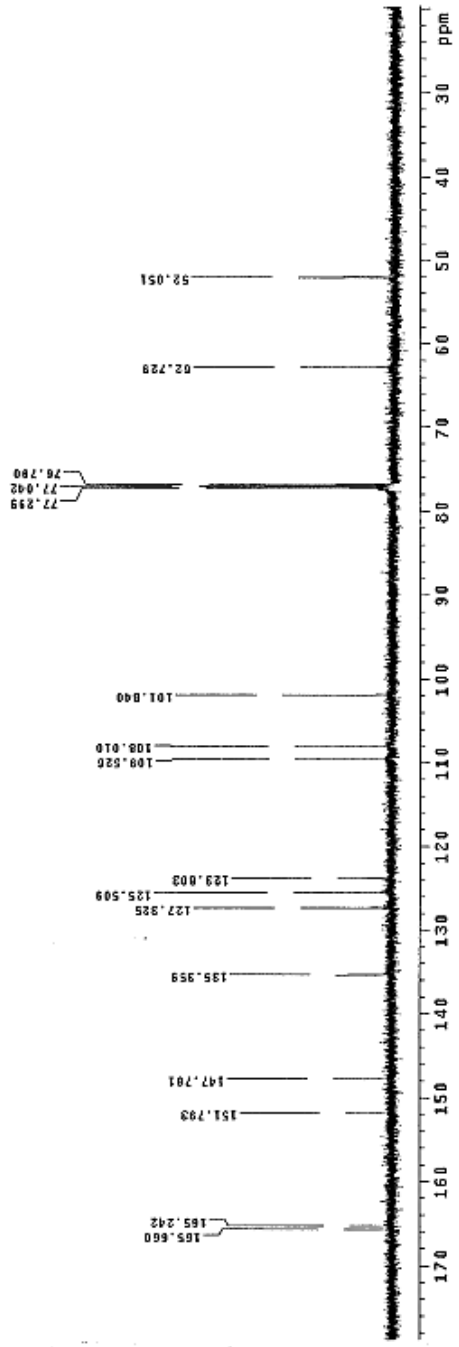
ppm
10
20
30
40
50
60
70
80
90
100
110
120
130
140
150
160
170
52.051
62.729
77.299
77.042
76.780
101.840
108.526
108.910
123.003
125.509
127.825
135.959
147.701
151.793
165.660
165.242

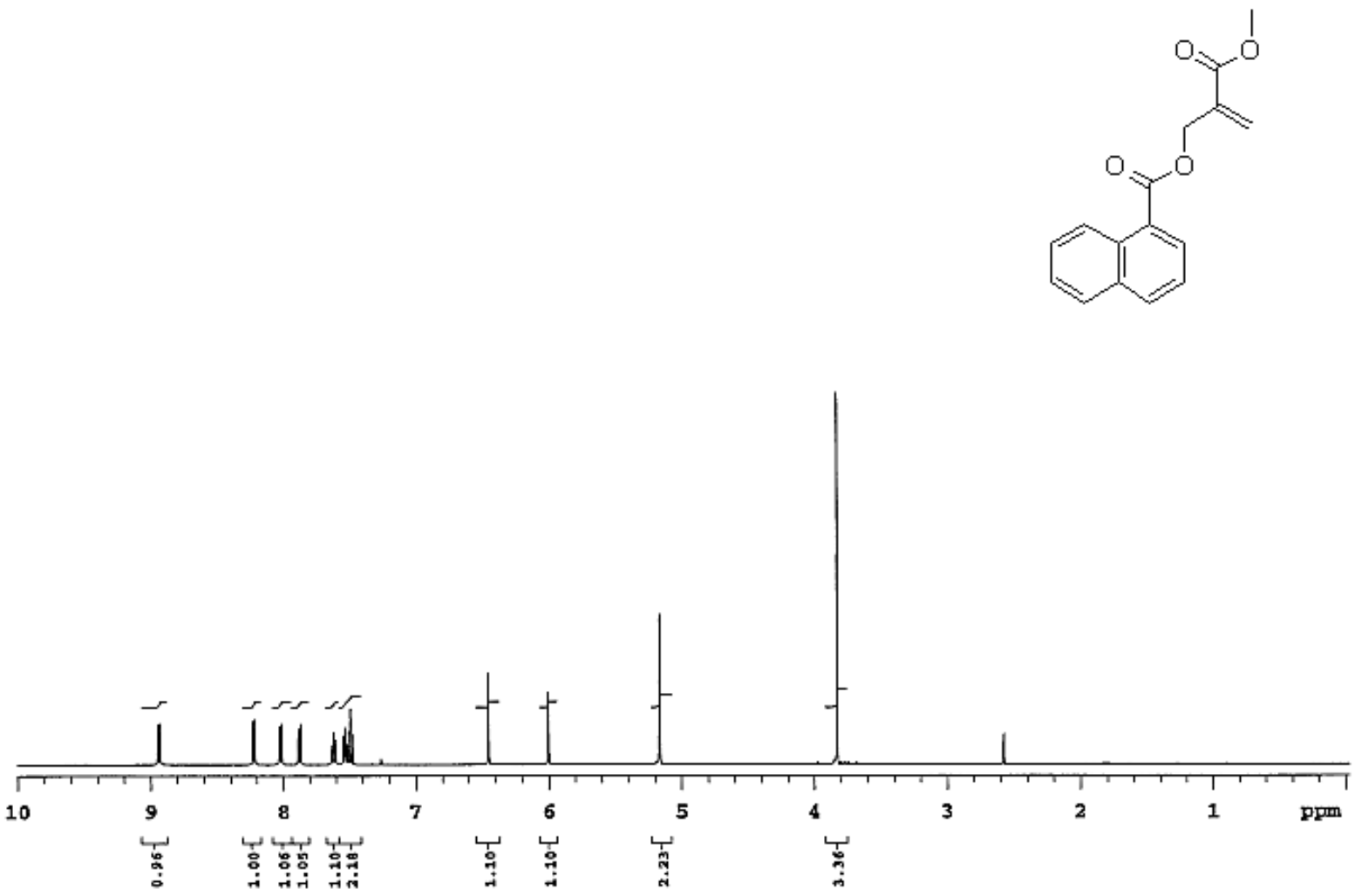
O
O
O
O
10
9
8
7
6
5
4
3
2
1
ppm
0.96
1.00
1.06
1.05
1.10
2.18
1.10
1.10
2.23
3.36

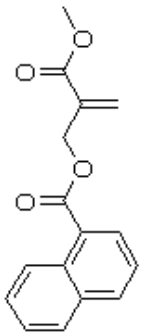

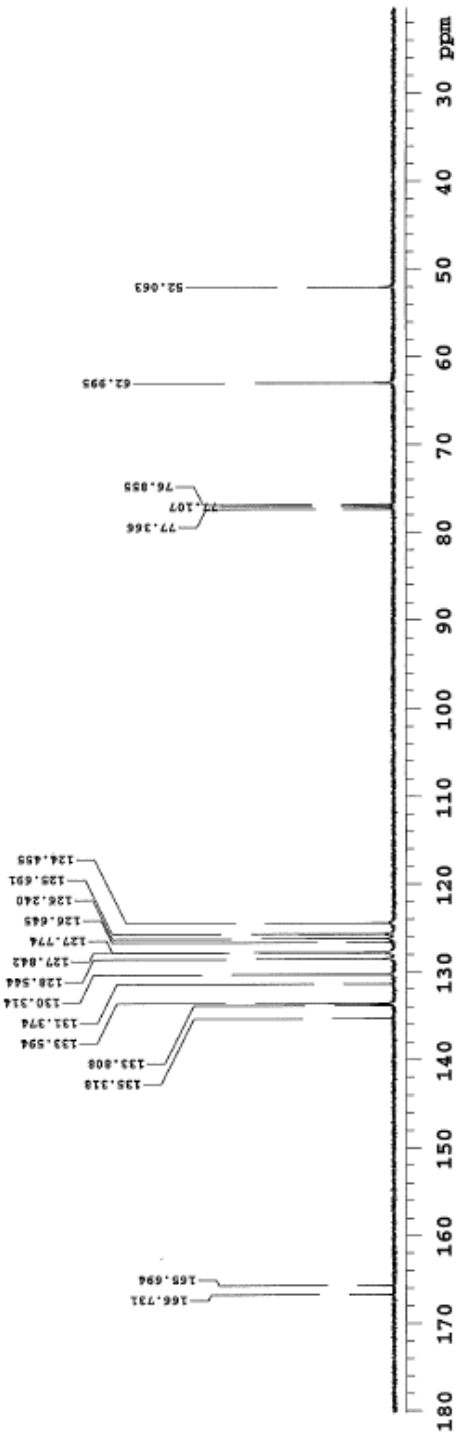
52.063
62.995
76.855
77.107
77.366
124.455
125.691
126.240
126.645
127.774
127.843
128.544
130.314
131.374
133.594
133.808
135.318
165.696
166.731
30
40
50
60
70
80
90
100
110
120
130
140
150
160
170
180
ppm

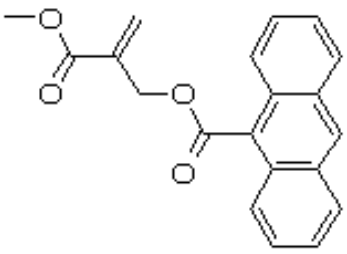

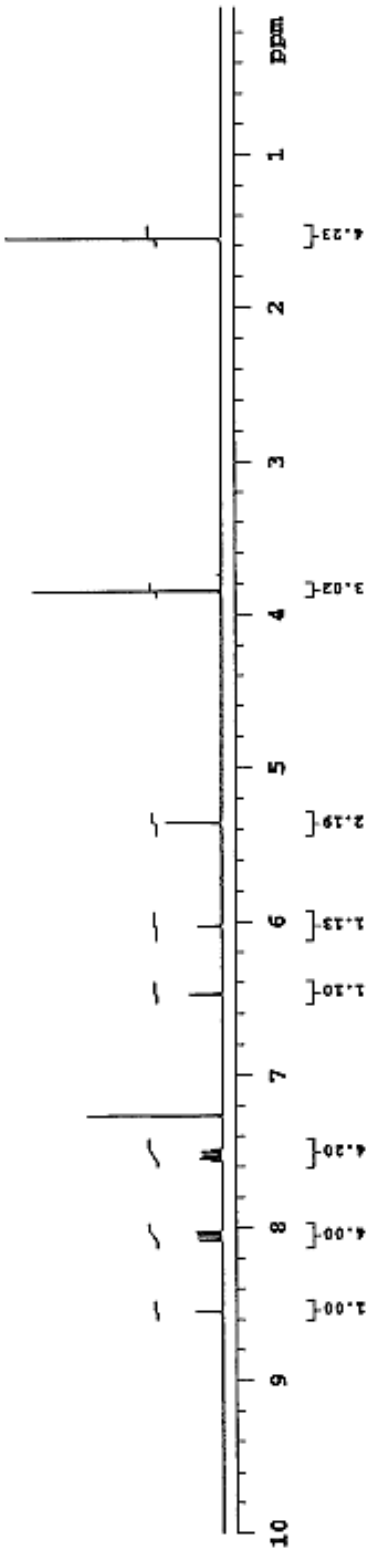
ppm
1
2
3
4
5
6
7
8
9
10
4.33
3.03
2.19
1.13
1.10
4.20
4.00
1.00

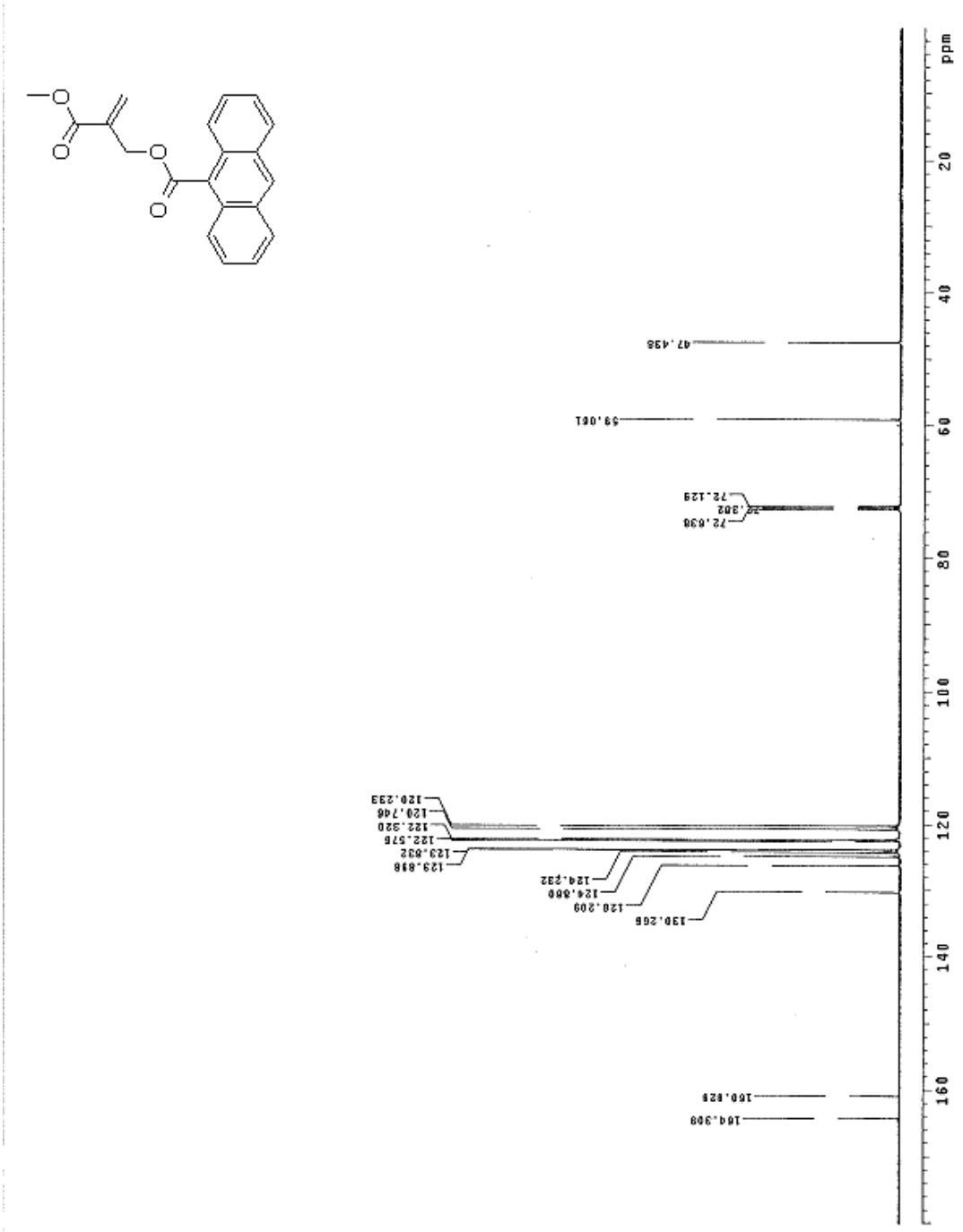
47.436
59.061
72.129
72.302
72.638
120.233
120.746
122.320
122.576
123.632
123.898
124.232
124.888
128.209
130.268
160.829
164.398
ppm

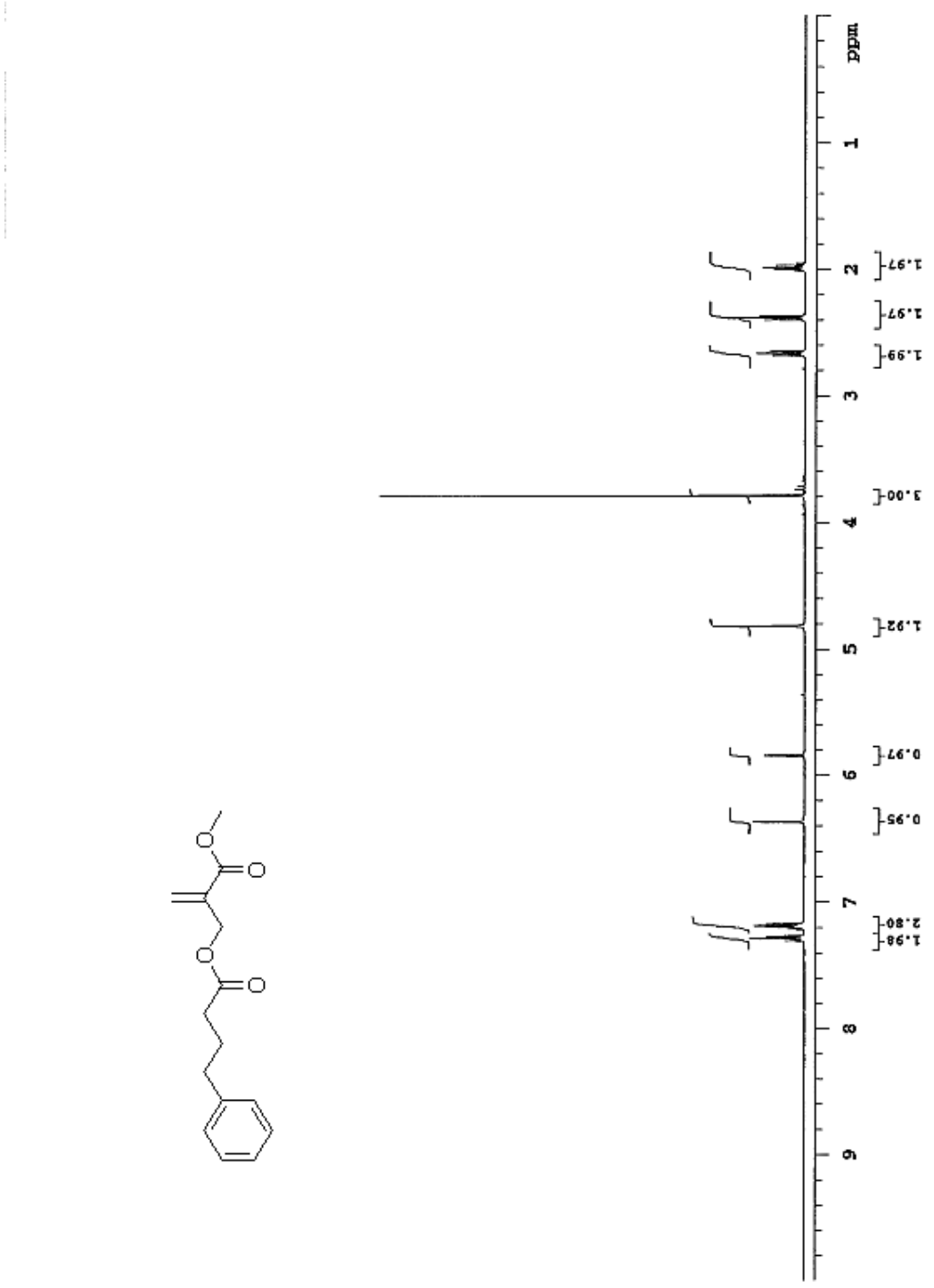
ppm
1
2
3
4
5
6
7
8
9
1.98
2.80
0.95
0.97
1.92
3.00
1.99
1.97
1.97

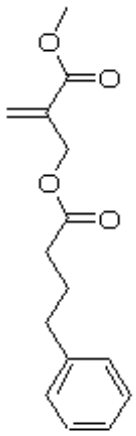

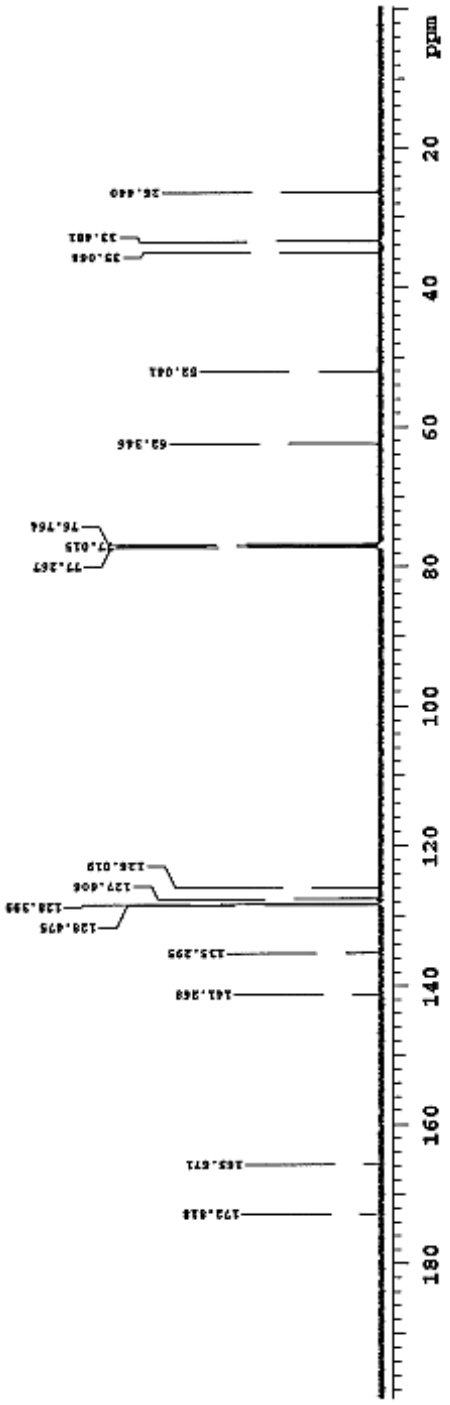
ppm
20
40
60
80
100
120
140
160
180
26.660
33.081
33.068
53.041
63.346
76.764
77.015
77.267
128.019
127.606
128.399
128.675
135.295
141.368
165.671
172.838

ppm
1
2
3
4
5
6
7
8
6.14
4.10
2.00
1.33
4.00

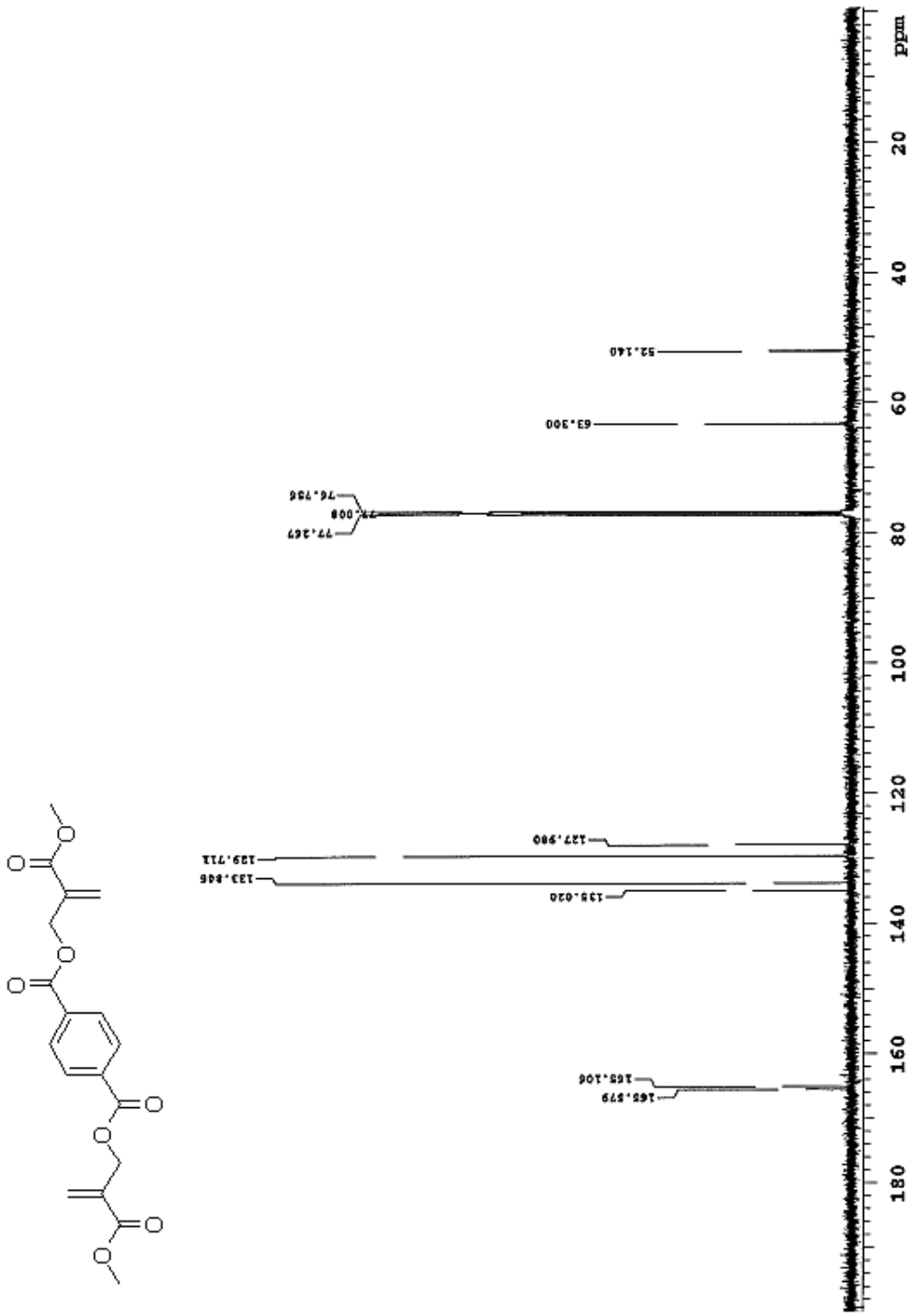
ppm
20
40
60
80
100
120
140
160
180
52.140
63.300
77.367
77.008
76.756
127.980
129.712
133.846
135.030
165.579
165.106

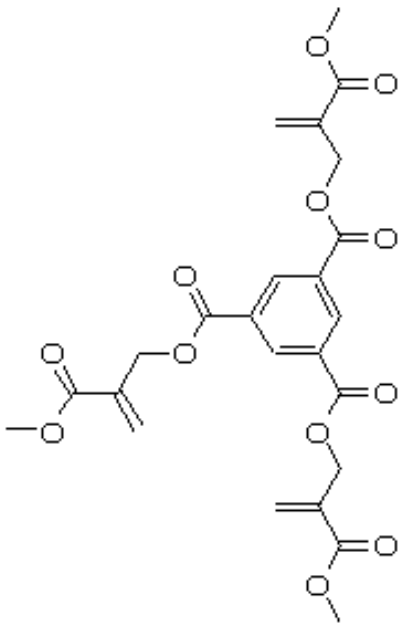

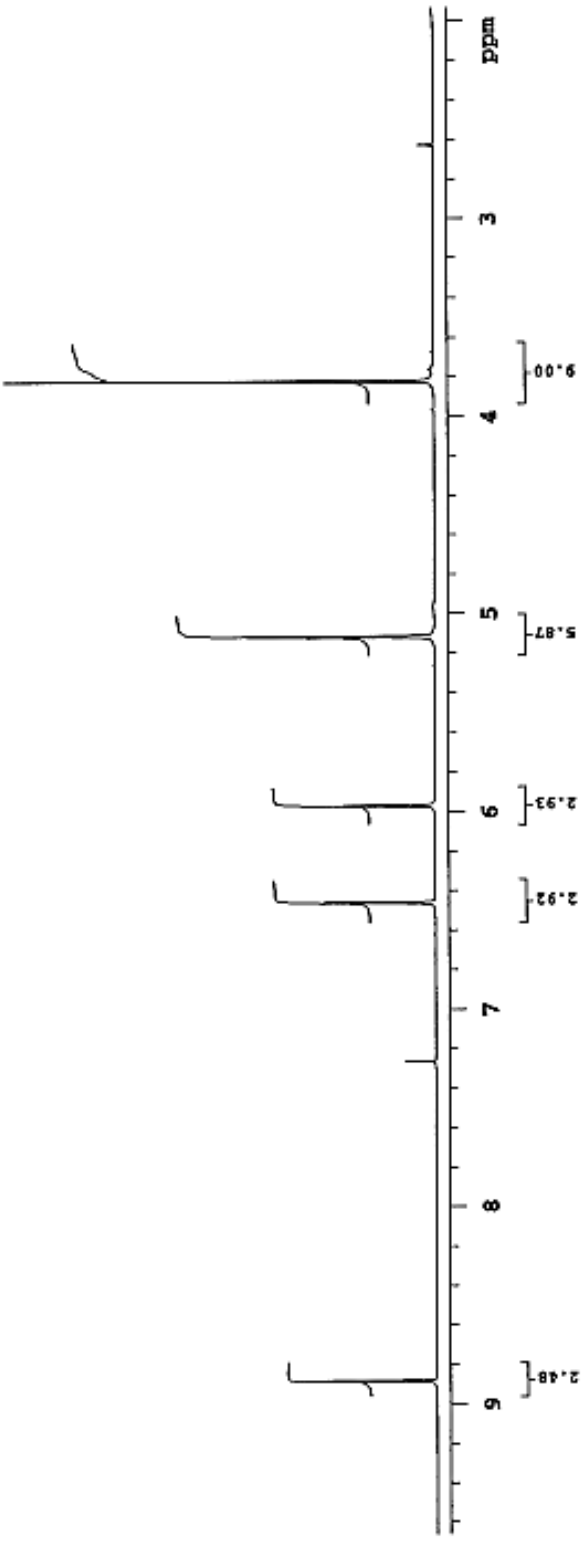
ppm
9
8
7
6
5
4
3
2.48
2.92
2.93
5.87
9.00

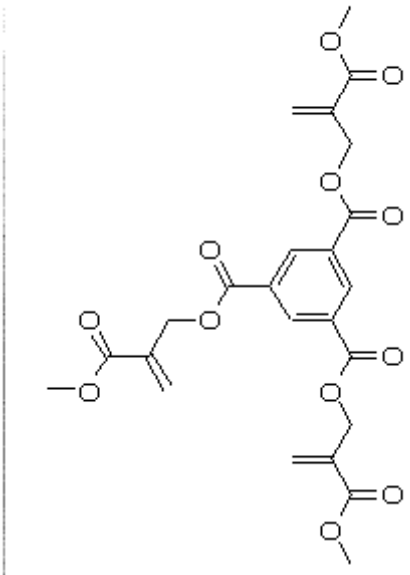

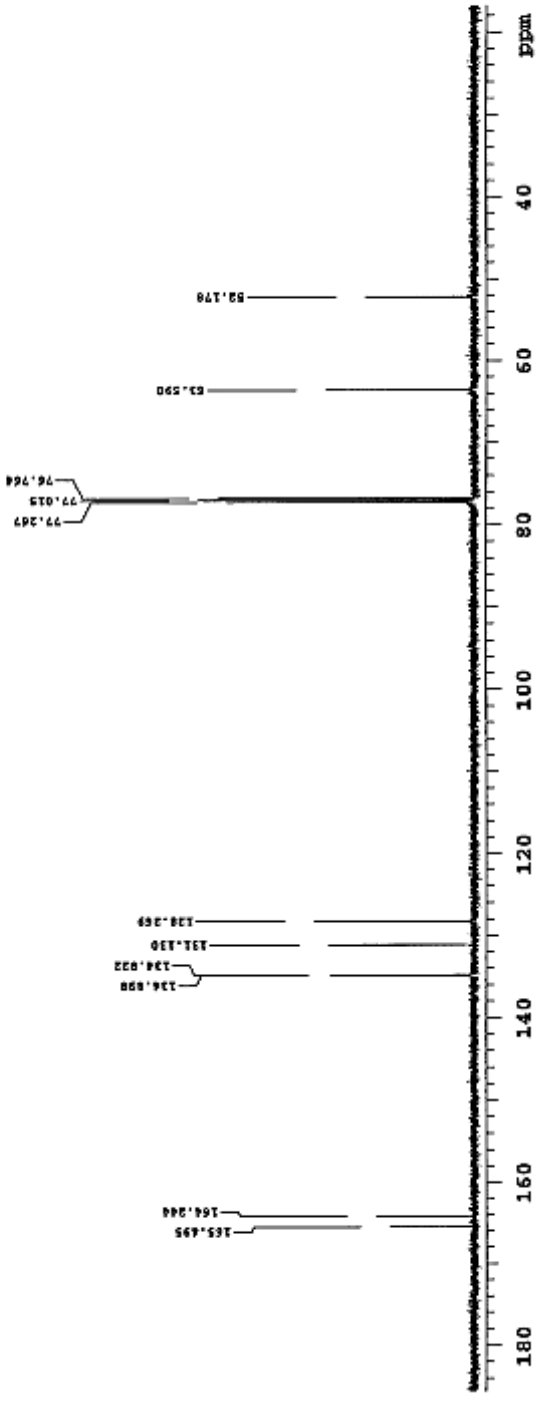
ppm
40
60
80
100
120
140
160
180
53.178
63.590
76.764
77.019
77.347
128.369
131.130
134.922
134.998
164.044
165.695

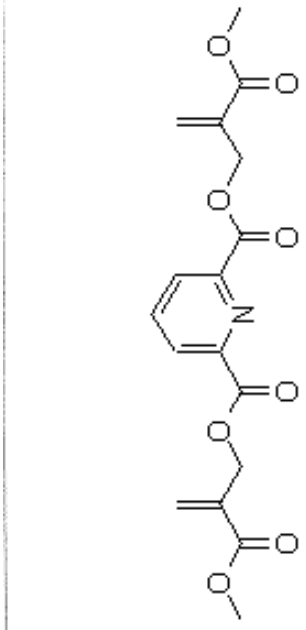

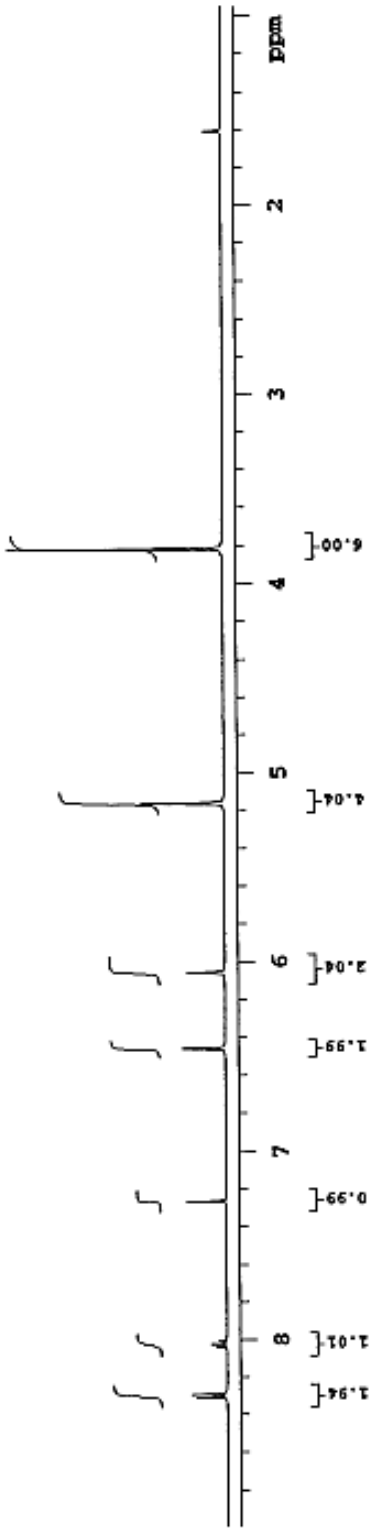
ppm
1
2
3
4
5
6
7
8
6.00
4.04
2.04
1.99
0.99
1.01
1.94

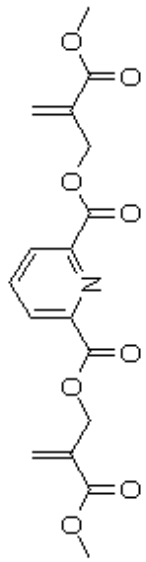

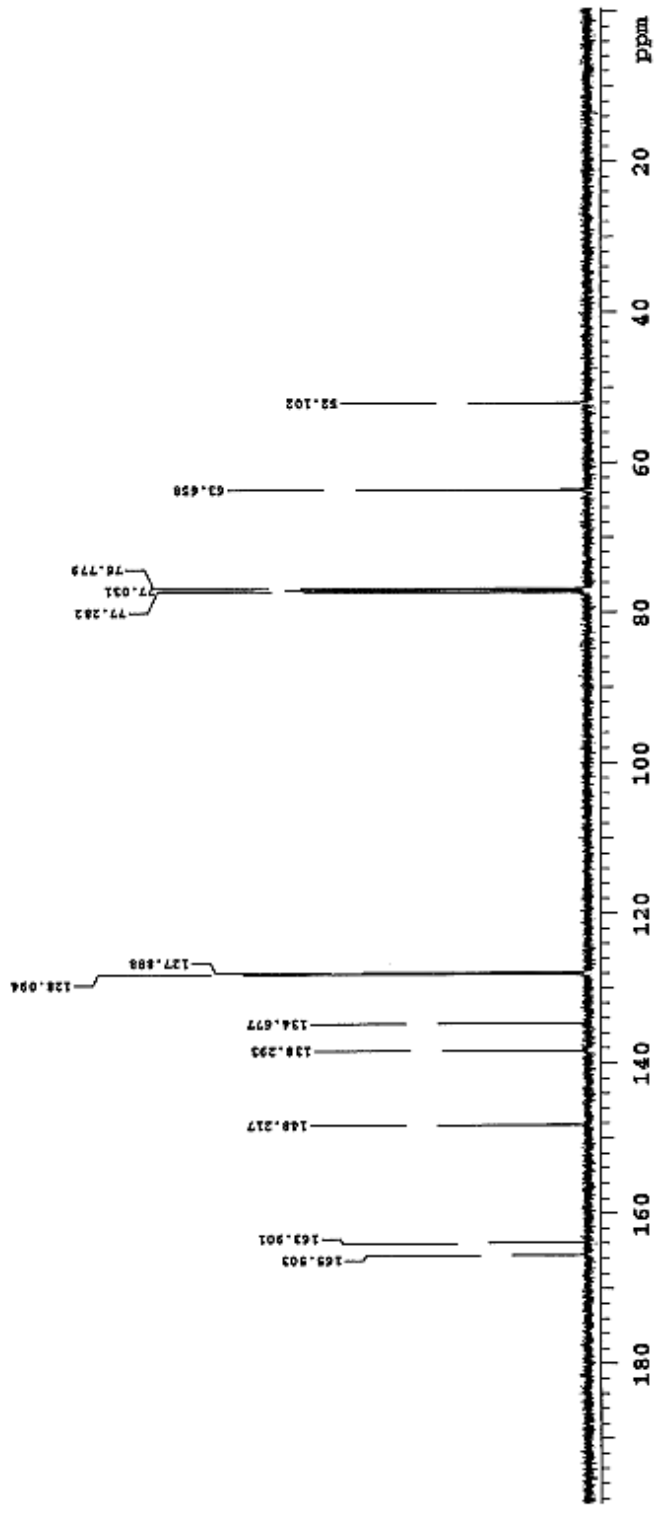
ppm
20
40
60
80
100
120
140
160
180
53.102
63.658
77.383
77.031
76.779
127.888
128.094
134.677
138.293
148.217
163.501
163.903

O
O
O
O
ppm
1
2
3
4
5
6
7
8
9
10

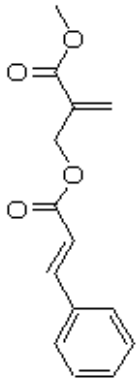

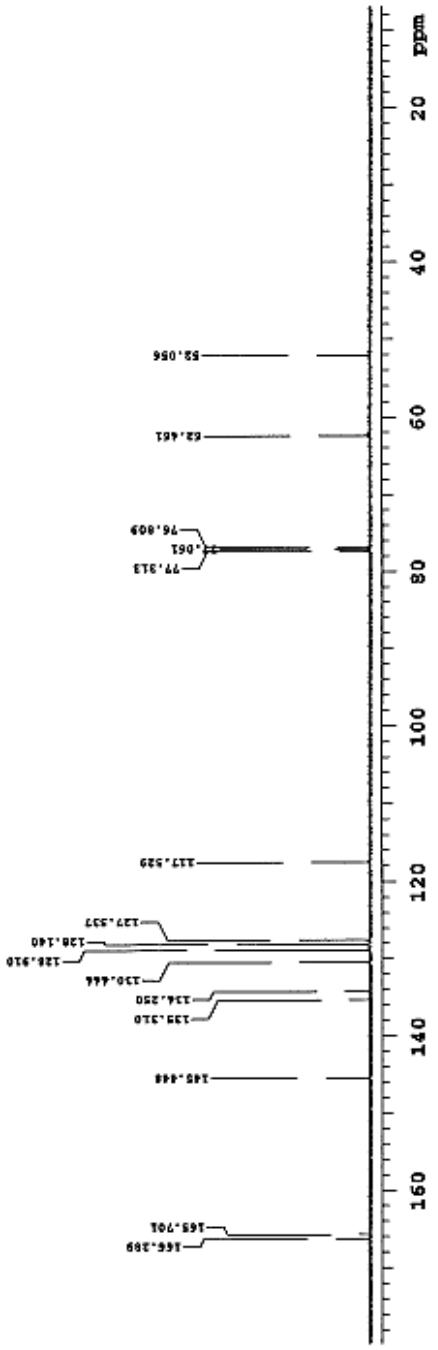
ppm
20
40
60
80
100
120
140
160
53.056
63.461
76.809
77.061
77.313
117.529
127.337
128.160
128.910
130.444
134.350
135.140
145.448
165.701
166.289

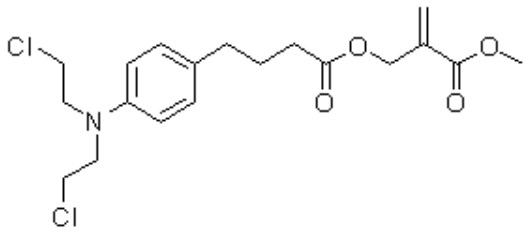
Cl
N
Cl
O
O
O
O

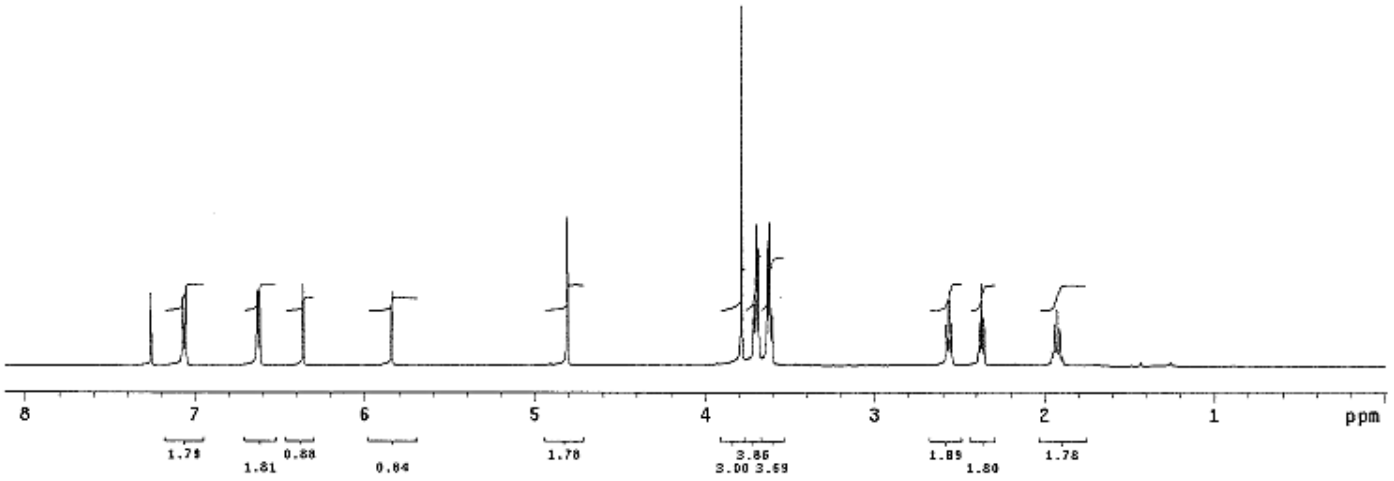
8
7
6
5
4
3
2
1
ppm
1.79
1.81
0.88
0.84
1.78
3.86
3.00 3.69
1.89
1.80
1.78

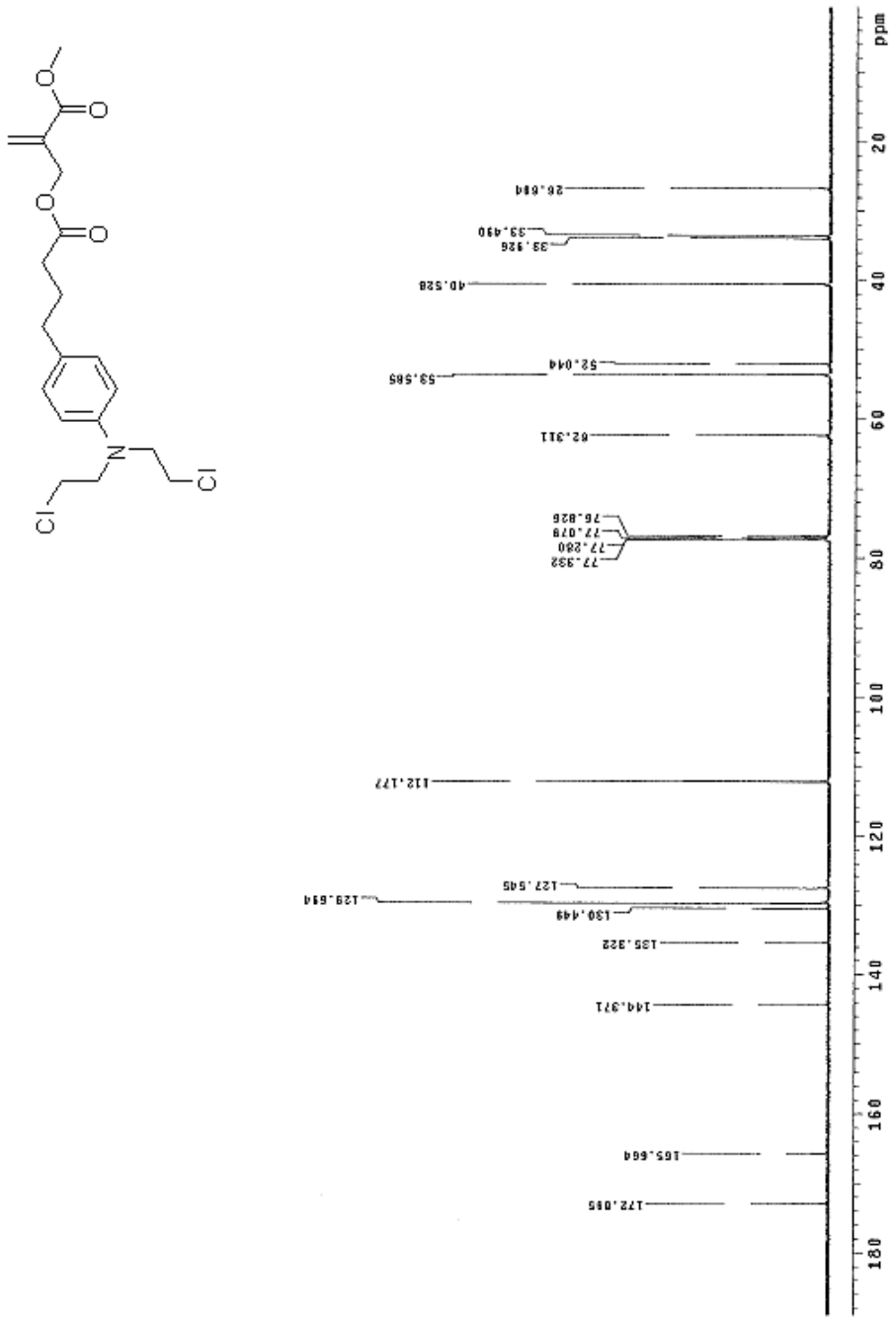
O
O
O
O
N
Cl
Cl
26.684
33.490
33.926
40.528
52.044
53.585
62.311
76.826
77.078
77.280
77.352
112.177
127.545
129.694
130.449
135.322
144.371
165.664
172.085
ppm
20
40
60
80
100
120
140
160
180

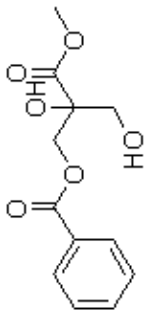
O
O
OH
O
HO
O
O

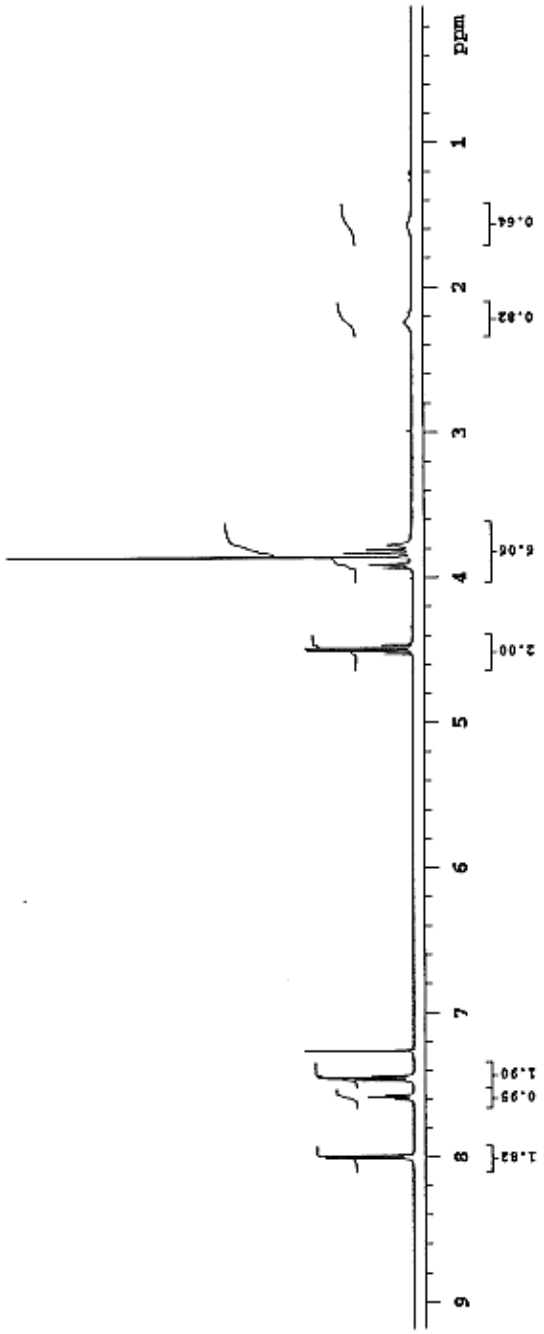
ppm
1
2
3
4
5
6
7
8
9
0.64
0.82
6.06
2.00
1.90
0.95
1.82

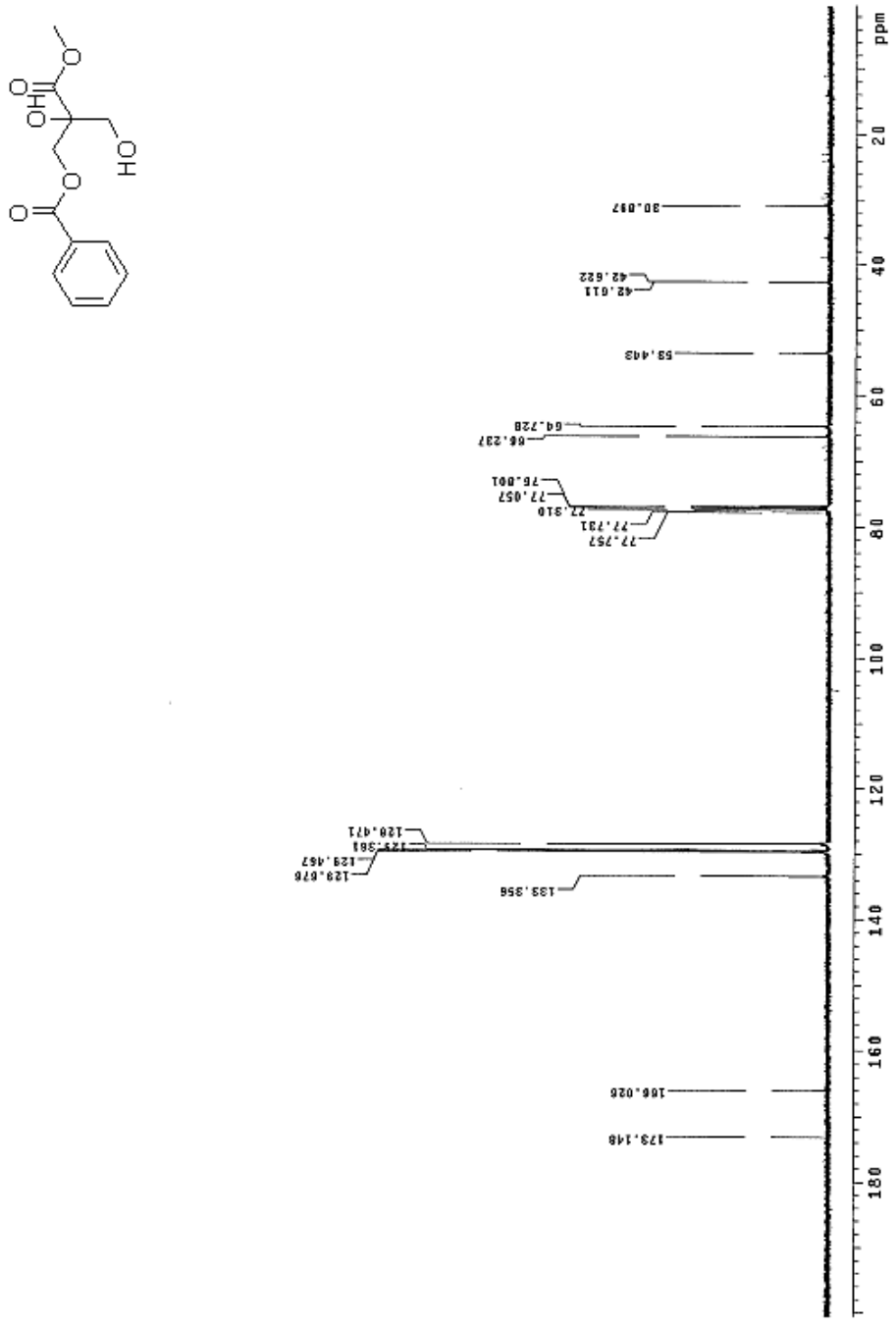
OH
O
O
O
O
HO
ppm
20
40
60
80
100
120
140
160
180
30.097
42.611
42.822
59.443
64.228
66.237
76.801
77.057
77.310
77.731
77.757
120.471
129.361
129.467
129.676
133.856
166.026
179.148